Title
Mechanisms of Mycobacterium tuberculosis Serine/Threonine Protein Kinase Activation

Author
Baer, Christina Elizabeth

Publication Date
2010

Peer reviewed|Thesis/dissertation

Mechanisms of *Mycobacterium tuberculosis* Serine/Threonine Protein Kinase Activation

by

Christina Elizabeth Baer

A dissertation submitted in partial satisfaction of the

requirements for the degree of

Doctor of Philosophy

in

Biophysics

in the Graduate Division of the University of California, Berkeley

Committee in charge:
Professor Tom Alber, Chair
Professor Carolyn Bertozzi
Professor Ehud Isacoff
Professor Bryan Krantz

Fall 2010

Mechanisms of *Mycobacterium tuberculosis* Serine/Threonine Protein Kinase Activation

Abstract

Mechanisms of *Mycobacterium tuberculosis* Serine/Threonine Protein Kinase Activation

by

Christina Elizabeth Baer

Doctor of Philosophy in Biophysics

University of California, Berkeley

Professor Tom Alber, Chair

Mycobacterium tuberculosis (Mtb) coordinates a wide variety of metabolic and cellular responses to changing external environments throughout the multiple stages of infection. Signaling kinases are critical for these responses. The *Mtb* genome encodes 11 Serine/Threonine Protein Kinases (STPKs) that function as important nodes of this sensing and response network, but the chemical and structural changes that mediate kinase activation have not been elucidated.

Autophosphorylation activates several of the *Mtb* STPKs, and kinase dimerization can activate receptor kinases for autophosphorylation through an allosteric dimer interface. Inter-kinase phosphorylation has been reported, but the function and specificity of these interactions remain unknown.

In this study, a biochemical approach was used to comprehensively map the cross-kinase trans-phosphorylation activity of the *Mtb* STPKs. The results reveal a pattern of kinase interactions that suggests each protein plays a distinct regulatory role in controlling cellular processes by phosphorylating other kinases.

The PknB and PknH STPKs act *in vitro* as master regulators that are activated only through autophosphorylation and also phosphorylate other STPKs. In contrast, the signal-transduction kinases PknE, PknJ and PknL are phosphorylated by the master regulatory STPKs and phosphorylate other kinases. The substrate STPKs PknA, PknD, PknF and PknK are phosphorylated by upstream STPKs, but do not phosphorylate other kinases. The delineation of the *Mtb* STPK signaling networks reveals for the first time the specific network of STPK phosphorylation that may mediate the intracellular signaling circuitry.

STPKS are activated and inhibited by phosphorylation at different residues. The regulatory role of the extensive *Mtb* STPK trans-phosphorylation network is unknown. Through mass spectrophotometry and mutagenesis, the amino acids targeted by each phosphorylation were identified. I find that key activation loop residues are the targets of both autophosphorylation and trans-phosphorylation. Mutation of the two conserved threonines in the activation loops of nine *Mtb* STPKs renders the kinases inactive. These results demonstrate that activation loop phosphorylation is a common mechanism of *Mtb* STPK activation.

To explore the structural implications of activation loop phosphorylation, I determined the crystal structures of the phosphorylated and unphosphorylated *Mtb* PknH kinase domain. The PknH kinase domain forms a back-to-back dimer observed previously in the structures of *Mtb* PknB and PknE. Amino-acid substitutions in the dimer interface fail to block kinase dimerization or autophosphorylation. Unexpectedly, the PknH activation loop is folded in the unphosphorylated form and disordered in the active, phosphorylated enzyme. These structures revealed that the back-to-back kinase dimer is a surprisingly stable structure that does not undergo global conformational changes with phosphorylation or nucleotide binding. Unlike the well-established, conformational regulatory mechanisms of eukaryotic STPKs, PknH activation may be a biochemical process mediated by changes in nucleotide affinity or activation loop disorder rather than remodeling of the overall kinase-domain architecture.

To establish the effects of stepwise phosphorylation of an *Mtb* STPK, I determined the structures of the PknK kinase domain modified with 0, 1, or multiple phosphoryl groups. PknK is one of the two solution STPKs in *Mtb* and is phosphorylated by multiple upstream kinases. Mass spectrophotometry revealed that the trans-phosphorylation and autophosphorylation reactions resulted in varying numbers of phosphate groups on this substrate protein. Crystal structures revealed that, like PknH, PknK does not undergo conformational remodeling following activation loop phosphorylation. Unlike many eukaryotic homologs, the unphosphorylated forms of PknH and PknK bind ATP analogs. These two examples suggest that phosphorylation activates the *Mtb* STPKs by directly changing the properties of the activation loop. Based on these results, I propose the testable new idea that activation loop phosphorylation may regulate the *Mtb* STPKs by directly changing the affinities for protein substrates or nucleotides. The absence of conformational remodeling of PknH and PknK upon activation loop phosphorylation implies that the prokaryotic and eukaryotic STPKs are regulated by different mechanisms.

Dedication

This thesis is dedicated to my father, Dr. Thomas Baer.
His passion for science inspired me from an early age.
His unfailing love and support helped my dreams become reality.
Daddy, this one is for you.

Acknowledgements

I thank Alejandra Cavasos, Seemay Chou, Nat Echols, James Fraser, Laurie Gay, Christoph Grundner, Ho-Leung Ng, Noelle Lombana, and Carl Mieczkowski for technical assistance and helpful discussions. I also thank Allyn Schoeffler, Bryan Schmidt, Richard Rhymer, Kevin Jude, George Meigs, and James Holton for X-ray crystallography assistance. Rotation students Thomas Burke and Allison Craney greatly contributed to the structural biology portions of this work. Cloning assistance was provided by Abbey Hartland and Scott Gradia in the QB3 MacroLab facility. I thank Anthony Iavarone for our collaboration. Tony's persistence and scientific curiosity greatly contributed to this work. Mass spectrometry analyses were performed at the QB3 Mass Spec Facility at UC Berkeley using the mass spectrometer acquired with support from the National Institutes of Health (grant number 1S10RR022393). Molecular graphics images were produced using the UCSF Chimera package from the Resource for Biocomputing, Visualization, and Informatics at the University of California, San Francisco (supported by NIH P41 RR001081). This work was supported by an NIH grant (P01AI068135) to Tom Alber.

I thank Udi Isacoff and Eva Nogales for inviting me to perform valuable rotations in their laboratories. I wish to thank the inspirational instructors and mentors I have had in graduate school for encouraging my interests. These professors include Carolyn Bertozzi, James Berger, Jennifer Doudna, Bryan Krantz, David Raulet and Russell Vance. I also thank the UC Berkeley Biophysics Graduate Group for providing me with the opportunity to pursue a graduate degree in science. The Biophysics Program has been a fantastic place for me to nurture my broad interests and to explore new scientific areas. I thank Kate Chase for her constant support as the Biophysics Student Affairs Officer. Her help navigating the administrative requirements for degree completion was invaluable.

I owe an enormous debt to Andrew Greenstein who, as my rotation mentor in the Alber Lab, introduced me to the *Mycobacterium tuberculosis* kinases and trained me in a wide range of techniques utilized in this thesis. His continued advice throughout my graduate career has proven invaluable. I thank Terry Lang for her support during my time in the Alber Lab. Terry, a constant source of advice and computer assistance, provided essential guidance over the course of my time in graduate school. I am grateful to Christine Gee for training me to do X-ray crystallography. Despite the distance between Australia and Berkeley, she is always ready and willing to help in any way that she can. Without her input and personal support, this project would not have been possible.

I thank my parents, Tom and Bobbi, for their constant love and support that carried me through the long years of graduate school. While my father is a source of my scientific aspirations, my mother is the foundation of my support system. Her motivational guidance and willingness to help in every way made this work a reality. My mom's work ethic and passion inspire me daily.

This dissertation would not have been possible without the long-distance support of my fiancé Jason. His willingness to endure a 3,000-mile separation for over 5 years allowed me to complete graduate school. Jason's enduring faith in the strength of our relationship and in my ability to become Dr. Baer allowed me to pursue my dream. With the deepest gratitude, I thank him for his patience.

Lastly, I am greatly indebted to Tom Alber for providing the opportunity to explore the intersection of molecular biology, biochemistry and structural biology. I thank him for being an

excellent mentor. Tom allowed me the freedom to pursue my interests while always providing valuable advice and suggestions. I am extremely grateful for his support throughout my graduate career.

Chapter 1

Introduction

Protein kinases comprise one of the most extensive and diverse gene families in eukaryotes (Manning, Whyte et al. 2002). This well-characterized class of enzymes regulates a wide variety of cellular processes. The sequencing of multiple prokaryotic genomes revealed the presence of many eukaryotic-like serine/threonine protein kinases (STPKs) in addition to the canonical bacterial response regulators, the histidine kinases (Hanks and Hunter 1995).

The prokaryotic STPKs were first identified in *Yersinia pseudoturberculosis* and *Myxococous Xanthus* (Hanks and Hunter 1995). Genes carrying the hallmarks of "eukaryotic-like" Ser/Thr phosphosignaling systems have been found in the genomes of archea and bacteria (Leonard, Aravind et al. 1998). The analysis of fully sequenced microbial genomes and sequences in the Global Ocean Sampling data base revealed that eukaryotic-like protein kinases now outnumber known histidine kinases (Kannan, Taylor et al. 2007). The increasing number of identified eukaryotic-like STPKs suggests that these signaling proteins may be at least as important in bacterial cellular regulation as two-component histidine kinases.

STPKs catalyze the transfer of the gamma-phosphate of adenosine tri-phosphate (ATP) to serine (Ser), threonine (Thr) or tyrosine (Tyr) residues. This class of enzymes performs three distinct functions: bind and orient the ATP phosphate donor as a complex with magnesium or manganese ions, bind and position the protein substrate, and catalyze transfer of the gamma phosphate from ATP to the acceptor hydroxyl group (Hanks and Hunter 1995). The resulting Ser, Thr, and Tyr phospho-esters are stable for weeks at neutral pH, requiring Ser/Thr/Tyr phosphatases to regulate this signal (Greenstein, Grundner et al. 2005). Careful regulation of the STPKs enables precise cellular responses to external signals, allowing bacteria to survive in a variety of changing environmental conditions.

Eukaryotic kinases exhibit a wide variety of regulatory mechanisms; however, prokaryotic STPK activation is not well understood. Universally, kinases are normally maintained in the off-state (Huse and Kuriyan 2002), only turning on in response to specific signals that relieve autoinhibition (Alber 2009). Multiple levels of control mediate activation of these proteins, from the binding of allosteric effectors to alterations in the kinase subcellular localization (Huse and Kuriyan 2002). While the on-state is defined by the chemical constraints required to bind a substrate and catalyze phosphoryl-transfer, the off-state is not subject to the same restrictions. As a result, different classes of kinases have evolved structurally diverse mechanisms of autoinhibition in the off-state (Huse and Kuriyan 2002; Alber 2009).

The genome of the pathogen *Mycobacterium tuberculosis (Mtb)* contains 11 STPKs. These proteins display striking structural similarity to their eukaryotic homologs, but discrepancies between the *Mtb* kinase structures and well-characterized eukaryotic kinases suggest differences in regulation. The 11 *Mtb* STPKs can be activated through trans-phosphorylation mediated by a "front-to-front" transient dimer or activated allosterically through a "back-to-back" interface (Greenstein, Echols et al. 2007; Mieczkowski, Iavarone et al. 2008). These two activation mechanisms result in a phosphorylated, and therefore active, kinase. The process of one kinase molecule phosphorylating another identical molecule is known as autophosphorylation. The mechanism of trans-autophosphorylation through the two interfaces is

fairly well established for the *Mtb* STPKs. Alternate mechanisms of activation and the conformational changes that result from phosphorylation remain unknown.

Inter-kinase trans-phosphorylation, phosphorylation of a kinase by another STPK in the *Mtb* kinome, has been reported (Kang, Abbott et al. 2005). However, the role of this interaction in kinase signaling pathways is not understood. Given the recent discovery of kinase-kinase regulatory cascades in *Myxococcus xanthus* (Nariya and Inouye 2005), cross-kinase phosphorylation potentially adds a level of regulatory control and increases the complexity of Ser/Thr phospho-signaling in *Mtb*. How specific are these interactions between the 11 *Mtb* STPKs? Does this kinase-kinase cross-talk act as an alternative activation pathway complementary to the known autophosphorylation activation mechanisms? Or is cross-kinase phosphorylation an inhibitory mechanism that regulates STPK activity? This thesis aims to answer these questions by defining these novel phosphor-Ser/Thr signaling pathways and characterizing the extent and function of cross-kinase phosphorylation.

For many kinases, activation is mediated by a series of biochemical events leading to structural remodeling that stabilizes the protein in the active conformation. The movement from the inhibited off-state to the active on-state is a crucial component of the kinase activation process. The autoinhibitory mechanism for the *Mtb* STPKs is unknown. Multiple crystal structures of the *Mtb* STPKs exist, but all are of active phosphorylated kinases. Through a series of structural studies, this work will explore the structural remodeling that may occur during activation. The structures of *Mtb* STPKs in various stages of activation provide valuable insights into the mechanism of activation.

Mycobacterium tuberculosis, the causative agent of tuberculosis (TB), infects an estimated 2.2 billion people globally and was the cause of 1.3 million deaths in 2008 (2009). The spread of HIV has dramatically increased the incidence of TB mortality, as the two pathogens work in concert to kill the human host. The rising human cost of TB infection and the emergence of bacterial strains resistant to the first and second line treatments have led to increased urgency to the search for new anti-mycobacterial drugs. New treatments for TB are needed to stem the tide of infection and to fight growing drug resistance. As eukaryotic STPKs have proven tractable drug targets in the fight against cancer (Huse and Kuriyan 2002), the homologous prokaryotic proteins are appealing targets for drug development. Many kinase inhibitors function to capture the kinase in the inactive or off state, preventing activation. The thorough biochemical and structural characterization of the all the mechanisms of kinase activation in *Mtb* may enable the development of similar molecular inhibitors for mycobacteria.

The *Mtb* genome contains a large number of signaling proteins in relation to its relative size (Greenstein, Grundner et al. 2005), making this pathogen an appealing system in which to study prokaryotic intracellular signaling and response pathways. Eleven histidine kinases with 11 cognate response regulators, 11 STPKs, 1 Ser/Thr phosphatase and 2 Tyr phosphatases are found in *Mtb* (Ortiz-Lombardia, Pompeo et al. 2003). The STPKs are in the PKN2 family of prokaryotic kinases, the most closely related to eukaryotic homologs (Kang, Abbott et al. 2005). The medical impact of *Mtb* infection combined with the potential for broad functional control of cellular processes afforded by the 14 regulatory proteins responsible for Ser/Thr phospho-signaling in *Mtb* provides strong rationale for investigating the mechanisms of these phospho-signaling systems (Greenstein, Grundner et al. 2005).

The *Mtb* Ser/Thr kinome consists of nine kinases anchored to the cell membrane by a single trans-membrane (TM) helix and two soluble solution kinases, (Figure 1.1). Three of the TM kinases, PknB, PknD and PknE, have extracellular domains known to be folded. The

structures of the PknB and PknD sensor domains have been solved, but the ligands for STPK extracellular domains remain unknown (Good, Greenstein et al. 2004; Barthe, Mukamolova et al. 2010).

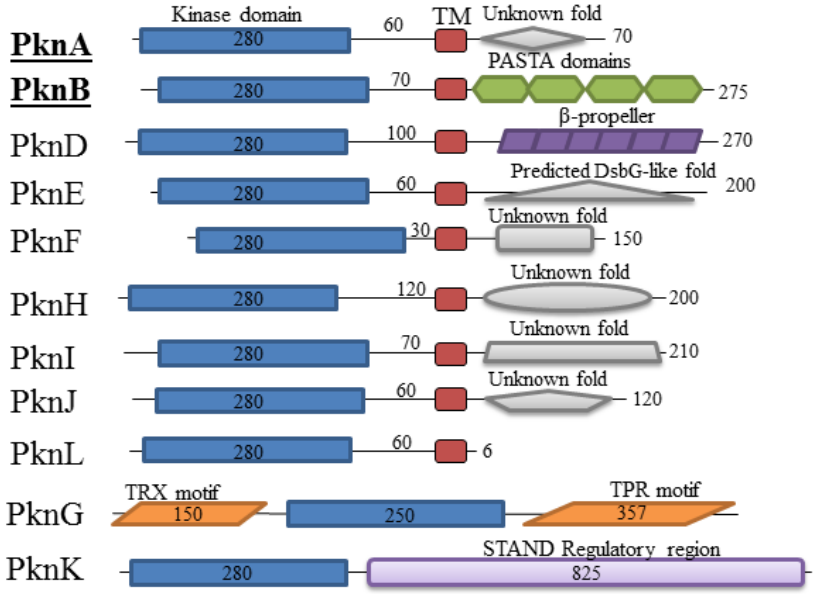

Figure 1.1 The Mtb Ser/Thr kinome contains 11 STPKS. The two essential kinases, PknA and PknB, are highlight in bold text. PknG and PknK are the two soluble kinases. The remaining 9 enzymes are predicted to be membrane-bound.

The catalytic domains of the STPKs can be divided into evolutionary clades based on sequence homology (Narayan, Sachdeva et al. 2007). PknA, PknB and PknL are found in the first clade and all three kinases are conserved across the mycobacterial genus. These three proteins are thought to be involved with cell divisions and cell wall synthesis. Notably, PknA and PknB are the only essential *Mtb* STPKs (Fernandez, Saint-Joanis et al. 2006). These two proteins are located in an operon with the Ser/Thr phosphatase pstP. The start and stop codons in this gene cluster overlap, an indication that transcription and translation maybe coupled and that these proteins may be expressed at similar levels in the cell (Kang, Abbott et al. 2005).

Overexpression and knockdown of PknA and PknB in *Mycobacterium smegmatis* (*Msmeg*) and *Mycobacterium bovis* (*Mbovis*) produce distinct cell shape phenotypes, suggesting a role for these proteins in cell growth and division (Kang, Abbott et al. 2005). PknA phosphorylates Rv0019c, an FHA (Fork-Head-Associated) domain-containing protein that is involved with cell division (Sureka, Hossain et al. 2010). The report that PknB is expressed in bacteria grown in macrophages supports a role for this protein in cell growth (Av-Gay, Jamil et al. 1999). Like PknA, PknB is known to phosphorylate proteins involved in cell wall synthesis such as PBPA (Penicillin-Binding-Protein A), a protein necessary for peptidoglycan synthesis (Dasgupta, Datta et al. 2006), Wag31, an essential protein that regulates cell morphology and polar cell wall synthesis (Kang, Nyayapathy et al. 2008), and FlpA, the flippase that supplies building blocks of peptidoglycan synthesis (Gee, Papavinasasundaram et al. 2010). PknB is also known to play a role regulating SigH, the stress-response sigma factor, through phosphorylation of the anti-sigma factor RshA (Greenstein, MacGurn et al. 2007). The involvement of these two

essential STPKs in a wide variety of cellular processes highlights the complex role played by each protein in cellular survival and proliferation.

The third member of this clade, the STPK PknL, phosphorylates the DNA-binding protein Rv2175c *in vitro* (Lakshminarayan, Narayanan et al. 2008; Cohen-Gonsaud, Barthe et al. 2009). Phosphorylation of Rv2175c appears to negatively regulate DNA binding activity (Cohen-Gonsaud, Barthe et al. 2009). The DNA targets of Rv2175c remain a source of speculation. Based on similarities to PknA and PknB, PknL has been proposed to be involved in cell division and morphology (Narayan, Sachdeva et al. 2007). While studies in *Corynebacterium glutamicum* of the conserved PknA, PknB, PknG and PknL homologs revealed that PknL phosphorylates an FHA domain protein that is homologous to the *Mtb* protein GarA, no role was identified for PknL in cell division (Fiuza, Canova et al. 2008; Schultz, Niebisch et al. 2009). The function of this nonessential STPK remains under investigation.

The second evolutionary clade of the *Mtb* STPKs contains the membrane-bound kinases PknD, PknE and PknH. These kinases are implicated in a variety of cellular processes, and all three proteins have extracellular sensor domains that are predicted to be folded. PknD, a membrane bound kinase with a five bladed β-propeller extra-cellular domain (Good, Greenstein et al. 2004), is implicated in sigma factor regulation and transcriptional control. Phosphorylation of Thr2 of the putative anti-anti-sigma-factor, Rv0516c, by PknD blocks binding of this protein to Rv2638, an anti-sigma-factor (Greenstein, MacGurn et al. 2007). Overexpression of PknD in *Mtb* influences SigF-mediated transcription, but the mechanism of control is unknown. In addition to PknD, PknB and PknE also phosphorylate anti- and anti-anti-sigma-factors *in vitro*. Transcriptional regulation through phosphorylation of sigma-factor regulator proteins may extend to multiple kinases *in vivo*. It is important to note that not all of the kinases phosphorylated these substrates and that the interactions are quite specific, so the identified kinase-substrate interactions are probably function as distinct signaling pathways (Greenstein, MacGurn et al. 2007).

One of the first STPKs identified as an active kinase, PknE contains a 200 amino acid extra cellular domain with sequence similarity to DsbG, the protein disulfide isomerase (Molle, Girard-Blanc et al. 2003). The PknE promoter responds to nitric oxide stress and deletion of PknE in *Mtb* results in increased apoptosis in the human macrophage *in vitro* model of infection (Jayakumar, Jacobs et al. 2008). Inhibition of macrophage apoptosis is an important *Mtb* survival mechanism that may be regulated in part by PknE. In addition to the anti- and anti-anti sigma factor substrates mentioned above (Greenstein, MacGurn et al. 2007), PknE phosphorylates the ABC transporter Rv1747 on an internal FHA domain (Grundner, Gay et al. 2005). FHA domains are phospho-threonine recognition motifs found in both eukaryotes and prokaryotes (Durocher and Jackson 2002; Pallen, Chaudhuri et al. 2002). Multiple FHA domain containing proteins are phosphorylated by the *Mtb* STPKs and many are phosphorylated by more than one kinase, suggesting complex signaling pathways (Grundner, Gay et al. 2005).

PknH, while nonessential, is increasingly recognized as a critical regulatory protein in *Mtb*. In liquid culture, a PknH knockout strain is more resistant to acidified-nitrite stress which indicates that PknH may regulate growth in response to nitric oxide stress *in vivo* (Papavinasasundaram, Chan et al. 2005). The *Mtb* PknH knockout strain displays significantly higher bacillary load in the mouse infection model (Papavinasasundaram, Chan et al. 2005). This hypervirulent phenotype is intriguing in light of a recent paper linking PknH to a two-component regulatory system, DosR/DevR, one of 11 pairs of defined two component systems in *Mtb* (Chao, Papavinasasundaram et al. 2010). PknH phosphorylates the response regulator

Rv3133, also known as DosR and DevR. Rv3133/DosR/DevR responds to hypoxia, nitric oxide and carbon monoxide stress *via* signaling through two cognate sensor kinases that activate a set of genes known as the dormancy (or DosR) regulon. The nitric oxide stress response links PknH and DosR/DevR, supporting a functional relationship between these two signaling proteins that may coordinate the intracellular response to environmental stress. Intriguingly, the deletion of devR/dosR resulted in a hypervirulent phenotype very similar to that reported for the PknH knockout strain (Parish, Smith et al. 2003).

PknH also known to phosphorylates EmbR, a DNA-binding protein that contains an FHA domain (Molle, Kremer et al. 2003). EmbR regulates the expression of the genes that mediate resistance to the anti-mycobacterial drug ethambutol (Sharma, Gupta et al. 2006). Recently, a structurally homologous regulatory protein, EmbR2, was identified in the *Mtb* strain CDC1551 (Molle, Reynolds et al. 2008). This gene is not found in the canonical *Mtb* lab strain, H37Rv, suggesting that further analysis of multiple *Mtb* strains may result in the discovery of additional proteins implicated in Ser/Thr phosphor-signaling. EmbR2 is phosphorylated by PknE and PknF, but not by PknH, and may inhibit PknH phosphorylation of EmbR (Molle, Reynolds et al. 2008). The ability of multiple kinases to indirectly control another kinase through phosphorylation of a regulatory protein suggests an intricate series of control mechanisms that have yet to be elucidated.

Clade 3 of the *Mtb* STPKs consists of PknF, PknI and PknJ. PknF is conserved across mycobacteria. This kinase may regulate glucose transport though phosphorylation of the FHA-domain-containing ABC transporter, Rv1747 (Deol, Vohra et al. 2005). Overexpression of PknF in the nonpathogenic model organism *Msmeg* significantly altered cell morphology and slowed growth (Deol, Vohra et al. 2005). In addition, overexpression of this protein impairs biofilm formation and sliding motility in *Msmeg*, providing further evidence for the regulatory role of PknF in the processes related to formation of proper cell wall architecture (Gopalaswamy, Narayanan et al. 2008).

In contrast to PknF, PknI and PknJ are found in only a small subset of mycobacterial species. Similar to the PknH knockout phenotype, the PknI deletion mutant is hypervirulent compared to wild-type *Mtb* in time-to-death studies in the SCID mouse model (Gopalaswamy, Narayanan et al. 2009). However, total bacillary load in this infection model was not assayed, so these results are not directly comparable. Macrophage infections with the PknI deletion strain revealed that the kinase may control bacterial growth post infection (Gopalaswamy, Narayanan et al. 2009). Little is known about the function of PknI *in vivo*, and no endogenous substrates have been identified for this kinase. PknI contains a single predicted transmembrane helix and an extra cellular domain that does not bear homology to any known fold.

The membrane bound kinase PknJ is the subject of a recent study that identified multiple substrate peptides. The peptide sequences were selected from the *Mtb* genome by similarity to the PknJ activation loop peptide (Jang, Stella et al. 2010). Four of the identified targets were confirmed *in vitro*: PknJ; EmbR; MmaA4/Hma, a methyltransferase involved in synthesis of mycolic acids; and PepE, a putative dipeptidase with proline specificity. While these results suggest a functional role for PknJ in nitrogen and amino acid metabolism through phosphorylation of PepE, this has yet to be confirmed (Jang, Stella et al. 2010). Pyruvate kinase A has also been identified as a PknJ substrate and the functional implications of this phosphorylation event have been incompletely characterized (Arora, Sajid et al. 2010).

The soluble kinases PknG and PknK are evolutionarily distinct from each other and from the rest of the *Mtb* STPKs. Widely distributed across pathogenic and nonpathogenic bacteria,

PknG is a multi-domain kinase containing a catalytic kinase domain fused to two TPR motifs of unknown function (Koul, Choidas et al. 2001). PknG plays a significant role during *Mtb* infection. This STPK increases intracellular survival by contributing to the inhibition of phago-lysosome fusion, an important step for *Mtb* survival within the host cell. The deletion of this gene in the attenuated vaccine strain *Mbovis* BCG results in lysosomal localization of mycobacteria, and *Msmeg* complemented with this gene can prevent phagosome-lysosome fusion (Chaurasiya and Srivastava 2009). PknG has been reported to selectively down regulate PKC-alpha expression during infection by directly degrading PKC-alpha. However, PKC-alpha is not a PknG kinase substrate and the PknG kinase domain by itself does not degrade PKC-alpha, leading to the speculation that one of the other domains must be responsible for this protease activity (Chaurasiya and Srivastava 2009). However, no homologues to a known protease are apparent in the PknG sequence.

PknK is present in both slow- and fast-growing mycobacteria (Narayan, Sachdeva et al. 2007). This soluble kinase contains a C-terminal regulatory domain connected to the catalytically active kinase domain by a flexible linker. The C-terminal region of PknK is homologous to the regulatory region of the *Escherichia coli* transcriptional regulator MalT (Kumar, Kumar et al. 2009). MalT-like proteins are part of the Signal Transduction ATPases with Numerous Domains (STAND) protein family. STAND proteins are large signaling hubs with a conserved multi-domain ATPase core, the nucleotide-binding oligomerization domain (Danot, Marquenet et al. 2009). These proteins exist in two states: a monomeric resting ADP-bound form, the off-state, and an ATP-bound oligomeric on-state competent for downstream signaling through effecter domains (Danot, Marquenet et al. 2009). The role of autophosphorylation and the effect of MalT domain activation on the kinase are unknown. While the *E.coli* MalT does not have a kinase domain, other STAND homologs do include a STPK (Danot, Marquenet et al. 2009). PknK is reported to phosphorylate VirS and multiple related proteins in the *Mtb* monoxygenase operon *mymA* (Kumar, Kumar et al. 2009). Co-expression of VirS and PknK appears to upregulate *mymA* transcription, although the exact role of PknK in this signaling pathway remains an open question (Kumar, Kumar et al. 2009).

The sole Ser/Thr phosphatase identified in the *Mtb* genome, Pstp, efficiently de-phosphorylates the STPKs (Chopra, Singh et al. 2003). Like many of the kinases, Pstp contains a single predicted TM helix and an extracellular domain.

A recent peptide screen identified 301 *Mtb* proteins as potential kinase substrates (Prisic, Dankwa et al. 2010). These 301 proteins contained 516 phosphorylation events, indicating that many proteins are multiply phosphorylated. A shared phosphorylated peptide sequence was identified for PknA, PknB, PknD, PknE, PknF and PknH, implying phospho-regulatory control of the same substrate proteins by multiple kinases. This result also suggests that factors in addition to peptide recognition mediate substrate specificity. Co-expression, co-localization and protein-protein interactions are likely factors involved in substrate recognition (Biondi and Nebreda 2003). Peptide screening to identify kinase substrates must be followed with further investigations, as some proteins identified as having multiple phosphorylation sites in this screen have only one site *in vivo* (Gee, Papavinasasundaram et al. 2010; Prisic, Dankwa et al. 2010). However, this study greatly expands the number of potential kinase substrates and suggests diverse roles for the *Mtb* STPKs in many cellular processes.

The *Mtb* STPKs may contribute to cellular survival under conditions of osmotic shock, nutrient starvation and NO stress encountered during infection by signaling response proteins. The implication of these enzymes in cellular processes essential for survival within the host

makes these proteins intriguing drug targets. The mycobacterial STPKs have only 30% sequence identity to human STPKs, facilitating the development of mycobacteria-specific kinase inhibitors (Wehenkel, Bellinzoni et al. 2008). The essential STPK PknB crystallizes in a complex with mitoxantrone, a compound used in cancer treatment, and this drug inhibits mycobacterial growth (Wehenkel, Fernandez et al. 2006). PknB mutants have also been crystallized with staurosporine, another kinase inhibitor, enabling an analysis of the specific active site residues that contact the inhibitor with an eye to improving inhibitor specificity (Mieczkowski, Iavarone et al. 2008). Screens of available kinase inhibitors have revealed certain extant compounds that display specificity for individual *Mtb* STPKs (Greenstein, MacGurn et al. 2007).

Eukaryotic Ser/Thr kinases have proven to be appealing drug targets for the treatment of cancer. The most recent successful kinase-targeted drugs take advantage of the wide structural variability in inactive kinase conformations by specifically binding the inactive form to inhibit catalytic activity (Simard, Grutter et al. 2009). Examples of these drugs are sorafenib (Nexavar; Bayer), nilotinib (Tasigna, Novartis), sunitinib (Sutent; Pfizer/Sugen), dasatinib (Sprycel; Bristol Myers Squibb), and lapatinib (Tykerb; GSK), which all target specific types of cancer (Simard, Grutter et al. 2009). Understanding mycobacterial STPK activation and the conformational changes that occur during the movement from the off-state to the on-state would allow the proven methodology of kinase inhibitor design to be applied to mycobacterial drug development.

Phosphorylation of the catalytic kinase domain is a common mechanism of STPK activation (Huse and Kuriyan 2002). Phosphorylation of a peptide known as the activation loop is required for kinase activity for all *Mtb* STPKs except PknG. The current model for *Mtb* STPK activation is depicted in Figure 1.2. Many of the STPKs contain a folded extracellular sensor domain, hypothesized to dimerize with another molecule upon ligand-binding.

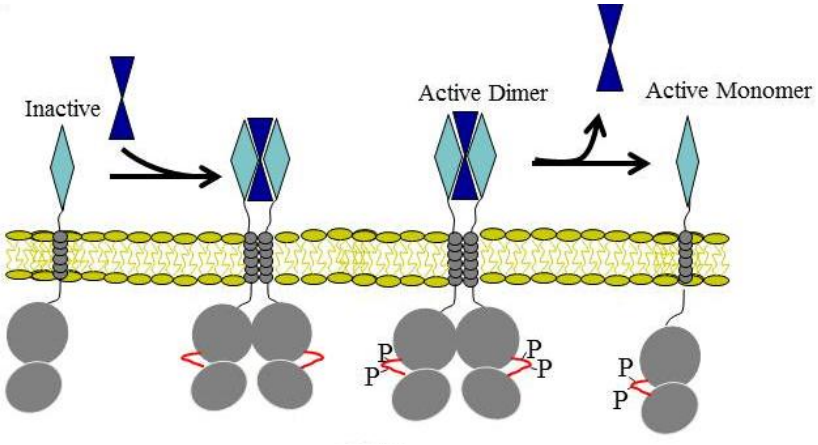

Figure 1.2 The ligand-induced dimerization model of kinase activation. Ligand binding to the inactive kinase leads to back-to-back dimerization. Allosteric activation through the dimer interface leads to activation-loop phosphorylation. Following release of the ligand, the active kinase monomer is now available to phosphorylate downstream substrate proteins.

Dimerization of the intracellular catalytic domains results in allosteric activation through the back-to-back interface (Greenstein, Echols et al. 2007). The crystal structures of the PknB and PknE kinase domains exhibit this characteristic back-to-back dimer (Figure 1.3a) (Young, Delagoutte et al. 2003; Gay, Ng et al. 2006). Biochemical investigations of the dimer interface revealed that this intermolecular interaction allosterically activates the PknB and PknD kinases

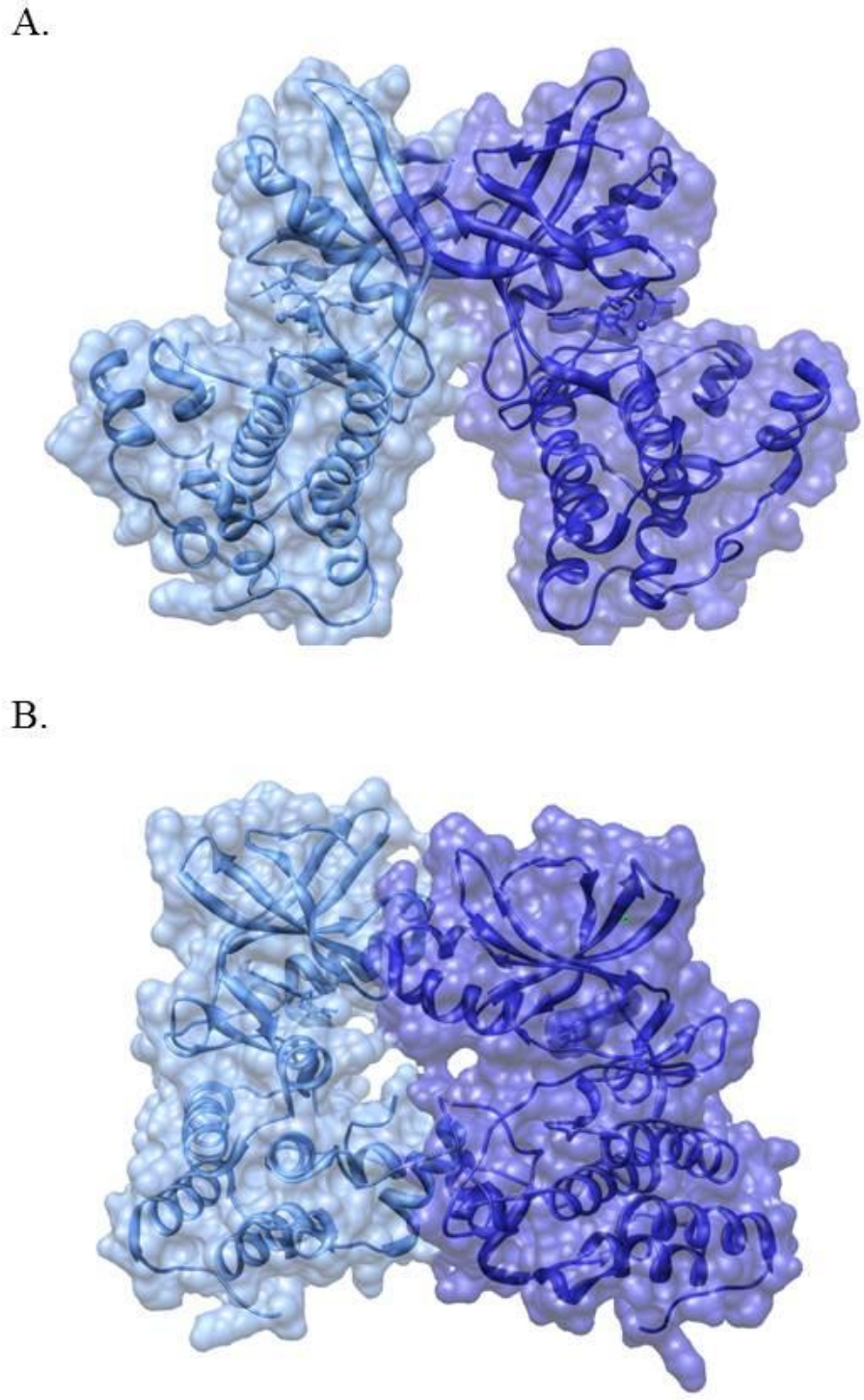

Figure 1.3 A) Active Mtb STPKs form a back-to-back dimer mediated through N-lobe contacts. Interactions through this dimer interface can activate the kinase allosterically. **B)** These proteins can also form a front-to-front dimer. Trans-phosphorylation is thought to occur through this interface.

(Greenstein, Echols et al. 2007). Additional crystal structures of PknB mutants demonstrated that the kinase domain can also form a front-to-front dimer (Figure 1.3b), likely activating the substrate kinase through direct phosphorylation on residues critical for activity (Mieczkowski, Iavarone et al. 2008).

The ligand-induced dimerization hypothesis models activation for the STPKs containing folded ECDs. However, several members of the *Mtb* kinome have extremely short ECDs or senor domains that are predicted to be unfolded. The activation mechanism for kinases that lack folded ECDs is unknown.

The "Master-Kinase Hypothesis" proposes that STPKS with folded ECDs, the master regulator kinases, are the upstream activators of kinases with shorter or unfolded ECDs, the substrate kinases. According to this hypothesis, ligand-induced dimerization would activate a master regulator STPK and subsequent phosphorylation of downstream substrate kinases would propagate signals through the appropriate intracellular response pathways.

The Master-Kinase Hypothesis supports a predictable and specific pattern of kinase interactions. To prevent signal confusion, each master regulator kinase must phosphorylate a specific subset of the downstream kinases. Probing this hypothesis is a critical part of investigating the activation pathways that occur throughout the STPK. Many *Mtb* STPK substrates apparently phosphorylated with different affinities by multiple kinases *in vitro* (Grundner, Gay et al. 2005; Greenstein, MacGurn et al. 2007; Gee, Papavinasasundaram et al. 2010). While the phosphorylation of substrate proteins by multiple STPKs has not been demonstrated to occur *in vivo*, the advantage to having multiple input signals for essential cellular processes in response to a variety of external environmental changes is clear. Delineating the activation mechanisms for the *Mtb* STPKs will produce a roadmap to the inter-kinase communication. This map will reveal any redundancy built into the *Mtb* Ser/Thr kinome and provide insights into the roles of each *Mtb* STPK in the complex intracellular signaling and response network.

Phosphorylation shifts STPK conformations by influencing the arrangements of key functional motifs. The crystal structures of the catalytic domains of PknB, PknE and PknG reveal that these three proteins share the classical Ser/Thr kinase fold common to eukaryotes and prokaryotes. The *Mtb* kinases have the two canonical domains: the N-lobe, consisting of β-sheets and a single regulatory α-helix, and the primarily α-helical C-lobe (Figure 1.4). Located in a deep cleft between these two domains is the ATP binding site. Important structural features include glycine-rich P-loop which folds over the ligand binding site, the Cα-helix, and the activation segment. The assembly of these structural motifs into the active conformation enables substrate recognition and phosphorylation.

The glycine-rich, phosphate binding loop contains the conserved sequence motif (GXGXyG) where y is usually a hydrophobic residue with a bulky side chain, such as tyrosine or phenylalanine (Huse and Kuriyan 2002). The glycine residues permit this 'P-loop' to approach the phosphates of ATP very closely and to coordinate these groups through backbone interactions. The sequence of this loop makes it flexible in the absence of ligand.

Figure 1.4 A) The structure of the PKA kinase domain (PDB code 1ATP) reveals features consistent with eukaryotic and prokaryotic kinases. The activation segment is highlighted in purple and the ATP ligand, highlighted in blue is located deep in the ligand binding cleft. **B)** Classical kinase features are visible in the PKA structure when rotated 90 degrees. The magnesium binding loop, the activation loop and the P+1 loop are all features of the activation segment. The P-loop forms essential contacts with the phosphate groups on the ATP molecule. Proper positioning of the Cα-helix is necessary for kinase activity.

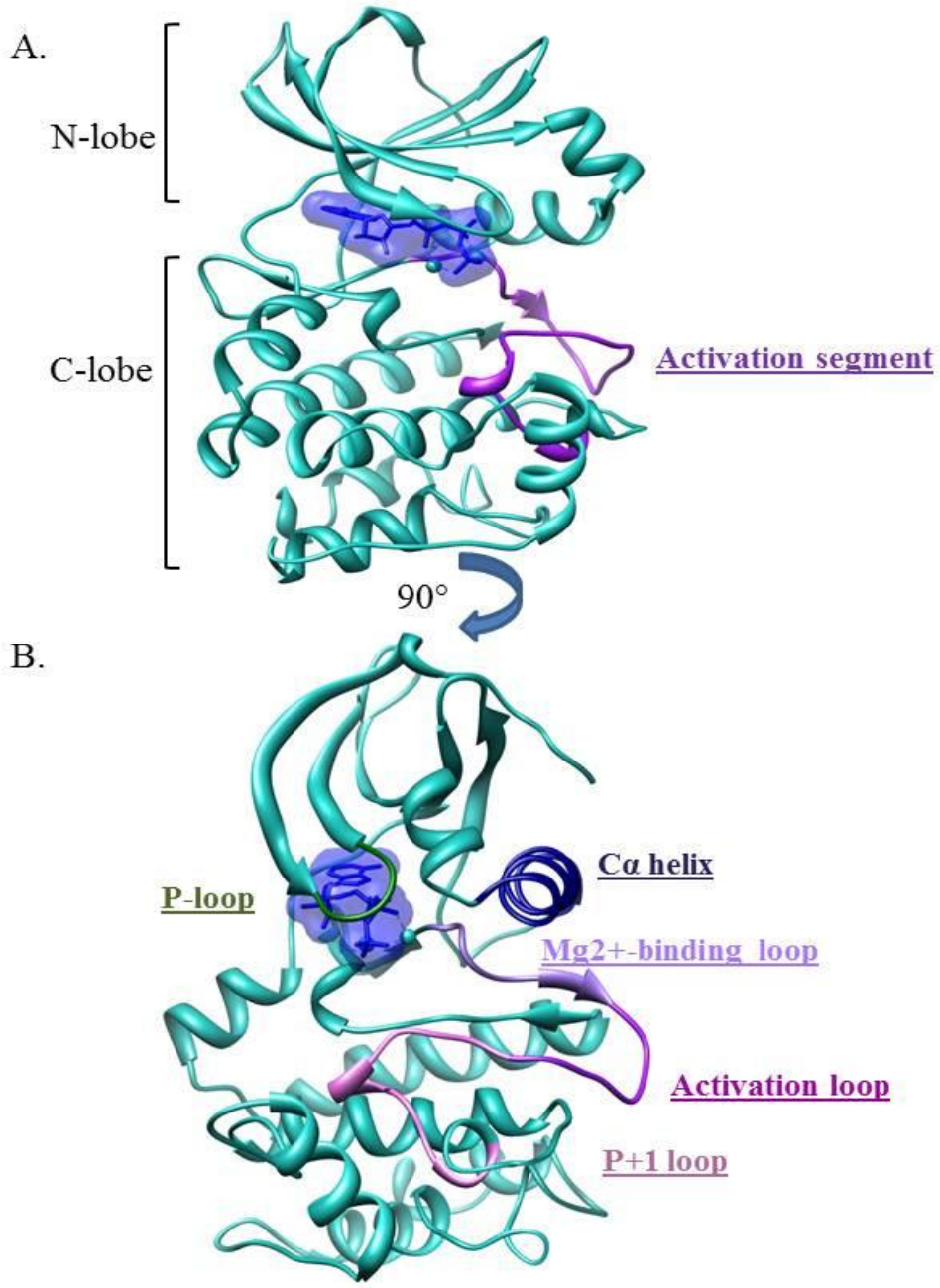

The C-terminal α-helix (Cα-helix) is a critical structural motif that can adopt dramatically different conformations depending on the kinase phosphorylation state. Significant movement coordinated through this helix can separate the N and C-lobes, opening the active site and allowing ATP binding in the active conformation of the kinase (Huse and Kuriyan 2002). An ion pair formed between a conserved Glu in this helix and a conserved Lys, which coordinates the α and β phosphates of ATP, is essential for kinase activity (Huse and Kuriyan 2002). The β- and γ-phosphates of ATP are coordinated by a complex network of H-bonding and ionic interactions with the metal ions, residues in the catalytic motif and amino acids in the loop located above the active site (Simard, Getlik et al. 2010).

Inactive kinases utilize different mechanisms to disrupt these interactions. Cyclin-dependent kinases (CDKs) become active upon binding the cognate cyclins (Huse and Kuriyan 2002). Without cyclin, the CDK Cα-helix rotates away from the active site, breaking the interaction between the conserved Glu and the Lys responsible for ATP coordination. The activating cyclin binds directly to this helix, resulting in an inward rotation that restores the atomic interactions necessary for ligand coordination and catalysis (Huse and Kuriyan 2002). Similarly, the Src family of kinases is regulated by SH2 and SH3 binding that stabilizes the Cα-helix in a conformation that prevents the Glu-Lys interaction (Xu, Doshi et al. 1999; Young, Gonfloni et al. 2001). In the active kinase conformation, the Cα-helix directly contacts the N-terminal side of the activation loop and the coordination of the catalytic loop Asp residue that is essential for activity. Kinase activation appears to be a coordinated event involving the coupling of activation loop phosphorylation and Cα-helix reorientation. The dynamic coupling of the Cα-helix and the activation loop phosphorylation allows information to pass between the active site and the allosteric regulatory sites at the back of the enzyme (Huse and Kuriyan 2002).

The activation segment generally contains 20 to 35 residues, beginning with the first of two tripeptide motifs, DFG, and ending with APE, the second motif (Nolen, Taylor et al. 2004). This DFG motif coordinates nucleotide-bound metal ions and senses the conformation of the Cα helix. This activation loop starts at the back of the ATP binding cleft, moves toward the lip of the cleft, wraps across the face of the C-lobe and twists in toward the hydrophobic core of the kinase in a classical active STPK structure (Figure 1.4) (Nolen, Taylor et al. 2004).

In the eukaryotic kinase PKA, phosphorylation of a Thr residue in the activation loop allows this residue to form an ion pair with a the conserved His in the Cα-helix (Madhusudan, Akamine et al. 2002). This interaction stabilizes the Cα-helix in the active conformation, enabling a network of interactions between the catalytic residues and the nucleotide phosphate donor. The phosphorylated activation loop also interacts with a conserved patch of basic residues on the C-lobe (Nolen, Taylor et al. 2004). STPKs regulated by activation loop phosphorylation have a conserved arginine immediately before the essential catalytic aspartate, this class of kinases in known as RD kinases in both eukaryotes and prokaryotes (Nolen, Taylor et al. 2004). The side-chain mediated interactions stabilize the activation loop and expose the substrate-binding surface.

Despite characteristic features, activation loops are quite diverse in sequence and structure in eukaryotic STPKs. This diversity is thought to contribute to substrate specificity. In the majority of active eukaryotic STPK structures, the activation loop is clearly ordered and, in many of these structures, forms part of a binding platform for a peptide substrate. However, the activation loop is not visible in the *Mtb* STPK structures despite phosphorylation of critical Thr residues. While the *Mtb* STPKs appear active based upon Cα-helix orientation and positioning of the catalytic residues, a full picture of the activated kinase has yet to emerge.

Eukaryotic kinases utilize a number of inhibitory mechanisms to prevent inadvertent activation. For example, the inactive form of the Src-family kinases is stabilized by a complex series of interactions initiated by the phosphorylation of a Tyr residue in the C-terminal region. Following the phosphorylation event, subsequent intramolecular binding of the phosphorylated peptide by the Src SH2 domain and the association of the SH3 domain with N-lobe of the kinase domain results in Src inhibition (Xu, Doshi et al. 1999; Young, Gonfloni et al. 2001). De-phosphorylation of the C-terminal tail disassembles this auto-inhibitory complex and permits activation through activation loop phosphorylation. Other kinases do not require inactivating cofactors, but instead are inhibited by remodeling of the activation loop. Like PKA and Src, insulin receptor kinase (IRK) is activated by phosphorylation. In the inactive form, the unphosphorylated activation loop sterically blocks ATP and substrate binding by folding into the active site. The loop is released following phosphorylation and refolds into a conformation that permits catalysis (Nolen, Taylor et al. 2004). The crystal structures of an *Mtb* STPK in the active and inactive forms would uncover biochemical and structural mechanisms that maintain the inactive conformation.

I undertook a two-fold biochemical and structure approach to investigate the mechanisms of *Mtb* STPK activation. A complete map of the cross-kinase interactions in the *Mtb* kinome is presented in Chapter 2. These data reveal that the *Mtb* STPKs can be classified into three functional groups: master regulator kinases, signal transduction kinases and substrate kinases. Investigation of these cross-kinase reactions revealed that both auto- and cross-phosphorylation reactions result in the addition of 1-3 phosphate groups on the substrate kinase, contrasting sharply with the hyperphosphorylated state observed following recombinant expression of the wild-type STPKs in *E.coli*. These specific interactions suggest additional mechanisms of kinase activation that expand the current model for STPK signaling in *Mtb*.

The functional role of cross-kinase phosphorylation is presented in Chapter 3. The transferred phosphates localize to the activation loop of the STPK and are critical for kinase activity. Cross-phosphorylation is a mechanism of *Mtb* STPK activation. Unlike many eukaryotic STPKs, phosphorylation has little impact on nucleotide binding and activation loop flexibility for the *Mtb* STPKs. These results suggest that the *Mtb* STPKs may maintain the catalytically inactive state through a unique mechanism.

Chapter 4 describes the first X-ray crystal structure of an unphosphorylated prokaryotic STPK, the master regulator kinase PknH. Multiple forms of this protein were crystallized enabling a comparison of the phosphorylated (active) and unphosphorylated (inactive) forms of the protein. Unphosphorylated PknH forms the characteristic back-to-back dimer observed in other *Mtb* STPK structures and is remarkably similar in conformation to the phosphorylated form. The PknH structures reveal that phosphorylation does not induce conformational remodeling in the *Mtb* master regulator STPKs.

X-ray crystal structures of PknK, a soluble *Mtb* STPK, are presented in Chapter 5. This monomeric protein was crystallized with zero, one, and two phosphates – each structure is a snapshot of the protein as it transitions from the off-state to the on-state. These crystal structures revealed that, like PknH, PknK does not undergo conformational remodeling following activation loop phosphorylation. Unlike many eukaryotic homologs, the unphosphorylated forms of PknH and PknK bind ATP analogs. The structures of PknH and PknK suggest that phosphorylation activates the *Mtb* STPKs by directly changing the properties of the activation loop. Based on these results, I propose the testable hypothesis that activation loop phosphorylation may regulate the *Mtb* STPKs by directly changing the affinities for protein

substrates or nucleotides. The absence of conformational remodeling upon activation loop phosphorylation implies that the prokaryotic and eukaryotic STPKs are regulated by different mechanisms.

Chapter 2

Mapping *Mtb* kinome cross-phosphorylation

Introduction

Autophosphorylation via inter- and intra-molecular interactions is the predominant activation mechanism for the *Mtb* kinases. With the exception of PknG, phosphorylation of the kinase domain is essential for *Mtb* STPK activity (Boitel, Ortiz-Lombardia et al. 2003; Molle, Girard-Blanc et al. 2003; Scherr, Honnappa et al. 2007). PknB phosphorylation has been confirmed *in vivo* by western blotting of cell lysates and this phosphorylation has been localized to the TQT motif found in the PknB activation loop (Kang, Abbott et al. 2005). Induced overexpression of PknD in *Mtb* in liquid culture led to the increased phosphorylation of cellular proteins, including PknD itself (Greenstein, MacGurn et al. 2007). Treatment with a PknD specific inhibitor, SP600125, led to decreased autophosphorylation of the kinase and trans-phosphorylation of substrate proteins, providing evidence that the *Mtb* kinases activate through autophosphorylation not only *in vitro*, but also *in vivo*. Treatment with the Ser/Thr phosphatase PstP abolishes activity of the STPK catalytic domains *in vitro* (Greenstein, Grundner et al. 2005)

Several studies have cataloged the number of phosphates on recombinant *Mtb* STPKs using mass spectrophotometry. These kinase domains appear to be phosphorylated in two distinct regions: the activation loop and the linker segment known as the juxtamembrane domain (Duran, Villarino et al. 2005). This pattern holds for PknB, PknD, PknE and PknF, all of the kinases investigated to date. The STPKs are heterogeneously phosphorylated with each protein displaying a distinct number of phosphates. PknD has as many as 14 phosphates, PknE has up to 13 phosphates and PknF has a maximum of 6 sites. Interestingly, the number of phosphates varies on each kinase and the additional phosphorylation sites in the intracellular domain outside the activation loop are not conserved. The varying location of phosphorylation sites on the kinase domains raises the question of the functional relevance of autophosphorylation. The link between activation loop phosphorylation and activity is clear; however, the role of juxtamembrane linker phosphorylation deserves further investigation.

In addition to autophosphorylation, PknA and PknB are reported to have cross-phosphorylation activity (Kang, Abbott et al. 2005). To eliminate the signal from autophosphorylation, catalytically inactive PknA and PknB mutants were constructed by changing the conserved Lys that coordinates ATP to Met. Phosphoryl transfer assays revealed that PknA trans-phosphorylates the inactive PknB kinase domain, but does not trans-autophosphorylate the catalytically dead PknA mutant. PknB phosphorylates both inactive mutants. The authors of this study interpreted these data to suggest the following preliminary model for kinase activation: PknA and PknB are co-localized within the cell, PknB is activated by the ligand binding to the extracellular domain (ECD), and, subsequently, active PknB activates PknA through trans-phosphorylation. Fully active PknA and PknB can then phosphorylate downstream substrates. This model is supported by the result that the *in vivo* kinase substrate Wag31 is weakly phosphorylated by PknA, not phosphorylated by PknB and is more significantly phosphorylated by a mixture of the two kinases, PknA and PknB.

In other organisms, STPK signaling cascades have been identified where a substrate kinase is activated through cross-phosphorylation by a different, autophosphorylated kinase. The activated substrate kinase then recognizes an intracellular substrate (Fiuza, Canova et al. 2008). *M. Xanthus* Pkn8, a membrane associated STPK, phosphorylates Pkn14, a cytoplasmic STPK, turning it on (Nariya and Inouye 2005). The activation of Pkn14 enables this protein to phosphorylate MrpC, a transcriptional regulator essential for development, on Thr residues. This signaling cascade provides the first experimental confirmation of a STPK-STPK activation cascade in prokaryotes. In addition, the result that a soluble STPK can be activated by a membrane-localized upstream STPK adds additional complexity to the proposed model for STPK activation. While the master kinase hypothesis concerns the activation of membrane-anchored STPKs without ECDs, the theory of ligand induced dimerization leading to autophosphorylation followed by cross-kinase activation through trans-phosphorylation can be extended to include the two cytoplasmic *Mtb* kinases, PknG and PknK. Based solely on the prediction that the receptor kinases with folded extracellular domains initiate signaling, the *Mtb* kinases could exhibit numerous cross-phosphorylation events. This hypothesis is readily testable *in vitro*.

The 11 *Mtb* STPKs contain a conserved catalytic domain. Each of the nine putative membrane-bound kinases is anchored by a single predicted trans-membrane helix connected to the C-terminus of the catalytic domain by a flexible linker, ranging from 30 to 125 amino acid residues in length. Kinase constructs consisting of the entire intracellular region or the kinase domain show comparable activities on the noncognate model substrate, myelin basic protein (MBP) (Duran, Villarino et al. 2005).

To comprehensively map kinase cross-phosphorylation *in vitro*, I assayed the 11 active *Mtb* STPKs for activity on the catalytically dead mutants of the same 11 kinases. Many of the positive phosphorylation reactions were confirmed by liquid-chromatography mass spectrophotometry to measure presence of phosphate groups. To gauge the consequences of phosphorylation, I mapped the modified sites in several kinase domains using mass spectrometry. Most *Mtb* kinases undergo autophosphorylation of the activation loop. Unexpectedly, the inactive substrate kinases were phosphorylated on a maximum of two sites, in sharp contrast to the autophosphorylation of additional sites observed in the active kinase domains. These studies define potential phospho-regulatory networks in a complete bacterial kinome.

Results

The catalytic activity of the kinase-domain constructs of the *Mtb* STPKs has been demonstrated previously for several of these proteins (Duran, Villarino et al. 2005). To assay for cross-phosphorylation, it is necessary to design not only active wild-type kinase constructs, but also to clone the inactive mutants to act as substrates. The full-length sequences of the STPKs in the *Mtb* H37Rv genome were analyzed using the hydrophobicity prediction servers, TMHMM and PredictProtein (Rost 2004) to locate the TM helix. Kinase-domain constructs were designed based on sequence alignments and secondary structure prediction using the PHYRE homology server (Kelley 2009). Various lengths of the kinases were cloned and expression was tested to optimize yield. Constructs were kept as close as possible to 280 amino acids, the predicted size of the catalytic kinase domain, while maximizing solubility. Table 2.1 lists the constructs utilized

in this chapter. Whenever possible, previously existing constructs were used, creating some variability in the expression plasmids.

The inactive kinases were generated using site-directed mutagenesis to change to Asn the catalytic Asp in the HRD motif (Greenstein, MacGurn et al. 2007). This mutation is more conservative than the Lys to Met mutation utilized in the initial report of cross-kinase phosphorylation and it has been previously demonstrated to abolish kinase activity (Kang, Abbott et al. 2005; Mieczkowski, Iavarone et al. 2008).

Proteins were expressed using auto-induction (Studier 2005). Wild-type PknA and PknB have reported cell toxicity when expressed in *E.coli*. Auto-induction prevents leaky T7-polymerase-driven expression and alleviates complications due to toxicity of the *Mtb* STPKs. All STPKs were purified using standard immobilized metal ion chromatography (IMAC) and size-exclusion chromatography (SEC) protocols. To enable separation of the wild-type and inactive kinases, the active kinases were tagged with 6xHis-MBP tag. The inactive kinases were expressed with this 6xHis-MBP tag and the tag was cleaved with the tobacco etch virus (TEV) protease. The tagged STPKs and the untagged inactive kinase domains differ in molecular weight by ~40 kDa.

Table 2.1

Protein	Length	Mutation	Tag	Tag cleavage site	Expression vector
PknA	1-279		HMBP	TEV	pHMGWA
PknA	1-279	D141N	His	Thrombin	pET28b
PknA	1-336		HMBP	TEV	pHMGWA
PknA	1-336	D141N	HMBP	TEV	pHMGWA
PknB	1-291		HMBP	TEV	pLIC2MT
PknB	1-279	D138N	His	Thrombin	pET28b
PknB	1-330		HMBP	TEV	pLIC2MT
PknB	1-330	D138N	HMBP	TEV	pLIC2MT
PknD	1-292		HMBP	TEV	pHMGWA
PknD	1-292	D138N	HMBP	TEV	pHMGWA
PknE	1-279		HMBP	TEV	pHMGWA
PknE	1-279	D139N	HMBP	TEV	pHMGWA
PknF	1-280		HMBP	TEV	pHMGWA
PknF	1-280	D137N	HMBP	TEV	pHMGWA
PknG	1-750		His	none	AmpR
PknG	1-750	D143N	His	none	AmpR
PknH	1-280		HMBP	TEV	pHMGWA
PknH	1-280	D139N	HMBP	TEV	pHMGWA
PknI	1-585		HMBP	TEV	pHMGWA
PknI	1-585	D137N	HMBP	TEV	pHMGWA
PknJ	1-286		HMBP	TEV	pHMGWA
PknJ	1-286	D125N	HMBP	TEV	pHMGWA
PknK	1-290		HMBP	TEV	pLIC2MT
PknK	1-290	D149N	HMBP	TEV	pLIC2MT
PknL	1-302		HMBP	TEV	pLIC2MT
PknL	1-302	D142N	HMBP	TEV	pLIC2MT
PknL	1-366		HMBP	TEV	pLIC2MT
PknL	1-366	D142N	HMBP	TEV	pLIC2MT

Catalytic activity of the wild-type kinases was confirmed using a radioactive phosphoryl transfer assay. A 10-fold molar excess of the FHA-domain containing protein GarA was

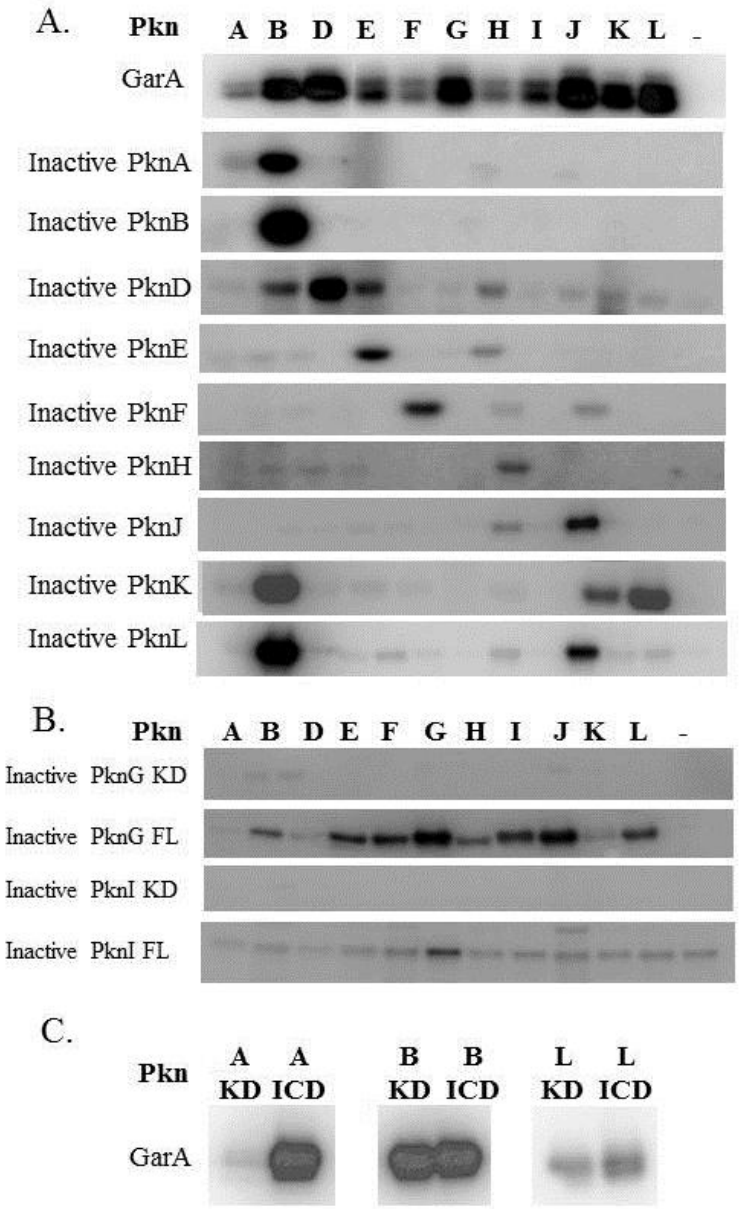

Figure 2.1 A) Autoradiographs of γ^{32}P phosphotransfer assays demonstrate that all kinase constructs are active on the FHA domain containing protein GarA. *In vitro* reactions reveal kinase-kinase interactions. Each lane contains a different active kinase, labeled horizontally across the top incubated with the analogous inactive kinase construct. **B)** The kinase domains of PknG and PknI are not phosphorylated by any of the other kinases. Full-length PknG and PknI are trans-phosphorylated. **C)** The kinase domains and full-length intracellular domains of PknA, PknB and PknL were incubated with GarA in γ^{32}P phosphotransfer assays to detect the relative activity of each enzyme.

incubated with each active STPK in the presence of 50 μM $MnCl_2$, 1 μCi γP32-ATP, and 50 μM ATP. The reactions were incubated for 30 minutes at room temperature and separated by SDS-PAGE. All kinases are active on GarA (Figure 2.1). This substrate protein contains a phosphor-threonine recognition motif, an FHA domain that is known to be targeted by the STPKs (Grundner, Gay et al. 2005; England, Wehenkel et al. 2009; Nott, Kelly et al. 2009). To date, GarA is the only protein known to be a substrate for all members of the *Mtb* Ser/Thr kinome. Previously the *Mtb* STPKs have been assayed for activity using the model substrate MBP, but not all of the *Mtb* kinases are active on this protein.

The same reaction protocol was utilized to test the 11 wild-type kinases against the 11 inactive mutants. For PknB, PknD, PknE, PknF, PknH, PknJ, PknK and PknL, the approximately 280-amino-acid catalytic domain is sufficient for kinase activity. The PknA 1-330 construct is substantially more active than the PknA kinase domain alone. The additional C-terminal 40 amino acid residues in the long construct may be necessary for substrate recognition or provide phosphorylation sites.

To investigate whether the presence of the juxtamembrane linker increased the activity of PknB and PknL, the two kinases closely related to PknA, full-length ICD kinase constructs were compared to the original kinase-domain proteins. PknA (Thakur, Chaba et al. 2008) and PknL activity are increased by including residues in the juxtamembrane linker (Figure 2.1). The full-length ICD PknA, PknB and PknL constructs were tested against all of the inactive substrate kinases to determine whether kinase length alters substrate specificity. These results are included in the final table of kinase-kinase interactions (Figure 2.3).

The PknG and PknI kinase domains alone are not active, so varying lengths of these proteins were tested for the ability to phosphorylate GarA. For PknG, the full-length protein is the most active form of the kinase. This result is unsurprising as PknG lacks Ser and Thr residues in the activation loop and is the only *Mtb* STPK that appears to have no phosphorylated residues in the catalytic domain (O'Hare, Duran et al. 2008). PknG contains an unknown number of phosphorylation sites in its C-terminal domain that may be necessary for activity (Cowley, Ko et al. 2004; Scherr, Honnappa et al. 2007). Given these results, I probed for cross-phosphorylation of PknG using both the inactive kinase domain and the full-length inactive mutant.

The PknI kinase domain and predicted ICD constructs are persistently inactive (Prisic, Dankwa et al. 2010). Despite presence of a predicted transmembrane helix (Figure 2.2), full-length PknI has been identified in the cytosol (Singh, Singh et al. 2006). This study also reported the PknI kinase domain to be active, a result that I could not reproduce (Gopalaswamy, Narayanan et al. 2004). Nonetheless, I found that full-length PknI is active on GarA and unexpectedly soluble in aqueous buffer. Full-length PknI is the only active form of this kinase produced for this study.

The PknJ and PknL kinase domains manifested persistent problems with solubility when expressed as recombinant protein. The hydrophobicity plot of PknJ reveals an unexpected membrane topology for this kinase with two predicted transmembrane helices (Figure 2.2). The location of a single TM helix in was defined experimentally, however, using PhoA and GFP fusions to different length constructs of PknJ (Jang, Stella et al. 2010). These results revealed that the single TM helix in this protein includes amino acids 334-363, leaving an extra cellular domain of 260 amino acids with no homology to a known fold. Kinase domain constructs of PknJ were purified following changes to the purification scheme as described in the methods, but the yield of this protein is lower than that of the other kinases.

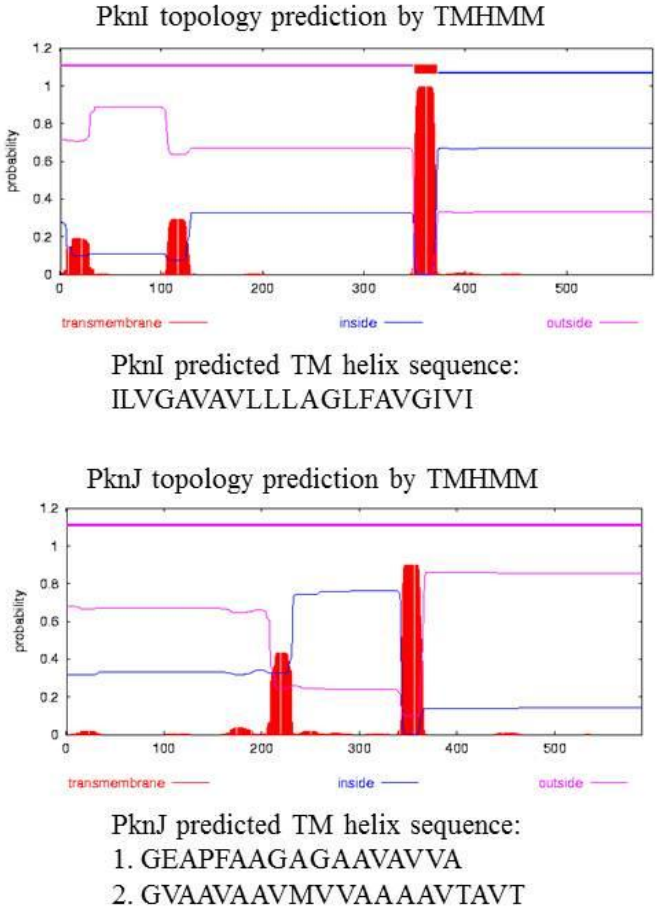

Figure 2.2 Hydrophobicity plots of PknI and PknJ show the predicted transmembrane helices for each kinase. The sequences of each predicted helix are listed below the plot.

The PknL kinase domain constructs are aggregated when expressed with a 6xHis-MBP tag. The inactive PknL kinase domain with a minimal 6xHis tag expresses in inclusion bodies. Solubilization with urea and refolding yielded a minimal amount of protein. This protocol was determined to be less than optimal for biochemistry due to unanswered questions about the proper refolding of the kinase domain. After testing multiple constructs, the kinase domain plus ~20 amino acids (amino acids 1-302) was the shortest stable form of this protein. This construct is soluble and stable for both wild-type and catalytically inactive PknL.

To identify cross-phosphorylation reactions with regulatory implications, I assayed both the inactive kinase domains and the full-length versions of these proteins. The full-length PknG and PknI proteins are very close in size to the other tagged wild-type kinases. As the wild-type kinases measurably autophosphorylate in these assays, it was necessary to remove the tags from the wild-type kinase when testing PknG and PknI as substrates. Each reaction was quenched with the addition of EDTA to chelate the divalent metal ions necessary for kinase activity. The 6xHis-MBP tags were then removed with TEV protease and the reactions were separated by SDS-PAGE. All reactions were repeated in triplicate for each kinase substrate (Figure 2.1).

This approach yielded a complete map of intermolecular kinase phosphorylation in the *Mtb* kinome (Figure 2.3). With the exception of PknL, the *Mtb* kinase domains show intermolecular autophosphorylation activity (diagonal, Figure 2.3). PknL does not autophosphorylate, but it is cross-phosphorylated by PknB and PknJ. Intermolecular autophosphorylation by PknA requires the full-length intracellular domain (ICD).

These data demonstrate that the master-kinase hypothesis does not accurately predict kinase-kinase phosphorylation. Notably, multiple kinases with folded extracellular domains (ECD)s are phosphorylated by other kinases that also have folded sensory domains. For example, PknD is phosphorylated by PknB, but does not cross-phosphorylate the other kinases.

To determine the extent of phosphorylation and to map the modified sites, I characterized several of the positive trans-phosphorylation reactions by liquid-chromatography mass spectrophotometry (LC-MS). Phosphorylated species were readily identifiable in the resulting mass spectra as peaks equivalent to the molecular weight of the unphosphorylated protein plus multiples of 80 daltons. The addition of phosphates to the substrate kinase appears to be very specific for each reaction. For example, the substrate kinases PknD and PknK were phosphorylated on 0-3 sites by PknB, PknD, PknJ or PknK (Figure 2.4).

The locations of phosphates were mapped on the substrate kinase PknD. The inactive PknD was phosphorylated overnight using PknB or PknD with an excess of ATP and $MnCl_2$. Kinase assays were separated by SDS-PAGE, digested with trypsin, modified with amino-ethanethiol and subjected to LC-MS/MS (Mieczkowski, Iavarone et al. 2008). This modification enables detection of phospho-peptides by a more sensitive method than searching the spectra for neutral loss corresponding to a phosphate group and allows the identification of multiply phosphorylated species. Completion of the phosphorylation reaction was probed using the phospho-reactive, Pro-Q Diamond Stain (data not shown).

Analysis of the resulting mass spectra revealed the presence of one major phosphopeptide that corresponds to the activation loop of PknD. Four threonines are located on the PknD activation loop. To identify the phosphorylation sites, the individual threonines were mutated to alanine. Each of these mutants was constructed in the inactive kinase background, making them suitable for assaying trans-autophosphorylation and trans-phosphoryalation. The activity of PknB and PknD were tested on each mutant protein using the γ^{32}P ATP assay. The intact masses of the phosphorylated mutants also were measured using LC-MS following phosphorylation with excess ATP and $MnCl_2$. The MS measurements demonstrated that the first two Thr residues in the PknD activation loop, Thr169 and Thr171, are the targets of both PknB and PknD. Alanine substitutions of Thr173 and Thr179 do not have a major impact on phosphorylation, indicating that these residues are not the main targets in the reactions.

Figure 2.3 A) Intermolecular kinase-domain interactions are denoted with an X. The active kinases are listed horizontally; the inactive kinase substrates are listed vertically. **B)** Cross-kinase phosphorylation including the PknA, PknB and PknL intracellular domain constructs.

A. Kinase-kinase interactions reported for kinase-domain constructs

	A	B	D	E	F	G	H	I	J	K	L
A		X									
B		X									
D		X	X	X							
E				X			X				
F					X		X		X		
G											
H							X				
I											
J							X		X		
K		X							X	X	
L		X							X		

B. Final kinase-kinase interaction chart

	A	B	D	E	F	G	H	I	J	K	L
A	X	X									X
B		X									
D		X	X	X							
E				X			X				
F					X		X		X		
G		X		X	X	X	X	X	X		X
H							X				
I						X		X			
J							X		X		X
K		X							X	X	
L		X							X		

Figure 2.4 A) LC-MS measurements of kinase activity on the inactive PknD substrate revealed that PknB and PknD transfer different numbers of phosphates on the PknD kinase domain. LC-MS traces for each reaction are displayed below the chart. **B)** LC-MS measurement of PknK kinase-kinase interactions also revealed differences in the number of phosphate groups transferred to the substrate depending on the identity of the active kinase in the reaction.

A.

Kinase	None	PknB	PknD
Phosphates detected on inactive PknD	0	0, 1, 2	1, 2
Phosphates detected on active PknD			7, 8

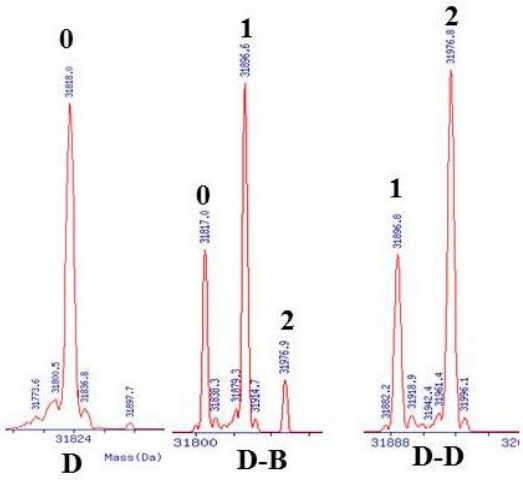

B.

Kinase	None	PknB	PknJ	PknK
Phosphates detected on inactive PknK	0	1	0, 1	2, 3

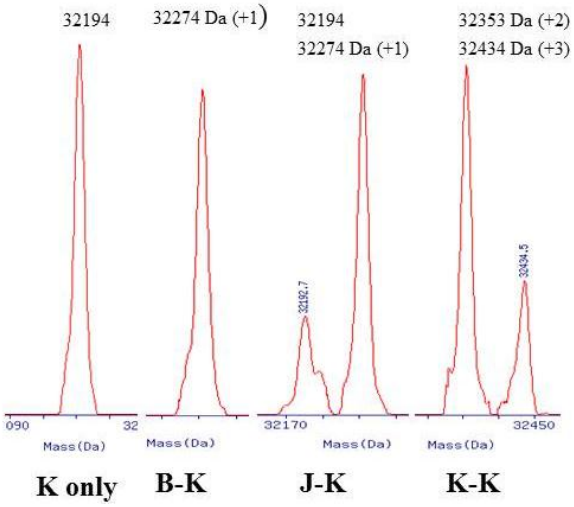

Discussion

The *Mtb* receptor kinases are generally regulated by phosphorylation of the activation loop (Boitel, Ortiz-Lombardia et al. 2003; Molle, Zanella-Cleon et al. 2006). Studies of PknD (Greenstein, Echols et al. 2007) and PknB (Lombana 2010) show that this process is initiated by intermolecular phosphorylation reactions. Consequently, to define the networks of STPK signaling in *Mtb*, I established the pattern of efficient intermolecular phosphorylation *in vitro*. This approach has been used to identify potential signaling partners of eukaryotic kinases, especially in pathways that lack scaffolding proteins that restrict kinase specificity (Canman, Lim et al. 1998). For histidine kinases in *Caulobacter crescentis*, the pattern of efficient *in vitro* phosphorylation of response regulators parallels the physiological activation pathways *in vivo* (Skerker, Prasol et al. 2005). These precedents suggest that a comprehensive, system-level profile of STPK phosphorylation can reveal candidate signaling networks based on kinase specificity. Of particular interest was to test the idea that receptor kinases with folded extracellular domains act as master kinases, initiating signals that are transduced to substrate STPKs that lack putative sensor domains.

The first step in this comprehensive analysis was to produce active kinase constructs. By adjusting the expressed protein boundaries, I obtained soluble constructs of the 11 *Mtb* STPKs that phosphorylate the substrate protein GarA (Figure 2.1). To date, GarA is the only protein known to be a substrate for all members of the *Mtb* Ser/Thr kinome.

Using these active kinase constructs to phosphorylate inactive mutants, I defined the complete pattern of intermolecular phosphorylation for the *Mtb* STPKs. The results show three striking features. First, autophosphorylation is the dominant phosphorylation event. All the STPKs except PknL phosphorylate otherwise identical inactive variants with a mutation in the critical active-site aspartate. For PknB, PknD and PknE, this autophosphorylation modifies the activation loop, stabilizing the active form of the kinase.

Second, PknB and PknH only undergo autophosphorylation. These are the predicted master kinases in the network. As expected for kinases that sit atop the signaling hierarchy, they both contain predicted folded extracellular sensor domains (ECDs), and other kinases do not phosphorylate them *in vitro*. Contrary to the master-kinase hypothesis, however, the presence of a folded sensor domain does not guarantee that an STPK acts as a master kinase. PknD, for example, contains a beta-propeller in the ECD, but it is phosphorylated efficiently by two other kinases. The observed pattern of cross phosphorylation may allow signals to propagate to specific STPKs that regulate distinct sets of downstream cellular proteins.

Third, an unanticipated feature of my results is that the initial intermolecular phosphorylation modifies only 1-3 sites on the substrate kinases. In the two cases I characterized, PknD and PknK, these initial phosphorylation events target the activation loop of the substrate kinase domain. This limited phosphorylation focused on the regulator machinery of the substrate kinase contrasts sharply with the phosphorylation of up to 14 sites on expressed active kinases (Molle, Zanella-Cleon et al. 2006). In addition, I find that different active STPKs phosphorylate a given substrate kinase with different efficiency. These results suggest that different signals may initially produce distinct phosphorylation states of the kinome with different relative activities of the STPKs.

The pattern of kinase phosphorylation *in vitro* is consistent with the limited information available about STPK phosphorylation in mycobacteria (Figure 2.3). In *Msmeg*, PknA and PknB autophosphorylate and PknB phosphorylates the inactive mutants of PknA (Kang, Abbott et al.

2005). In addition, PknD overexpression in *Mtb* promotes PknD phosphorylation, and this apparent autophosphorylation reaction is inhibited by a PknD-specific kinase inhibitor. The systematic interactions seen *in vitro* (Figure 2.3) afford additional candidate functional interactions *in vivo*.

In addition to the master regulatory kinases PknB and PknH, the *Mtb* kinome phosphorylation map also reveals signal propagation kinases that are activated by auto- and trans-phosphorylation, and are capable of propagating the phospho-signal to downstream kinases. PknE, PknJ and PknL are intermediary signaling kinases.

Substrate kinases autophosphorylate and are phosphorylated by multiple master regulator kinases, but do not cross-phosphorylate other STPKs. PknA, PknD, PknF and PknK are substrate kinases. PknG is an exception to this emerging pattern of phospho-signaling relays because the kinase domain is not phosphorylated for activation and the role of phosphorylation on the C- and N-terminal domains is unknown.

PknB, one of the two essential STPKs in *Mtb*, is known to play a significant role in cell division, cell morphology and stress response to environmental changes. This kinase contains a folded extracellular domain that is hypothesized to bind cell-wall fragments as a signaling and response mechanism (Barthe, Mukamolova et al. 2010). In addition to autophosphorylation, PknB trans-phosphorylates multiple members of the STPK family: PknA, PknD, PknJ and PknL. These interactions were not predictable based on sequence similarity as PknA and PknL cluster into a clade with PknB, but PknD and PknJ do not. PknD and PknJ both have extensive ECDs. The result that these predicted sensor receptor kinases can be phosphorylated by another sensor kinase was unexpected. These interactions provide evidence that the presence of a folded ECD alone is not predictive of the role played by an individual protein in STPK signaling pathways.

The second master regulator kinase, PknH, contains a folded ECD and phosphorylates multiple kinases. The PknH extracellular domain has homology to some lipid binding proteins, but the structure remains unsolved and the ligand for this domain is unknown. By sequence similarity, PknH groups with PknE and PknD. PknH phosphorylates PknE, but not PknD, and two members of a different clade: PknF and PknJ.

PknE, PknJ, and PknL form a unique class of intermediary signal transduction kinases that are phosphorylated by the upstream master kinase regulators, but are also able to phosphorylate downstream substrate kinases. PknE autophosphorylates and is phosphorylated by PknH. This kinase is able to phosphorylate PknD. The PknE-PknD interaction is specific, as PknE does not phosphorylate any other *Mtb* STPKs. The PknE kinase domain is also able to allosterically activate the PknD kinase domain through a back-to-back dimerization interface (A. Greenstein, unpublished results). This result, in combination with the trans-phosphorylation map, suggests that the PknE-PknD interaction may activate the substrate kinase in response to unique set of cellular conditions.

PknJ contains 260 amino acids C-terminal of the predicted TM helix location. The PknJ kinase domain is phosphorylated in *trans* by PknH and PknL. This kinase phosphorylates the substrate kinases PknF and PknK. PknJ both phosphorylates and is phosphorylated by PknL. This interaction may function as part of a phospho-signaling regulatory circuit, the functional implications of these interactions are worthy of further investigation.

The third member of the signal propagation class of *Mtb* STPKs is PknL. The PknL ECD contains only 6 amino acids, suggesting that a mechanism other than ligand-induced dimerization is necessary to activate this STPK. Indeed, PknL is phosphorylated by PknB and by PknJ. Once activated, PknL phosphorylates PknA and PknJ.

The kinases PknA, PknD, PknF and PknK are clear downstream substrate STPKs that lack the ability to transfer phosphates to any other catalytic kinase domains. All of these proteins phosphorylate additional substrate proteins such as GarA (Chao, Wong et al. 2010). PknD and PknF contain extensive ECDs suggesting that these proteins sense an environmental ligand, but are also involved in cellular responses to ligands that activate other upstream activator STPKs.

The soluble kinase PknG is transphosphorylated by multiple STPKs. As the kinase domain of this protein is not phosphorylated, the phosphorylation sites on the full-length protein are likely located in the N- and C-terminal domains. Phosphorylation of these sections of the protein has been previously reported (Cowley, Ko et al. 2004; Scherr, Honnappa et al. 2007; O'Hare, Duran et al. 2008). Because the functional role of phosphorylation on PknG is not understood, these instances of kinase-kinase phosphorylation are considered kinase-substrate interactions, rather than a continuation of the kinase-kinase activation network.

Phosphorylation on the kinase domain is known to be essential for kinase activity for the *Mtb* STPKS (Greenstein, Grundner et al. 2005). Multiple phosphorylation sites have been identified on the catalytic domain (Molle, Zanella-Cleon et al. 2006). Is kinase cross-phosphorylation an activating mechanism or inhibitory? How many phosphates are transferred in each reaction? Does the number and location of these phosphoryl groups vary depending on the identity of the phosphorylating enzyme? To address these questions, we defined the sites in PknD and PknK phosphorylated by multiple STPKs. Differing numbers of phosphates were detected on the substrate proteins.

PknB and PknD phosphorylate the inactive PknD substrate on 1-2 sites in the activation loop (Figure 2.4). In contrast, PknD autophosphorylates during protein expression at up to 14 sites depending on the length of the construct (Molle, Zanella-Cleon et al. 2006). Two populations of auto-phosphorylated PknD were detected with the kinase-domain construct used in these biochemical experiments, seven or eight phosphates respectively. In striking contrast, PknB phosphorylates inactive PknD at zero, one, or two sites. PknD adds one or two phosphates to the activation loop of inactive PknD.

The identification of PknK as a substrate kinase that is phosphorylated by multiple membrane-bound STPKs is surprising given that this protein is localized to the cytosol. PknB and PknJ transferred a specific number of phosphates to the inactive PknK substrate. PknB and PknJ phosphorylate a single residue on the PknK kinase domain; PknK autophosphorylation involves the addition of two to three phosphates. These data parallel the PknD results with the addition of a limited number of phosphates on the substrate kinase. The location of these transferred phosphates on the catalytic domain of each kinase would provide some insight into the regulatory role of cross-kinase phosphorylation.

Phosphorylation sites for both auto- and trans-phosphorylation are located on the activation loop of PknD (data not shown). The location of the phosphorylation sites was confirmed by changing each of the four threonines in the PknD activation loop to alanine. The first two threonines in the PknD activation loop are the main phosphorylation sites targeted by both PknB and PknD. Phosphorylation on the activation loop suggests that cross-phosphorylation activates the targets.

These results provide new perspectives on the process of STPK activation (Figure 2.5). Activation requires the formation of a “back-to-back” dimer through N-lobe contacts observed in the crystal structures of PknB and PknE. Dimerization triggers an allosteric conformational change that promotes intermolecular STPK phosphorylation (Greenstein, Echols et al. 2007). Ligands that stabilize the back-to-back dimer thus indirectly promote activation loop

phosphorylation events that produce active STPKs able to modify downstream cellular substrates.

Figure 2.5 The kinase-kinase interaction map suggests two mechanisms for the activation of transmembrane kinases. Back to back dimerization can result in activation through autophosphorylation. Front-to-front inter-kinase interactions are another potential mechanism of activation. Soluble kinases are autophosphorylated and are trans-phosphorylated by transmembrane kinases.

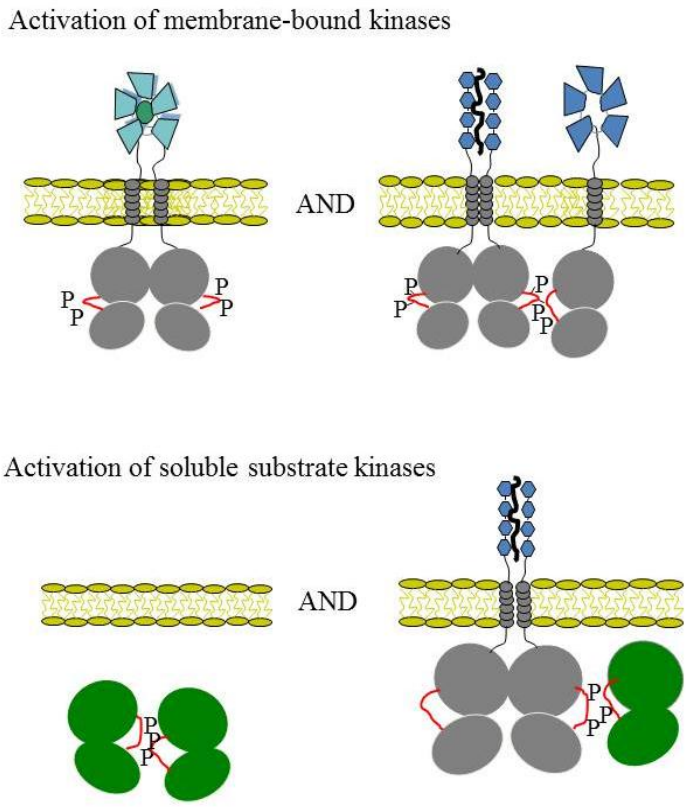

Here I identified the specific STPK targets of this initial intermolecular phosphorylation. As expected, autophosphorylation of the activation loop is the dominant mode of regulation. I also observe a specific pattern of STPK cross-phosphorylation. This map of STPK cross-talk recapitulates functional interactions between PknA and PknB and affords new hypotheses for the spread of signals through the *Mtb* kinome.

As anticipated for functional phosphorylations, the *in vitro* cross-phosphorylation reactions showed similar efficiencies as the autophosphorylation reactions of the STPK. Moreover, for the cross-phosphorylation reactions of PknD and PknK, we mapped the modifications to key regulatory Thr residues in the activation loop. Thus, the efficiency and specificity of the phosphorylations meet critical requirements of functional modifications.

I also found that the initial intermolecular phosphorylation modifies only 1-3 sites on the target inactive kinase, in comparison to up to 14 phosphorylation sites detected on active STPK intracellular domains. This discrepancy suggests that a combination of inter- and intramolecular phosphorylation events produces the hyperphosphorylated recombinant kinase domains detected previously (Molle, Zanella-Cleon et al. 2006). The initial, efficient phosphorylation of the

activation loop of PknD and PknK casts doubt on the functional relevance of the phosphorylation of other sites. Phosphorylation of the solution kinase PknK by the receptor kinases provides evidence for an additional unanticipated aspect of STPK activation. Previously, autophosphorylation was the only recognized activation mechanism for PknK. The cross-phosphorylation map reveals protein-protein signaling interactions between transmembrane and soluble STPKs. In general, however, the soluble STPKs do not phosphorylate the transmembrane receptor STPKs.

The studies presented in this chapter demonstrate the wide-spread nature of kinase-kinase phosphorylation across the entire *Mtb* STPK family. The distinct pattern of these kinase interactions carries broad implications for intracellular signaling and coordinated response to extracellular environmental changes. The transfer of 1-2 phosphates to critical residues in the PknD activation loop may be indicative of a general mechanism for kinase activation. The functional relevance of this initial phosphorylation event will be addressed in the following chapter.

Methods

Construct design and cloning

DNA sequences from the Tuberculist webserver (http://genolist.pasteur.fr/TubercuList/) analyzed for predicted trans-membrane helices with the TMHMM (http://www.cbs.dtu.dk/services/TMHMM/) and PredictProtein webservers (Rost 2004). The boundaries of the catalytic kinase domains for each gene were determined using the PHYRE homology prediction server (Kelley 2009). N-terminal intracellular domain of each kinase domain was truncated to the predicted catalytic domain based on the PHYRE results. *Mycobacterium tuberculosis* H37Rv genomic DNA from the Mycobacteria Research Laboratories at Colorado State University is the cloning template for all genes utilized in this study. Kinase domains were cloned into the Gateway vector pHMGWA which includes N-terminal 6X-His and maltose binding protein (MBP) tags, followed by a tobacco etch virus protease site (Busso, Delagoutte-Busso et al. 2005). The PknA and PknB kinase domains were cloned into the pET28b expression vector (Novagen) by Carl Mieczkowski and Noelle Lombana respectively. The full-length PknG expression clone was obtained from Carl Mieczkowski. The final PknB, PknK and PknL expression constructs were made by the QB3 Macrolab facility using ligation independent cloning. Each of these constructs includes the N-terminal 6XHis-MBP tag followed by a TEV protease site.

Multiple sequence alignment of the kinase domains using ClustalW allowed identification of the catalytic Asp residue that I mutated in each protein to create the inactive mutant (Chenna, Sugawara et al. 2003). Each Asp-to-Asn mutant was constructed using 2-primer site-directed mutagenesis. For constructs in the Gateway vectors, mutagenesis PCR was performed with Herculase II fusion polymerase (Stratagene) and DMSO. For constructs in the pLIC2MT vector (QB3 MacroLab), successful mutagenesis required PCR with the Pfu Ultra II fusion polymerase (Stratagene).

Protein expression and purification

Proteins were expressed in *E. coli* BL21 CodonPlus (Stratagene) using auto-induction. Cultures were grown at 37°C for 8 hours and shifted to 18-22 °C for 18-24 hours. The pellets were harvested by centrifugation and stored at -80 °C. For purification, each pellet was resuspended in Ni-IMAC A buffer (300 mM NaCl, 25 mM HEPES pH 8.0, 25 mM Imidazole, 0.5 mM TCEP, and 10% glycerol with 250 µM AEBSF protease inhibitor). The cells were lysed by sonication and the resulting suspension clarified with centrifugation. The soluble portion was run on a 10ml nickel equilibrated HiTrap chelating Sepharose column and each column was washed extensively with Ni-IMAC A buffer prior to elution. Ni-IMAC B buffer (300 mM NaCl, 25 mM HEPES pH 8.0, 25 mM Imidazole, 0.5 mM TCEP, and 10% glycerol) eluted the 6X His tagged proteins from the Ni IMAC resin. Wild-type kinases were further purified using size-exclusion chromatography (SEC) with a HiLoad 26/60 Superdex S75 column run in SEC buffer (150 mM NaCl, 25 mM HEPES pH8.0, 0.5 mM TCEP and 20% glycerol).
After the first IMAC column, the 6XHis-MBP tag was removed from the inactive kinase domains with His-tagged TEV protease. Following tag cleavage and dialysis, a second Ni-IMAC step was performed to remove the cleaved tag and the TEV protease. The purified proteins separated from any aggregate by SEC as described above. All proteins were concentrated to >1 mg/ml and frozen in SEC buffer. Protein stocks were maintained at -80°.

In vitro kinase assays

In a total reaction volume of 20 µl, the final concentration of substrate protein was 25 µM and the final concentration of active 6XHis-MBP tagged kinase was 1 µM. Reactions were run in SEC buffer. The reaction was initiated with the simultaneous addition of 1 µCi of [γ-^{32}P]ATP (6000 Ci/mmol and 10 mCi/ml; MP Biomedicals), ATP (Sigma) and $MnCl_2$ to a final concentration of 50 nCi/µl, 50 µM, and 50 µM. The reaction was allowed to proceed for 30 minutes at room temperature and quenched with the addition of SDS-PAGE reducing load dye. The reactions were separated by SDS-PAGE on 4-20% Mini-PROTEAN TGX Tris-Glycine gels (Bio-Rad). The gels soaked in Coomassie Brilliant Blue stain for 30 minutes and destained for 1 hr in 30% Methanol, 5 % glycerol solution. The gels were then dried. Radioactivity was quantified with a Molecular Dynamics Typhoon 860 phosphoimager.

To detect trans-phosphorylation on the full-length PknI and PknG constructs, it was necessary to cleave the 6XHis-MBP tags from the active kinases prior to running the reactions on SDS-PAGE. The reactions were initiated as described above and allowed to proceed for 30 minutes. The reactions were quenched by the simultaneous addition of EDTA to 20 mM and 6 µg of TEV protease. Tag-cleavage was allowed to proceed at room temperature for 2 hours. Following the addition of SDS-PAGE reducing load-dye, the reactions were separated by SDS-PAGE, stained, dried and imaged as described above.

LC-MS sample preparation

In a total reaction volume of 100 ul, the final concentration of substrate protein was 25 µM and the final concentration of active 6XHis-MBP tagged kinase was 1 µM. Proteins were incubated with 1 mM ATP (Sigma) and 1 mM $MnCl_2$ for 12-20 ours at 4 °C.

LC-MS analysis of intact proteins

Acetonitrile (Fisher Optima grade, 99.9%) and formic acid (Pierce 1 mL ampules, 99+%) and water purified to a resistivity of 18.2 MΩ·cm (at 25 °C) using a Milli-Q Gradient ultrapure water purification system (Millipore, Billerica, MA) were used to prepare mobile phase solvents for liquid chromatography-mass spectrometry (LC-MS).

Intact protein kinases were analyzed using an Agilent 1200 series liquid chromatograph (LC; Santa Clara, CA) that was connected in-line with an LTQ Orbitrap XL hybrid mass spectrometer equipped with an Ion Max electrospray ionization source (ESI; Thermo Fisher Scientific, Waltham, MA).

The LC was equipped with C_8 guard (Poroshell 300SB-C8, 5 µm, 12.5 mm × 2.1 mm, Agilent) and analytical (75 mm × 0.5 mm) columns and a 100 µL sample loop. Solvent A was 0.1% formic acid/99.9% water and solvent B was 0.1% formic acid/99.9% acetonitrile (v/v). Sample solutions contained in 0.3 mL polypropylene snap-top vials sealed with rubber septa caps (Wheaton Science, Millville, NJ) were loaded into the Agilent 1200 autosampler compartment prior to analysis. For each sample, approximately 100 picomoles of analyte was injected onto the column. Following sample injection, analyte trapping was performed for 5 min with 99.5% A at a flow rate of 90 µL/min. The elution program consisted of a linear gradient from 35% to 95% B over 34 min, isocratic conditions at 95% B for 5 min, a linear gradient to 0.5% B over 1 min, and then isocratic conditions at 0.5% B for 14 min, at a flow rate of 90 µL/min. The column and sample compartment were maintained at 35 ºC and 10 ºC, respectively. The autosampler injection needle was washed after each sample injection to avoid cross-contamination between samples.

The connections between the LC column exit and the mass spectrometer ion source were made using PEEK tubing (0.005" i.d. × 1/16" o.d., Western Analytical, Lake Elsinore, CA). External mass calibration was performed prior to analysis using the standard LTQ calibration mixture containing caffeine, the peptide MRFA, and Ultramark 1621 dissolved in 51% acetonitrile/25% methanol/23% water/1% acetic acid solution (v/v) (2003). The ESI source parameters were as follows: ion transfer capillary temperature 275 ºC, sheath gas (nitrogen) flow rate 25 (arbitrary units), ESI voltage 2.0 kV, ion transfer capillary voltage 33 V, tube lens voltage 125 V. Mass spectra were recorded in the positive ion mode over the range m/z = 500 to 2000 using the Orbitrap mass analyzer, in profile format, with a full MS automatic gain control target setting of 5×10^5 charges and a resolution setting of 6×10^4 (at m/z = 400, full width at half maximum peak height) (Marshall and Hendrickson 2008). Raw mass spectra were processed using Xcalibur software (version 4.1, Thermo) and measured charge state distributions of proteins were deconvoluted using ProMass software (version 2.5 SR-1, Novatia, Monmouth Junction, NJ).

LC-MS/MS sample preparation and analysis

To enable identification of phosphorylation sites, 2-aminoethylthiol modification of trypsin digested phosphorylated kinase substrates was performed. Kinase reactions were performed as described above for LC-MS measurement in 100 ul volume. Following the overnight incubation, 25 ul of the sample was desalted/delipidated by methanol-chloroform precipitation. This sample was resuspended in SDS-PAGE load dye and separated by SDS-PAGE. ProQ Diamond stain was used to probe for phosphorylation following the manufacturer's instructions (Invitrogen). The proteins were separated by SDS-PAGE and extracted following the trypsin digestion protocol available on the UCSF Mass Spec facility website (http://ms-facility.ucsf.edu/ingel.html). 2-aminoethanethiol modification and MS/MS measurements were performed as described (Mieczkowski, Iavarone et al. 2008).

Trypsin-digested protein kinases were analyzed using a quadrupole time-of-flight (Q-Tof Premier, Waters, Milford, MA) tandem mass spectrometer that was connected in-line with an ultraperformance liquid chromatograph (nanoAcquity UPLC, Waters).

The UPLC was equipped with C_{18} trapping (20 mm × 180 µm) and analytical (100 mm × 100 µm) columns and a 10 µL sample loop. Solvent A was 99.9% water/0.1% formic acid and solvent B was 99.9% acetonitrile/0.1% formic acid (v/v). Sample solutions contained in 0.3 mL polypropylene snap-top vials sealed with rubber septa caps (Wheaton Science, Millville, NJ) were loaded into the nanoAcquity autosampler compartment prior to analysis. For each sample, approximately 1 to 10 picomoles of trypsin-digested protein was loaded onto the column. Following sample injection, trapping was performed for 5 min with 100% A at a flow rate of 3 µL/min. The injection needle was washed with 750 µL each of solvents A and B after injection to avoid cross-contamination between samples. The elution program consisted of a linear gradient from 25% to 40% B over 60 min, a linear gradient to 95% B over 0.33 min, isocratic conditions at 95% B for 7.67 min, a linear gradient to 1% B over 0.33 min, and isocratic conditions at 1% B for 11.67 min, at a flow rate of 500 nL/min. The analytical column and sample compartment were maintained at 35 ºC and 8 ºC, respectively.

The column was connected to a nanoelectrospray ionization (nanoESI) emitter mounted in the nanoflow ion source of the Q-Tof mass spectrometer. The nanoESI source parameters were as follows: nanoESI capillary voltage 2.3 kV, nebulizing gas (nitrogen) pressure 0.15 mbar, sample cone voltage 30 V, extraction cone voltage 5 V, ion guide voltage 3 V, and source block

temperature 80 ºC. No cone gas was used. The collision cell contained argon gas at a pressure of 8×10^{-3} mbar. The Tof analyzer was operated in "V" mode. Under these conditions, a mass resolving power[2] of 1.0×10^4 (measured at m/z = 771) was achieved, which was sufficient to resolve the isotopic distributions of the singly and multiply charged precursor ions and fragment ions measured in this study. External mass calibration was performed immediately prior to analysis, using solutions of sodium formate. Survey scans were acquired in the positive ion mode over the range m/z = 400-1800, in continuum format, using a 0.95 s scan integration and a 0.05 s interscan delay. In the data-dependent mode, up to five precursor ions exceeding an intensity threshold of 35 counts/second (cps) were selected from each survey scan for tandem mass spectrometry (MS/MS) analysis. Real-time deisotoping and charge state recognition were used to select 2+, 3+, 4+, 5+, and 6+ charge state precursor ions for MS/MS. Collision energies for collisionally activated dissociation (CAD) were automatically selected based on the mass and charge state of a given precursor ion. MS/MS spectra were acquired over the range m/z = 50-2500, in continuum format, using a 0.95 s scan integration and a 0.05 s interscan delay. Ions were fragmented to achieve a minimum total ion current (TIC) of 30,000 cps in the cumulative MS/MS spectrum for a maximum of 4 s.

To avoid the occurrence of redundant MS/MS measurements, real time exclusion was used to preclude re-selection of previously analyzed precursor ions over an exclusion width of ± 0.5 m/z unit for a period of 120 s. To acquire MS/MS spectra of chemically modified peptides of interest with optimal signal-to-noise ratio, the m/z values of the precursor ions of interest were defined in an include list to preferentially select the ions of interest, over an inclusion width of ± 0.15 m/z unit, over other detected masses for MS/MS, and these selected ions were fragmented to achieve a minimum TIC of 50,000 cps in the cumulative MS/MS spectrum for a maximum of 15 s.

The data resulting from LC-MS/MS analysis of trypsin-digested proteins were processed using ProteinLynx Global Server software (version 2.3, Waters), which performed background subtraction (threshold 35% and fifth order polynomial), smoothing (10 times, over three channels), and centroiding (top 80% of each peak and minimum peak width at half height four channels) of the mass spectra and MS/MS spectra(Savitzky and Golay 1964). The processed data were searched against the amino acid sequence(s) of the protein(s) of interest using the following criteria: precursor ion mass tolerance 100 ppm, fragment ion mass tolerance 0.1 Da, and the following variable post-translational modifications: Met oxidation, Asn/Gln deamidation, Ser/Thr dehydration, Ser/Thr phosphorylation, chemical conversion of phosphoserine to aminoethylcysteine, and chemical conversion of phosphothreonine to β-methylaminoethylcysteine (Knight, Schilling et al. 2003). The MS/MS spectra were manually inspected to verify the presence of b and y-type fragment ions which, in combination with the measured precursor ion masses, uniquely identify the peptides (Roepstorff and Fohlman 1984).

Chapter 3

Kinase cross-phosphorylation is an activation mechanism

Introduction

The 11 *Mtb* STPKs cross-phosphorylate in a distinct and specific pattern. The map of these trans-phosphorylation reactions suggests the division of the *Mtb* kinome into three distinct functional classes: master regulator kinase, signal propagation kinase and substrate kinase. Kinase-kinase activation or inhibitory cascades also have been identified in other bacteria. In *M. xanthus*, Pkn8, a membrane associated STPK, phosphorylates Pkn14, a soluble STPK. This activation mechanism for Pkn14 leads to the downstream phosphorylation of the essential transcriptional regulator MrpC on Thr residues (Nariya and Inouye 2005). The locations of the phosphate groups transferred between these different proteins are an important indication of the functional role for these cross-kinase signaling interactions. Phosphorylation of the activation loop is a common kinase activation mechanism.

Although some eukaryotic kinases autophosphorylate on the activation loop, many depend on an upstream kinase for activation (Gao, Toker et al. 2001). In eukaryotes, PDK-1 is the upstream kinase for a number of other protein kinases such as Akt/protein kinase B, p70 S6 kinase and protein kinase C (PKC). Following phosphorylation on the activation loop, PKC phosphorylates two residues in the C-terminus through an intramolecular interaction. Autophosphorylation of these secondary sites is essential for full activity. PKC is inhibited when PDK-1 binds and occludes the autophosphorylation sites. PKC regulation of the kinase is a two-part process involving first trans-phosphorylation and then autophosphorylation. This example highlights the sequential nature of kinase activation. In the case of the *Mtb* STPKs, the question remains: are the phosphates placed by cross-phosphorylation reactions localized to the activation loop? If so, is this process sufficient for full kinase activation?

Activation loop phosphorylation is recognized as essential for activity in several prokaryotic STPKs. The activation loop Thr in *Bacillus subtilis* PKC is important for activity, as mutations in this residue significantly reduce trans-phosphorylation activity (Madex, Stensballe et al. 2003). This STPK is frequently compared to the *Mtb* kinases as phosphorylated residues on PKC are clustered to the activation loop and the juxtamembrane region, a pattern that is repeated in the *Mtb* kinome. PknB, a master regulator *Mtb* STPKs, has two critical Thr residues in the activation loop. Individual mutation of these residues to Ala resulted in 10- to 20-fold reductions in activity on MBP than the wild-type kinase, while the double Thr-to-Ala mutant is 300-fold less active than wild type (Duran, Villarino et al. 2005; Boitel, Ortiz-Lombarida et al. 2003). Likewise, the Ala substitution of the potential phosphorylation site Thr170, in the PknH activation loop greatly reduces autophosphorylation activity (Molle, Kremer et al. 2003). These data suggest that the two master regulator kinases, PknB and PknH require activation loop phosphorylation for full kinase activity.

The pattern of activation loop phosphorylation extends to the signal propagation kinases PknJ and PknL. The three Thr residues in the PknJ activation loop, Thr168, Thr171 and Thr173, have been mutated to Ala. The resulting triple mutant was not autophosphorylated (Jang, Stella et al. 2010). Trans-phosphorylation activity is presumed to be abolished for the triple mutant;

however, this experiment was not performed. The double activation loop Thr mutant in the soluble kinase PknK shows a complete loss of auto- and trans-phosphorylation ability (Kumar, Kumar, et al. 2009). The PknL double Thr-to-Ala mutant is less autophosphorylated when expressed in *E.coli* than the wild-type kinase (Canova, Veyron-Churlet et al. 2008). In addition to the double Thr motif, the activation loop of PknL contains multiple Ser residues. Individual mutation of these residues yields autophosphorylation signals similar to the wild-type protein, suggesting that these serines are not targets of autophosphorylation. The PknL double Thr-to-Ala mutant does not phosphorylate the cognate substrate Rv2175. This activation loop double mutation renders the kinase inactive.

Activation loop phosphorylation also has been reported for the substrate kinases PknA and PknD. Individual Thr-to-Ala mutations in the activation loop render PknA significantly impaired in autophosphorylation ability and eliminate trans-phosphorylation on a substrate (Thakur, Chaba et al. 2008). The PknD activation loop peptide is reported to be the acceptor site for multiple phosphate groups (Molle, Zanella-Cleon et al. 2006); however, these data have not been confirmed with direct mutations. Identification of these primary phosphorylation sites in the activation loop is key to understanding the role of auto- and trans-phosphorylation in *Mtb* STPK activation. Multiple additional Ser and Thr residues in the activation loops raise questions concerning the potential for functional secondary phosphorylation sites located in this defined region of the protein.

Secondary phosphorylation sites in STPKs can be upstream or downstream of the primary phosphorylation site (Nolen, Taylor et al. 2004). These sites are usually conserved in subfamilies and are only found to be phosphorylated following phosphorylation of the primary residue. In the MAP kinase ERK2, phosphorylation at both the primary and secondary sites is required for full activity as phosphorylation of the second residue is essential for ligand binding. The mitogen activated kinase kinase, MEK, is activated by phosphorylation on two activation loop serines, Ser218 and Ser222 (Gopalbhai, Jansen et al 2003). Phosphorylation of the upstream residue Ser212 significantly reduces kinase activity and appears to result in kinase inhibition. Mutation of Ser212 to a phospho-mimic residue, Asp, completely abolishes the phosphorylation of exogeneous substrates *in vitro*. Experimental evidence demonstrates that mutation of the Ser to acidic residues such as Asp does not prevent phosphorylation of the activation loop or substrate binding. As a result, Ser212 is thought to be involved with catalysis as no significant conformational rearrangement is noted following simulated phosphorylation of this residue. Because multiple residues have been identified as autophosphorylation targets in the *Mtb* STPKs, it is possible that some of these residues function not as part of the activation mechanism, but instead to inhibit the kinase. The active STPKs are hyperphosphorylated when expressed in *E. coli*. Liquid-chromatography mass spectrometry (LC-MS) measurements of the intact mass for many of these proteins reveals that the kinase domain may be decorated with as many as 14 phosphates (Molle, Zanella-Cleon et al. 2006). The functional role of these multiple phosphorylation sites is not understood. Identification of the residues involved in kinase cross-phosphorylation is the first step to elucidating the function of these interactions, be it activation, inhibition, or substrate recognition.

Utilizing the comprehensive, system-level kinase phosphorylation map presented in the preceding chapter, the phosphorylation patterns resulting from the identified cross-phosphorylation reactions were investigated. Sequence alignment of the *Mtb* STPKs revealed a high level of conservation of Thr and Ser in the activation loop sequences. Mutations were made to these residues and the mutant proteins were tested for auto- and trans-phosphorylation. The

contribution of activation loop phosphorylation to ligand binding and activation loop flexibility was assayed using series of florescence polarization and limited proteolysis.

Results

The DNA sequence of the substrate kinase PknD was analyzed for potential activation loop phosphorylation sites. Four threonine residues in the PknD activation loop were mutated to alanine. Each Thr-to-Ala mutant was constructed in the Asp-to-Asn inactive kinase mutant background to eliminate autophosphorylation ability. Intact mass measurements of the mutants following phosphorylation reactions using active PknD or active PknB revealed that the two N-terminal Thr residues are the main phosphorylation sites (Figure 3.1).

Figure 3.1 LC-MS measurements of the single PknD activation-loop Thr-to-Ala single mutants revealed different patterns of phosphorylation depending on the activating kinase. **A)** This set of plots depicts the inactive PknD mutants phosphorylated by PknB. **B)** The LC-MS traces of the intact PknD Thr-to-Ala mutants phosphorylated by PknD.

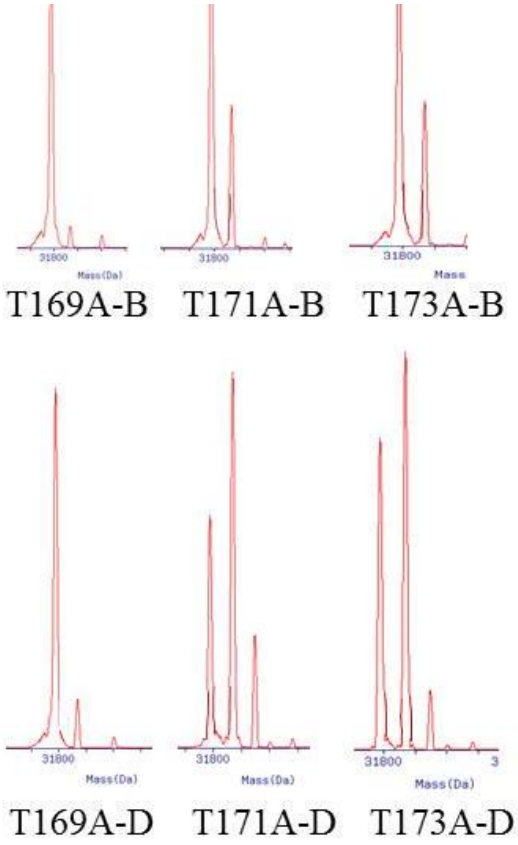

These results demonstrate that the first two Thr residues in the activation loop are the most strongly phosphorylated in both auto- and trans-phosphorylation reactions. A sequence alignment using ClustalW reveals that these two residues are commonly conserved throughout

the STPK family (Figure 3.2). Because a double mutation is necessary for maximum reduction in PknB activity (Duran, Villarino et al. 2005; Boitel, Ortiz-Lombarida et al. 2003), I constructed double mutants of the first two activation loop Thr in all of the *Mtb* STPKs to test their general

Figure 3.2 A sequence alignment of the 11 *Mtb* STPKs with ClustalW highlights conserved features in activation segment peptide. The DFG motif highlighted in red forms the critical residues for magnesium binding in the ligand binding cleft. The residues targeted by autophosphorylation and trans-phosphorylation are boxed in yellow. The APE motif, highlighted in blue, represents the C-terminal end of the activation segment.

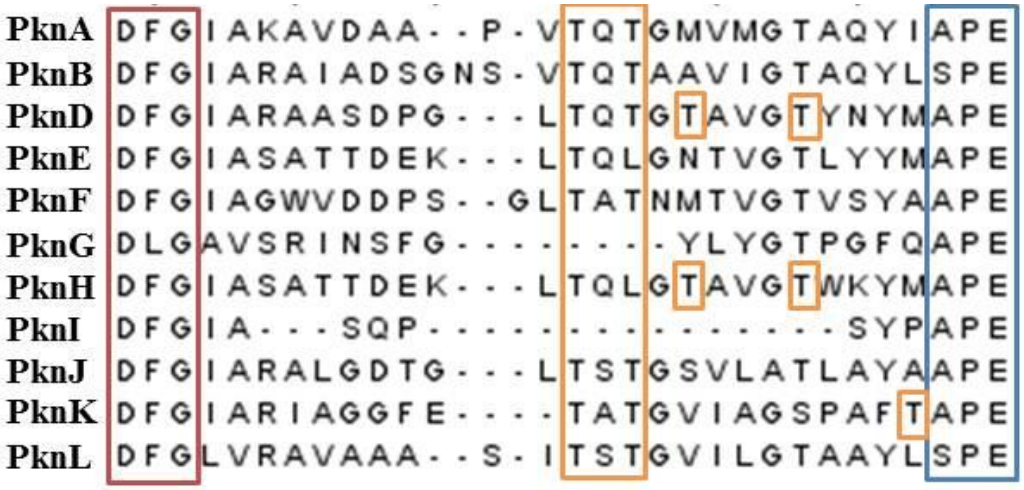

role in *Mtb* STPK activation. The PknJ and PknL activation loop sequences contain an intervening Ser residue between the two targeted threonines (Figure 3.2). To remove the possibility of phosphorylation targeted to this residue, the TST motif was mutated to AAA for these two proteins.

Each of the double mutants were made in the wild-type kinase background, to test the impact of these mutations on substrate phosphorylation, and in the inactive Asp-to-Asn mutant kinase to test the impact of the mutations on trans-autophosphorylation and trans-phosphorylation in cross-kinase interactions (Table 3.1). The double Thr-to-Ala mutants in the wild-type and inactive STPK background behaved identically to the fully active kinases throughout purification. A comparison of the size-exclusion chromatography traces for each mutant and the wild-type homolog revealed no change in the estimated protein size, an indication that the mutations do not destabilize the proteins.

The activity of each kinase with the Thr-to-Ala double mutation in the wild-type background was assayed against GarA. A 10-fold excess of GarA was incubated with each mutant STPK for 30 minutes are room temperature in the presence of γ^{32}P ATP, unlabeled ATP, and $MnCl_2$. Strikingly, the Thr-to-Ala mutation abolished auto- and trans-phosphorylation activity for all STPKs tested (Figure 3.3). This result demonstrates that these activation loop residues are essential for kinase activity. The exact mechanistic role played by the individual threonines has yet to be determined. These residues may be involved with switching the kinase to an active conformation or with substrate recognition.

Table 3.1

Protein	Length	Mutation	Tag	Tag cleavage site	Expression vector
PknA	1-279	T172/174A	HMBP	TEV	pHMGWA
PknA	1-279	D141N/T172/174A	His	none	pET28b
PknA	1-330	T172/174A	HMBP	TEV	pHMGWA
PknA	1-330	D141N/T172/174A	HMBP	TEV	pHMGWA
PknB	1-291	T171/173A	HMBP	TEV	pLIC2MT
PknB	1-279	D138N/T171/173A	His	none	pET28b
PknB	1-330	T171/173A	HMBP	TEV	pLIC2MT
PknB	1-330	D138N/T171/173A	HMBP	TEV	pLIC2MT
PknD	1-292	T169/171A	HMBP	TEV	pHMGWA
PknD	1-292	D138N/T169/171A	HMBP	TEV	pHMGWA
PknE	1-279	T170/175A	HMBP	TEV	pHMGWA
PknE	1-279	D139N/T170/175A	HMBP	TEV	pHMGWA
PknF	1-280	T173/175A	HMBP	TEV	pHMGWA
PknF	1-280	D137N/T173/175A	HMBP	TEV	pHMGWA
PknG	1-750		His	none	AmpR
PknG	1-750	D143N	His	none	AmpR
PknH	1-280	T170/174A	HMBP	TEV	pHMGWA
PknH	1-280	D139N/T170/174A	HMBP	TEV	pHMGWA
PknI	1-585		HMBP	TEV	pHMGWA
PknJ	1-286	T171/S172/T173A	HMBP	TEV	pHMGWA
PknJ	1-286	D125N/T171/S172/T173A	HMBP	TEV	pHMGWA
PknK	1-290	T179/181A	HMBP	TEV	pLIC2MT
PknK	1-290	D149N/T179/181A	HMBP	TEV	pLIC2MT
PknL	1-302	T173/175A	HMBP	TEV	pLIC2MT
PknL	1-302	D142N/T173/175A	HMBP	TEV	pLIC2MT
PknL	1-366	T173/175A	HMBP	TEV	pLIC2MT
PknL	1-366	D142N/T173/175A	HMBP	TEV	pLIC2MT

Figure 3.3 Cross phosphorylation reactions with the wild-type STPKs and the double Thr-to-Ala kinase mutants reveals the mutations abolish trans-phosphorylation activity on GarA.

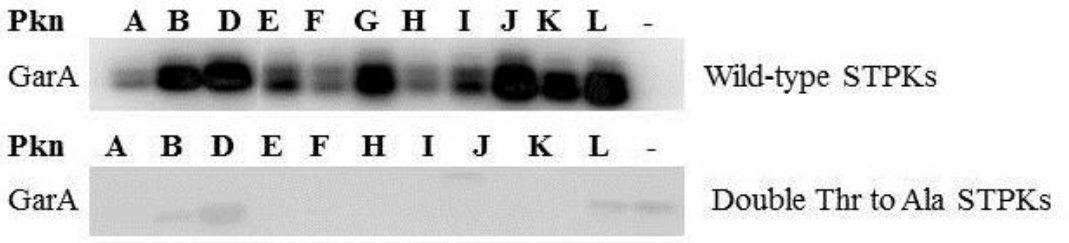

PknG, the sole *Mtb* STPK without phosphorylated residues in the activation loop, efficiently phosphorylates GarA (Figure 3.3). This kinase-substrate interaction implies that a phosphorylated TXT motif is not essential for substrate recognition, even though GarA contains a Forkhead-Associated (FHA) domain that recognizes phospho-Thr residues in a peptide context. The divergence of the PknG activation loop is emphasized by the sequence alignment of the entire *Mtb* Ser/Thr kinome (Figure 3.2). The activity of all 11 kinases on GarA, despite such wide variation in activation loop sequence, suggests that additional factors must be involved in substrate identification.

To explore local sequence determinants of substrate recognition, I tested the kinase trans-phosphorylation interactions defined in the STPK phosphorylation map using the catalytically inactive double Thr-to-Ala mutants as the substrates. The wild-type STPKs were unable to phosphorylate many of the double Thr-to-Ala mutants (Figure 3.4). These results demonstrate that the activation loop threonines are the targets of phosphorylation in *trans*.

To probe the impact of activation loop phosphorylation on ligand binding, a series of fluorescence polarization (FP) experiments were performed with the wild-type PknB kinase domain and the double Thr-to-Ala PknB mutant in the wild-type background. Fluorescently labeled non-hydrolyzable ATP analogs can be used in high-throughput assays to probe the binding of ligands to the kinases. An FP assay has been developed utilizing Bodipy-ATPγS and previously utilized to screen for PknB kinase inhibitors (Marimuthu, unpublished results). The affinity of this ATP analog was determined by generating protein saturation curves for PknB, (Figure 3.5A).

The dissociation constant (K_d) for wild-type PknB was determined to be in the single digit micro-molar range from the protein saturation curve at a constant ligand concentration of 25 nM. This value is comparable to the PknB K_d determined previously (Marimuthu, unpublished results). The protein saturation curves for PknB wild-type, PknB Thr171/173Ala and inactive PknB Asp138Asn were determined. The PknB Thr171/173Ala mutant has a saturation curve nearly identical to the wild-type protein while the inactive PknB mutant appears to bind the Bodipy-ATP with slightly higher affinity. The calculated EC50s for these proteins are reported in Figure 5.3.

To probe the impact of phosphorylation on the ligand binding affinity of PknB, the K_ds of the adenosine nucleotides were determined from a series of indirect competition assays. In these reactions, increasing concentrations of ATP, ADP and AMP were used to reduce the concentration of free PknB, which leads to the release of the fluorescently labeled ATP analog. These experiments not only provide information about the relative binding affinity of each PknB construct, but also reveal any change in the affinities of the adenosine nucleotides. Surprisingly, the wild-type kinase and the Thr-to-Ala double mutant display similar affinities for ATP and ADP (Figure 3.5). The PknB Thr171/173Ala mutant does not bind AMP at the concentrations tested. These results indicate that the presence of phosphate groups on the activation loop does not control the affinity of ATP or ADP. Moreover, the ATP β- and γ-phosphates are important for nucleotide binding.

In many eukaryotic kinases, the activation loop conformation is stabilized by interactions between the phosphorylated residues and a patch of basic residues. These residues are conserved in PknB (Young, Delagoutte et al. 2003). Limited proteolysis can be used to identify flexible segments in an otherwise well-folded structure. The PknB activation loop sequence contains a single trypsin site and multiple predicted cleavage sites for the proteases thermolysin and chymotrypsin. Limited proteolysis reactions were performed with several ratios of

PknB/protease at 20 °C for 30 minutes (Anderson and Cole 2008). The reactions were quenched with 6xSDS-load dye and heated to 90 °C for 10 minutes prior to separation by SDS-PAGE. To assay for ligand-induced activation loop stability, the experiment was repeated in the presence of the ATP. Curiously, the PknB Thr-to-Ala double mutant appears somewhat more stable than the wild-type PknB kinase domain in the absence of ligand (Figure 3.6).

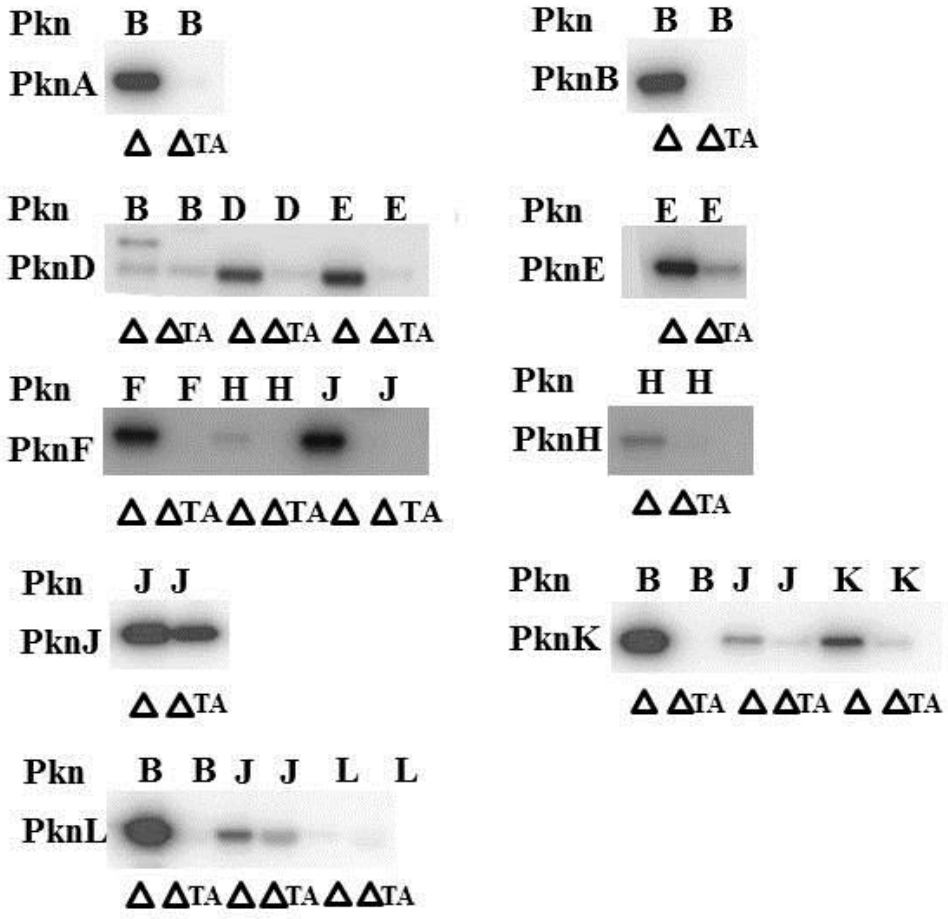

Figure 3.4 γ^{32}P phosphoryl transfer assays reveal that mutations of the activation loop Thr residues reduce or abolish trans-phosphorylation of the substrate kinase. The active kinases are listed on the top of each panel and the inactive substrate is indicated on the side.

A.

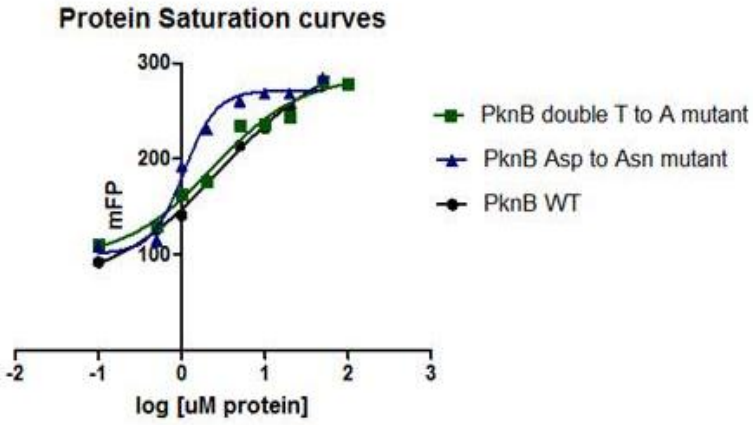

PknB WT	PknB double T to A mutant	PknB D138N
EC50 = 3.031 uM	EC50 = 2.4 uM	EC50 = 1.066 uM
Hillslope = .6483	Hillslope = .8177	Hillslope = 2.228

B.

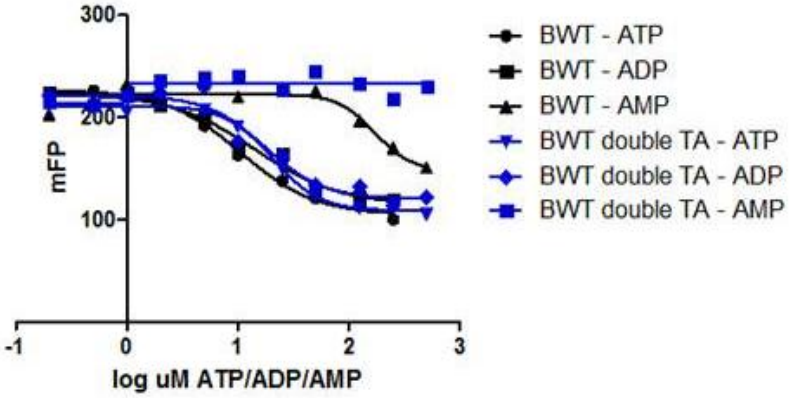

PknB WT	PknB double Thr to Ala
EC50 - ATP = 10.56 uM	EC50 - ATP = 20.51 uM
EC50 - ADP = 14.28 uM	EC50 - ADP = 17.49 uM
EC50 - AMP = 171.4 uM	EC50 - AMP = -

Figure 3.5
A) Fluorescence polarization studies at constant ligand concentration and increasing protein concentration provide the Kd for wild-type PknB, PknB T171/173A and PknB D138N.
B) Increasing concentrations of competing ligand titrate away the fluorescently labeled ATP analog for each protein.

Figure 3.6
Limited proteolysis of PknB with thermolysin reveals no change in protein stability with the addition of 1 mM ligand. However, the PknB Thr171/173Ala mutant is more stable in the presence of protease than the wild-type protein. The Thr-to-Ala double mutant is less stable following the addition of ATP.

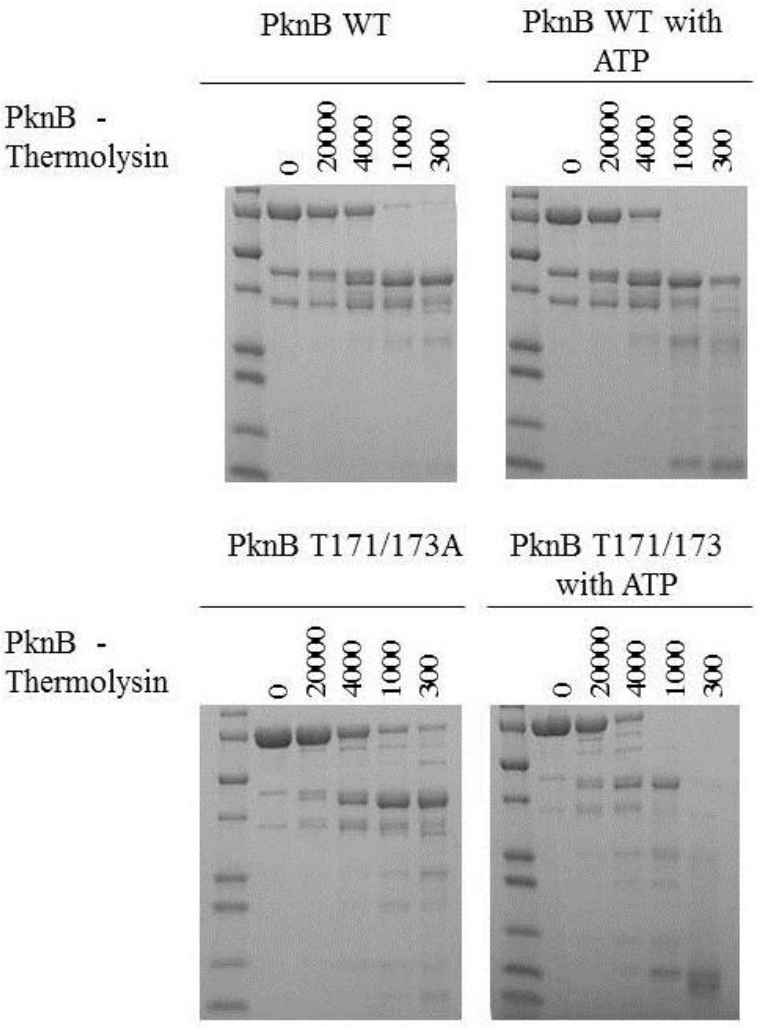

Discussion

The location of auto- and transphosphorylated residues in the kinase domain can be indicative of function. Activation loop phosphorylation is associated with activity for many eukaryotic and prokaryotic kinases. MKK1 and ERK2, two Ser/Thr kinases found in eukaryotes, have phosphorylation sites in the activation loop. Both enzymes must be phosphorylated on these residues for full activity (Boitel, Ortiz-Lombardia et al. 2003). The prokaryote *C. glutamicum* contains four STPKs: PknA, PknB, PknG and PknL (Fuiza, Canova et al. 2008). The *C. glutamicum* PknA and PknB have conserved phosphorylation sites located in the activation loop. The ThrSerThr motif found in the *Mtb* PknL activation loop is SerGlnAsp in the *C. glutamicum* ortholog, but the kinase is still autophosphorylated on this motif (Fuiza, Canova et al 2008). The conservation of this phosphorylation site despite sequence variation is indicative of a functionally important motif.

Sequence alignments of the 11 *Mtb* STPKs highlight significant conservation of threonines in the activation loop (Figure 3.2). Individual mutation of each potential phosphorylation site in this region for PknD highlighted the significance of the bi-phosphorylation motif. To measure the impact of the TXT motif on kinase activity, the Thr-to-Ala double mutants in the otherwise wild-type background were tested for the ability to phosphorylate the substrate GarA. The activation loop mutations abolished the trans-phosphorylation activity of each kinase. Common to many of the kinases, the TXT motif is necessary for activity.

Double Thr-to-Ala mutants in all 10 Mtb STPKs containing this motif reveal that all trans-phosphorylation reactions initially target the TXT motif. The Thr residues are phosphorylated during autophosphorylation and are identified in this work as being the targets of all cross-kinase trans-phosphorylation. These results demonstrate that trans-autophosphorylation and inter-kinase cross-phosphorylation have similar activating functions.

The precise mechanistic function of the activation loop threonines in the kinase activation process is unknown. Increased nucleotide- and substrate-binding affinity may occur due to phosphorylation-induced structural remodeling of the substrate-binding region, which encompasses the activation loop and portions of the C-terminal domain. In eukaryotic kinases, phosphorylated residues in the activation loop can have distinct roles in ligand binding and stabilization of the substrate protein (Prowse, Deal et al. 2001). The eukaryotic MAP kinase ERK2 is phosphorylated as Thr183 and Tyr185 in the activation loop. Phosphorylation at the latter residue acts as a switch that independently controls ATP binding, while the phosphorylation at both residues stabilizes the phosphor-acceptor substrate. In the CDKs, the unphosphorylated activation loop creates a blockade of the active site that inhibits ATP binding.

Remarkably the wild-type *Mtb* PknB kinase domain and the double Thr-to-Ala mutant displayed nearly identical affinity for Bodipy-ATP. The EC50 values are 3 µM for the wild-type kinase and 2.4 µM for the double Thr-to-Ala mutant. In competition assays, the IC50s of ATP, ADP and AMP for wild-type PknB measured here are 10.5 µM, 14.2 µM and 171.4 µM respectively. These values are comparable to the previously measured values of 4.5 µM, 6.5 µM for ADP and 181 µM for AMP (Marimuthu et al, unpublished results). I measured remarkably similar IC50 values for the PknB Thr-to-Ala double mutant for ATP and ADP - 20 µM and 17.5 µM, respectively. However, interaction with AMP differs greatly between the two proteins. At measured concentrations up to 0.5 mM, AMP does not displace Bodipy-ATP from the PknB Thr-to-Ala mutant. The presence of phosphorylated residues appears to be important for ligand

recognition if the ligand lacks phosphate. The two activation loop threonines are not required for ligand binding, but do appear to be important for ligand identification. The intracellular concentration of these nucleotides is estimated to be 3.5mM for ATP and 120 μM for ADP based on metabolic measurements of *E. coli* in mid-log phase growth (Buckstein, He et al. 2008). The conditions assayed were sufficient to test for ADP and AMP competition at concentrations similar to those expected within the cell. Further studies of PknB with individual Thr-to-Ala mutations in the activation loop would serve to probe the individual role of each phosphorylated residue. An intact TXT motif is not essential for ligand binding, but does appear to be important for the recognition of AMP *in vitro*.

The inactive Asp138Asn PknB mutant displays a higher affinity for Bodipy-ATP than the wild-type kinase or the double Thr-to-Ala mutant (Figure 3.5). These data support the finding that the activation loop Thr residues are not necessary for nucleotide binding, as the inactive PknB mutant is unphosphorylated. Unexpectedly, phosphorylation also does not increase ATP affinity, suggesting that the unphosphorylated PknB activation loop does not block the ATP binding site.

Limited proteolysis experiments reveal that the PknB Thr171/173Ala mutant is more stable in the presence of proteases than the wild-type protein. The addition of ligand appears increase the protease activity on the double mutant, suggesting that the kinase exhibits more flexibility with ATP bound in the ligand binding cleft. These results are consistent with the structures of active, phosphorylated PknB, which exhibit little electron density for the activation loop, indicative of flexibility in this segment. A structure of an inactive, unphosphorylated Mtb STPK may enable visualization of the activation segment.

The work presented in this chapter reveals that trans-phosphorylation, be it auto- or cross-phosphorylation, targets the same residues in the activation loop. For all of the *Mtb* STPKs except PknG, these phorphorylations are required for kinase activation. The TXT motif found in many of the *Mtb* STPKs is the conserved trans-phosphorylation element. The consistent targeting of this activation loop sequence indicates that auto- and cross-phosphorylation are complementary activation mechanisms that result in STPK signaling.

Methods

Construct design and cloning

Multiple sequence alignment of the kinase domains using ClustalW enabled identification of the TXT motif located in each kinase domain (Chenna, Sugawara et al. 2003). Each Thr-to-Ala double or triple mutant was constructed using 2-primer site-directed mutagenesis. For constructs in the Gateway vectors, PCR was performed with Herculase II fusion polymerase (Stratagene) and DMSO. For constructs in the pLIC2MT vector (cloned by MacroLab), successful mutagenesis required PCR with the Pfu Ultra II fusion polymerase (Stratagene).

Protein expression and purification

Proteins were expressed and purified as described in the methods for Chapter 2 using auto-induction (Studier 2005). The Thr-to-Ala double mutants in the wild-type background were purified with Ni-IMAC and subjected to SEC to remove aggregate. The inactive kinases with the Thr-to-Ala double mutations were purified by Ni-IMAC, TEV protease was used to cleave the 6xHis-MBP tag and a second Ni-IMAC step was run to remove the tag and the TEV. The proteins were then separated from aggregate by SEC. Each protein was concentrated and flash frozen in buffer containing 20% glycerol.

In vitro kinase assays

Kinase reactions with [γ^{32}P]ATP were performed as described in Chapter 2.

Fluorescence Polarization Assays

Fluorescence polarization assays were performed with BodipyFL-ATP-γ-S (Invitrogen). The excitation and emission wavelengths for the fluorophore are 485 nm and 535 nm respectively. Varying concentrations of purified proteins were incubated with 25 nM BodipyFL-ATP-γ-S in 75 mM NaCl, 12.5 mM HEPES pH 8.0, 0.25 mM TCEP, 10% glycerol, 1 mM $MgCl_2$ and 1 mM $MnCl_2$ for 20 minutes at room temperature. The mP value of the fluorescent ligand upon binding to the proteins was measured using a Wallac-Victor plate reader. GraphPad Prism software was used to plot the graphs and to calculate the Kd and EC50 values.

For the competition FP assays, 4 µM protein was incubated with 25 nM BodipyFL-ATP-γ-S in the buffer described above for 20 minutes. Stock solutions of ATP, ADP, and AMP were made in 1 M HEPES pH 8.0 and added to each sample at the appropriate concentration. The fluorescence polarization measurements were taken and analyzed as described above.

Limited Proteolysis

Limited proteolysis of PknB and PknB Thr171/173Ala was performed as described (Anderson and Cole 2008). Briefly, 20 µg of kinase was incubated with varying amounts of trypsin, chymotrypsin, and thermolysin. To determine the impact of ligand binding on protein stability, these assays were also performed in the presence of 1 mM ATP and 1 mM AMP-PNP, both with 1 mM $MnCl_2$. The reactions were incubated for 30 minutes at room temperature and quenched with SDS-PAGE loading dye. The samples were immediately boiled for 10 minutes and separated by SDS-PAGE. The gels were stained with Coomassie Brilliant Blue dye.

Chapter 4

X-ray crystal structures of the Master Regulator kinase PknH

Introduction

A switch between active and inactive conformations regulates the activities of protein kinases. Characteristic features of the active form contrast with diverse inactive conformations defined in studies of eukaryotic kinases. Multiple crystal structures have been determined of the active forms of the *Mtb* STPKs PknB, PknE and PknG (Ortiz-Lombardia, Pompeo et al. 2003; Young, Delagoutte et al. 2003; Gay, Ng et al. 2006; Scherr, Honnappa et al. 2007). The structure of an inactive *Mtb* STPK has not been reported. Ser/Thr kinases frequently adopt unique autoinhibitory conformations to prevent spurious activation. Structural analysis of an inactive *Mtb* STPK will provide insight in the conformational changes that occur as a result of activation by phosphorylation.

Eukaryotic and prokaryotic Ser/Thr kinases share a common fold consisting of a bilobal structure (Figure 4.1). The N-lobe contains a five-stranded β-sheet and one α-helix that is referred to as the Cα-helix. The C-lobe is mainly alpha helical. ATP binds in a deep grove, the active site, between the lobes and sits beneath the phosphate binding loop, the P-loop, which contains a conserved glycine rich motif. The glycine residues in this flexible loop closely approach the phosphates of ATP and coordinate these reactive groups through back-bone interactions while conserved aromatic side chains also found in the P-loop cap the site of phosphate transfer (Huse and Kuriyan 2002). The activation loop is proximal to the active site and provides a platform for the peptide substrate. In eukaryotic kinases, phosphorylation of this loop stabilizes it in an extended conformation that enables substrate binding.

The structure of active PKA, the first kinase crystal structure to be solved, shows a phosphorylated residue in the activation loop interacting with a pocket of positively charged residues on the surface of the C-lobe (Nolen, Taylor et al. 2004). Later structures of this kinase in the inactive form demonstrate that the unphosphorylated activation loop has multiple conformations and is disordered. Activation loops in the eukaryotic kinases are quite diverse in sequence and in structure. This diversity may contribute to substrate recognition and specificity. All eukaryotic kinases regulated by phosphorylation of the activation loop contain a conserved arginine residue immediately preceding the conserved catalytic aspartate in this loop (Nolen, Taylor et al. 2004). The *Mtb* STPKs, with the exception of PknG, contain these signature residues making them members of the 'RD' family of kinases.

The analysis of 19,000 eukaryotic-like protein kinase sequences revealed residue conservation across the main family divisions (Kannan, Taylor et al. 2007). Ten residues were identified as mediating the core function of the catalytic domain. These amino acids are conserved across the major divisions of life. Six of these residues are involved in substrate binding and catalysis. The remaining residues are part of a hydrogen-bonding network that links the characteristic DFG motif with substrate binding regions (Kannan, Taylor et al. 2007). The DFG motif coordinates the catalytically essential magnesium or manganese cations at the active site and stabilizes the Cα-helix (Steichen, Iyer et al 2009).

Allosteric mechanisms of activation have been reported for multiple eukaryotic and prokaryotic kinases (Greenstein, Echols et al. 2007). Residues implicated in catalysis have been closely examined for many kinases; however, mechanisms of allosteric signaling through structural features distant from the active site remain to be fully defined.

Recent analysis of STPK structures reveals two intra-molecular networks of connectivity that control ATP binding and enzyme regulation (Kornev, Tarylor et al. 2009). These motifs,

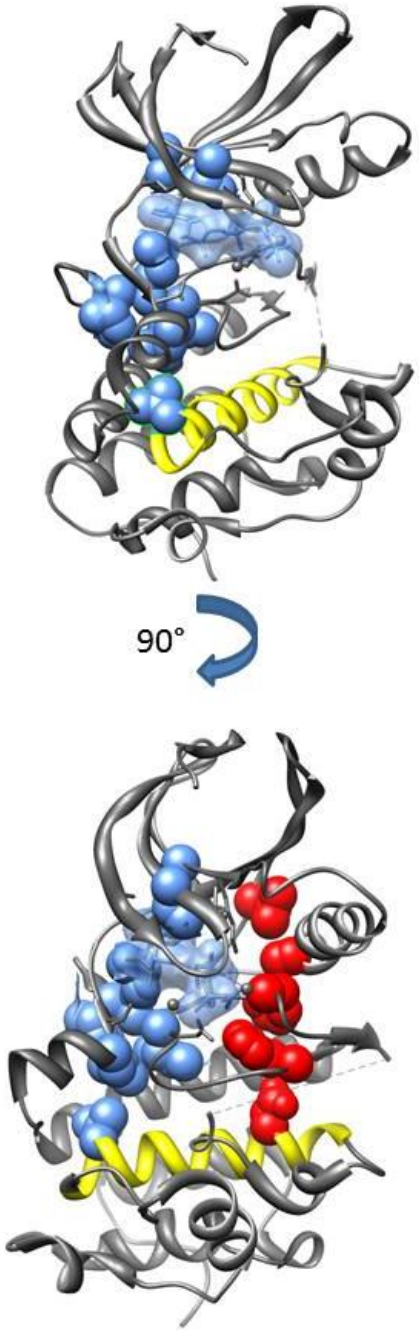

Figure 4.1 The structure of the wild-type PknB kinase domain contains intact C- and R-spines. The C-spine residues are highlighted in blue and the R-spine residues are depicted in red. Both spines are anchored by terminal residues on a buried helix known as the F helix (yellow).

referred to as 'spines', form two spatially conserved but noncontiguous hydrophobic regions that encompass residues from both the N- and the C-lobes (Figure 4.1). The catalytic spine (C-spine) is conserved in all kinases and controls catalysis through ATP localization. The regulatory spine (R-spine) contains activation loop residues and part of the Cα helix (Figure 4.1). These stacks of hydrophobic amino acids are conserved among STPKs, but are non-contiguous in sequence, making the individual residues difficult to identify. The assembly of these conserved hydrophobic spines depends on the activation state of the kinase. An intact R-spine is present in all active kinases, but is frequently disturbed in the inactive conformation. Analysis of the kinase spine alignment provides an additional metric for determining the activation state of the protein.

Comparisons of the crystal structures of phosphorylated and unphosphorylated kinases also provide insight into the wide variety of conformational changes that occur during activation. In switching from the inactive to active state, the Cα-helix typically undergoes a dramatic shift in position toward the active site, opening the ATP binding cleft and enabling interactions with the N-lobe and between the lobes. A conserved ion pair formed between a Glu in the Cα-helix and a Lys residue in the N-lobe bridges the nucleotide and helps to stabilize the Cα-helix in the active conformation. In PKA and IRK, the active kinase is characterized by a hydrogen bond between the RD arginine and the carboxyl oxygen of a residue in the magnesium binding loop. This interaction is absent in many inactive structures and may serve to stabilize the N-terminal anchor of the activation loop (Nolen, Taylor et al. 2004). An active kinase is characterized by the lobes closed around ATP, a fully structured phosphorylated activation loop anchored to C-lobe by interactions between the phospho-residues and the basic binding pocket, the presence of a conserved ion pair that helps coordinate the kinase-nucleotide interaction, and fully assembled internal hydrophobic spines. The two residues, the Asp in the DFG motif and an Asn at the back of the ATP binding cleft, coordinate the Mg^{2+} ions.

Analysis of the extant *Mtb* STPK structures in light of these considerations reveals that these kinases show features of both inactive and active conformations. None of the structures of phosphorylated PknB contain density for the activation loop. This disorder may be caused by heterogeneous phosphorylation as PknB has multiple phosphorylation sites on the activation loop (Boitel, Ortiz-Lombardia et al. 2003; Young, Delagoutte et al. 2003). While active kinases with disordered activation loops are unusual, the crystal structures of the C-terminal Src kinase Csk and PDK1 have no density for multiple residues in the tip of the activation loop (Biondi, Komander et al. 2002; Ogawa, Takayama et al. 2002). Substrate binding may be required to stabilize the activation loop of the *Mtb* STPKs. Lack of activation loop density is not an indication that the kinase is inactive, but does suggest fundamental differences in mechanism between the eukaryotic and prokaryotic STPKs.

The recent analysis of 24 active kinase structures revealed significant structural diversity in the activation segment which contrasts starkly with the striking level of structural conservation in the N- and C-terminal ends of this peptide (Nolen, Taylor et al. 2004). The ends of the activation segment, the anchor points, adopt the same conformation in the active state, regardless of the activation loop structure. The conserved DFG sequence in the magnesium binding loop features prominently in the interactions that stabilize the N-terminal anchor. The phenylalanine in this motif interacts with two hydrophobic residues in the Cα-helix, solidifying the interaction between the N and the C lobes. The β9 strand, located C-terminal to the DFG motif forms three hydrogen bonds with β6 (Figure 4.2). In inactive kinases, this interaction is disrupted, altering the conformation of the anchor segment and magnesium-binding loop. This altered arrangement

of the residues essential for magnesium binding prevents the appropriate positioning of the ATP phosphates for phosphoryl-transfer. Disruption of this loop also impacts the positioning of the Cα-helix, preventing interactions necessary for catalysis. The C-terminal end of the activation segment begins in the middle of the P+1 loop. This region of the kinase enables formation of the substrate-binding interface in eukaryotic kinases. A conserved Ser or Thr residue linking the P+1 loop to the catalytic loop is the first residue of the C-terminal anchor. Hydrogen bonds between this residue and the amino acids utilized for catalysis are a hallmark of an active STPK.

The activation segment anchors are intact in all PknB structures solved to date. The N-terminal end of this peptide forms the canonical H-bonds between β6 and β9 (Figure 4.2). In contrast, the apo-PknE structure displays significant conformational changes in this anchor. The N-terminal end of the PknE activation segment is shifted into the active site, with the phenyalanine ring of the DFG motif located in the ATP binding cleft (Figure 4.2). Both the PknB and PknE structures lack density for the activation segment between the DFG motif and the P+1 loop, hindering analysis of the active kinase conformation. The first structured residue on the C-terminal end of the activation segment is the conserved Thr residue that links the P+1 loop to the catalytic loop. The side chains of this amino acid are in different conformations in the PknB and PknE structures, preventing the formation of hydrogen bonds between the Thr and the residues in the catalytic loop. The altered conformation visible for this amino acid in both *Mtb* kinase structures may be due to disorder in the activation loop.

In the active PknB structures, the conserved Lys40 located immediately above the ATP-binding interacts with the α- and β-phosphates and forms an ion pair with the conserved Glu59 in the Cα-helix (Figure 4.3) (Young, Delagoutte et al. 2003). The structures of PknB bound to nucleotide analogs show the closed conformation with the P-loop dropping down to interact with the phosphates in the binding cleft. The apo-PknE structure is remarkably similar to the PknB active kinase structures in regards to positioning of the N and C-lobes (Figure 4.4). The positioning of the N-terminal activation segment linker in the ATP binding site likely maintains the overall conformation of the kinase in the absence of ligand. Active ligand-bound PknB exhibits a fully intact R-spine (Figure 4.5). As expected for an inactive kinase conformation, the apo-PknE R-spine is disturbed. Assembly of the R-spine is frequently viewed as a consequence of activation loop phosphorylation (Kornev and Taylor 2010); however, ligand binding appears to be necessary for PknE R-spine formation as this structure is of the phosphorylated, active kinase. The C-spine assembles around the adenine ring of bound ATP, integrating the N- and C-lobes (Kornev, Taylor et al. 2008). The C-spine depends on the presence of ATP, while the R-spine is thought to depend on activation loop phosphorylation. Like the R-spine, the C-spine is fully assembled in PknB (Figure 4.5).

The conservation of these structural features indicates that regulatory motifs identified in eukaryotic kinase structures are conserved in prokaryotic STPKs. A unique conformation is adopted by the PknE C-spine, as this apo-protein lacks the ligand adenosine ring normally utilized to form the vertebrae connecting the N- and C-lobes. Instead, the DFG-Phe is positioned in place to form this essential connection. Despite the lack of a ligand, the PknE C-spine is fully formed. This displacement of the DFG motif prevents formation of the R-spine, suggesting that C-spine assembly may be required to stabilize the protein in the absence of ligand.

PknB and PknE crystallize in a characteristic back-to-back dimer, similar to the conformation of human PKR (Greenstein, Echols et al. 2007). The dimer interface contains multiple conserved residues (Av-Gay, Jamil et al. 1999; Young, Delagoutte et al. 2003)

A.

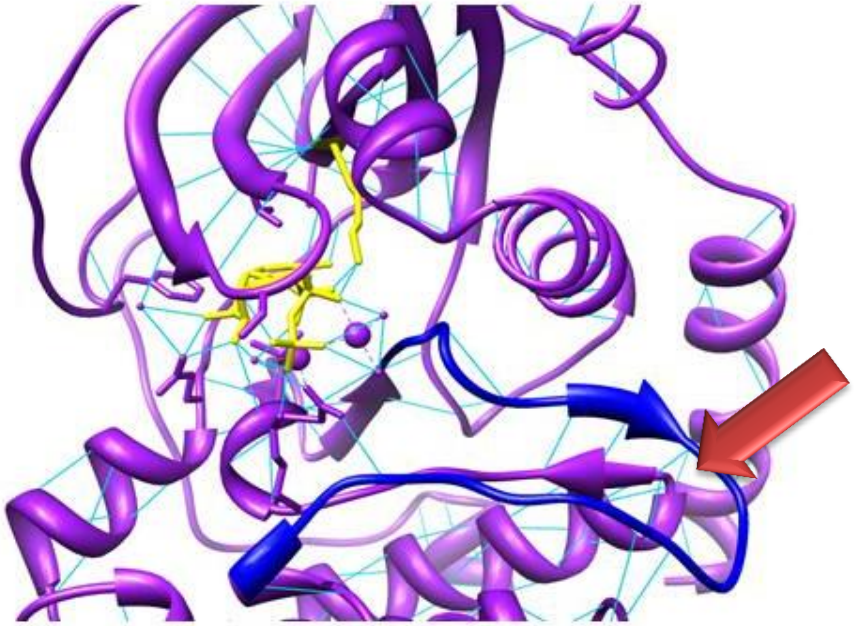

B.

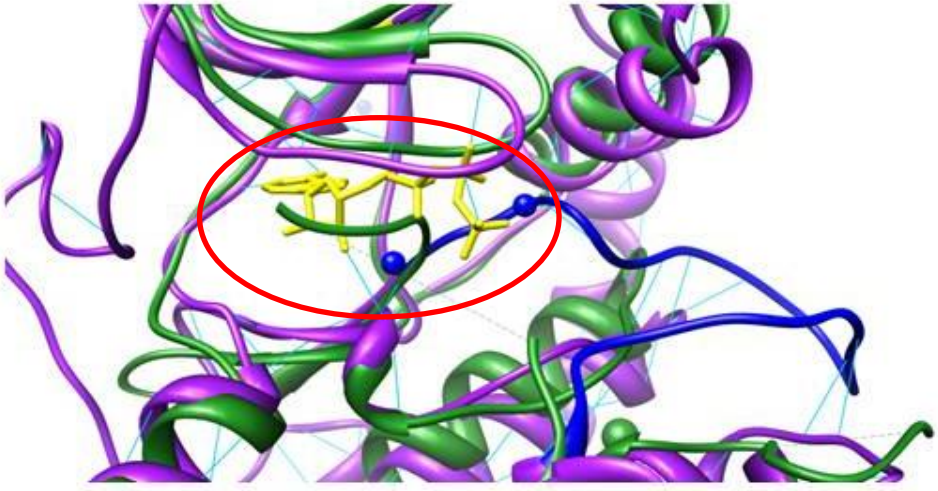

Figure 4.2 A) The canonical Ser/Thr kinase structure of active PKA (1ATP) contains full activation segment density, highlighted in dark blue. The invariant Lys residue, in yellow, contacts the ATP, also in yellow. Hydrogen bonds are depicted as aqua lines. Three H-bonds are responsible for locking the activation loop in the active conformation and are emphasized by the red arrow. **B)** A superposition of the apo-PknE structure (PDB ID 2H34) (green) with the PKA structure (purple) highlights the altered conformation of the N-terminal anchor of the PknE activation segment, visibly overlapping the ATP binding site (circled).

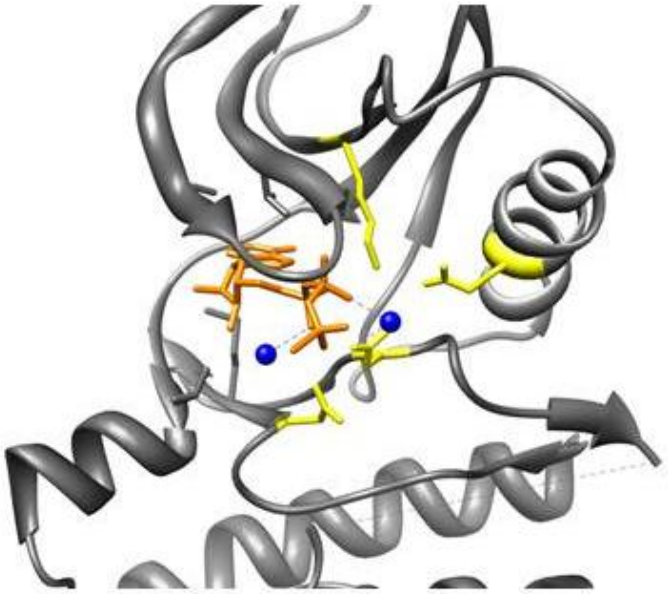

Figure 4.3 The residues in the PknB monomer (grey) responsible for coordinating the bound ATP and the magnesium ions (yellow). The metal ions are colored blue and the ATP molecule in the ligand binding cleft is orange.

including Asp10, Leu33 and Arg76 that form crucial intersubunit interactions necessary for dimer formation (Figure 4.6). An intermolecular ion pair between Arg76 and Asp10 in the N-lobe makes hydrophobic contacts with Leu33 and an intramolecular hydrogen bond with a proximal Tyr to stabilize the dimer (Young, Delagoutte et al. 2003).

Formation of a similar back-to-back dimer activates several eukaryotic kinases including PKR and Ire1 (Alber 2009). PKR, the human double-stranded RNA dependent protein kinase, is activated by dimer formation in response to double-stranded RNA binding to the ligand-binding domain (Greenstein, Echols et al. 2007). The Ire1 dimer mediates assembly of a larger oligomer that stimulates the cleavage of physiological substrates by the attached ribonuclease domains. An inducible dimerization system has been used to probe the role of STPK dimerization for the *Mtb* kinases PknB and PknD. In both cases, dimerization of the unphosphorylated kinase resulted in activation. This result implies that phosphorylation, and therefore activation, are mediated by this allosteric interface. Conservation of the back-to-back dimer formation is indicative of an ancient structural feature with an important role in Ser/Thr phospho-signaling.

Sequence analysis of the STPKs indicates that the dimer interface residues are more similar among the three distinct evolutionary clades (ABL, DEH, FIJ) (Greenstein, Echols et al. 2007). N-lobe dimer interface mutants of PknB crystallize as monomers in a variety of conformations. One such structure also revealed an unusual front-to-front dimer in which the subunits are offset along the contacts in the G-helix (Mieczkowski, Iavarone et al. 2008). This asymmetric kinase pair shows features expected for an autophosphorylation complex, with one monomer serving as the substrate and the other monomer serving as the active enzyme. The activation loop of the enzymatic kinase is ordered, while this loop in the substrate kinase is disordered with the ends positioned at the entrance to the active site of the enzymatic kinase. This crystal structure provides a potential view of the trans-phosphorylation reactions that activate the *Mtb* STPKs. However, the structure of an inactive *Mtb* STPK remains to be solved.

Figure 4.4. A) The PknB structure (dark gray) is superimposed on the apo-PknE structure (green) as a dimer. This overlay highlights the difference in the back-to-back dimer interface of these two proteins. **B)** An overlay of the PknB and apo-PknE kinase domain reveals the nearly identical orientation of the N- and C-lobes.

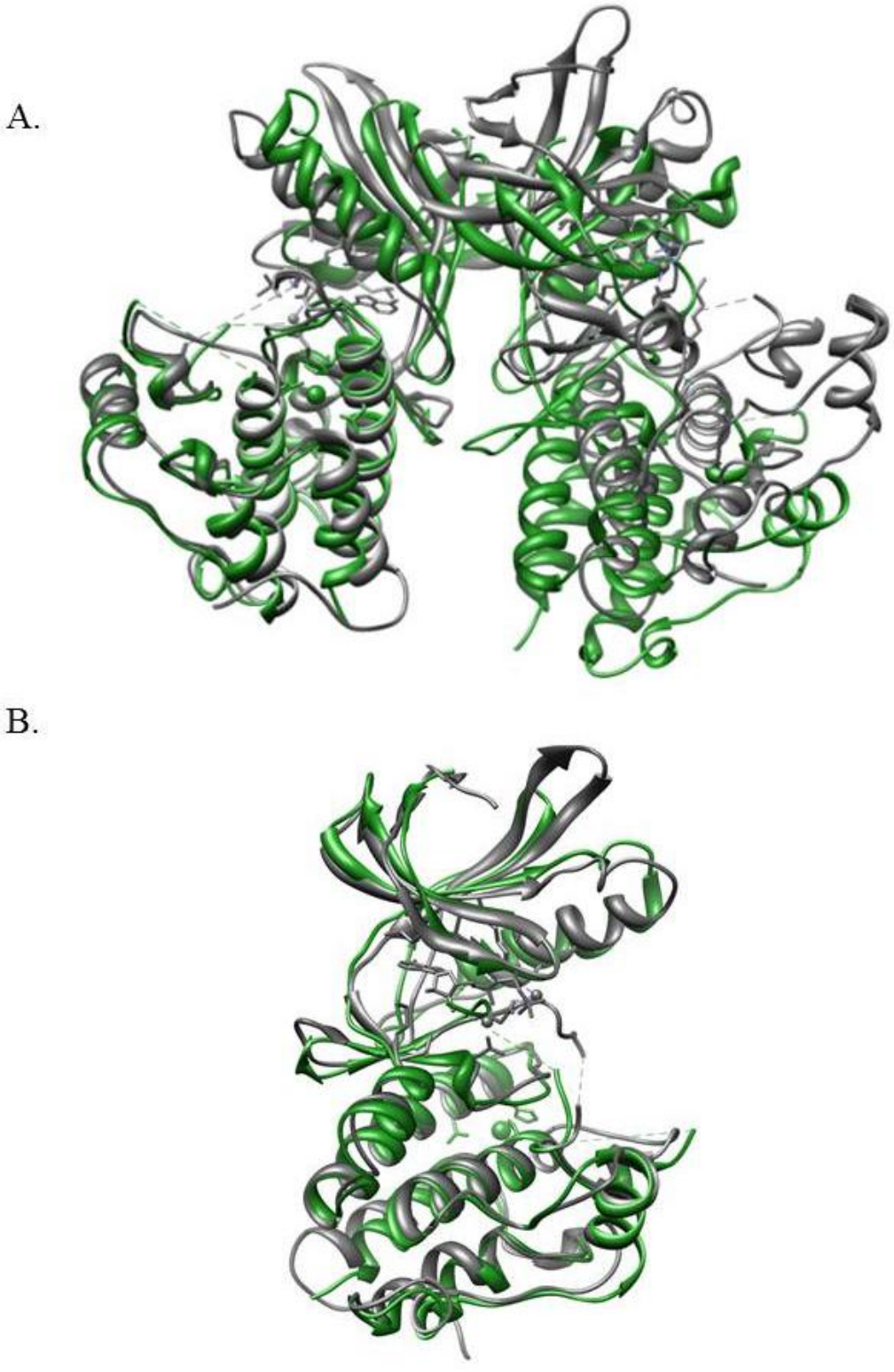

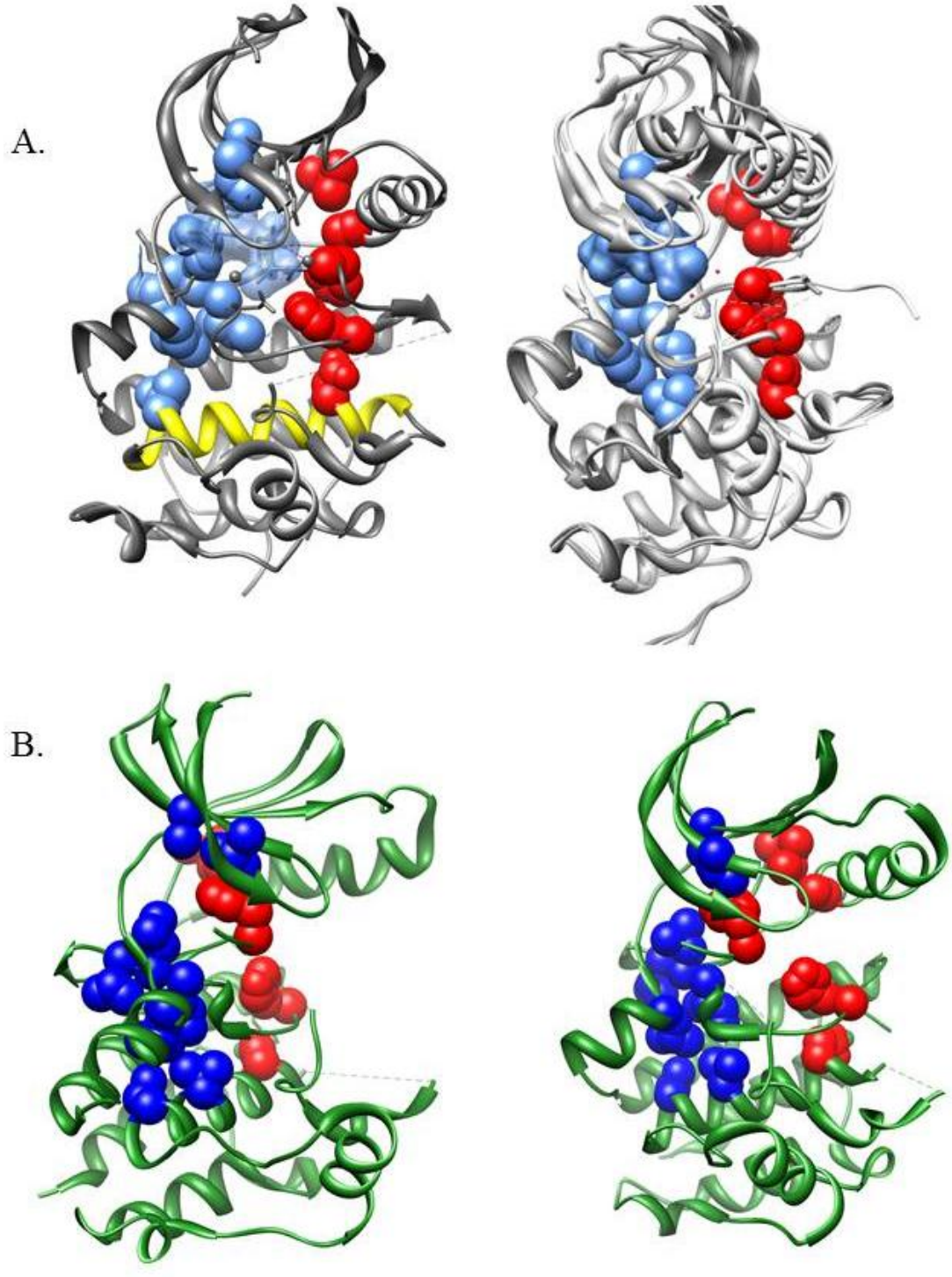

Figure 4.5 A) The PknB structure contains an intact C-spine (blue) and R-spine (red). The F helix is highlighted in yellow. **B)** The apo-PknE structure contains an intact C-spine completed by the final ordered N-terminal residue on the activation segment. This residue slips out of the R-spine (red) and takes the position of the adenosine ring from ATP in the PknE structure.

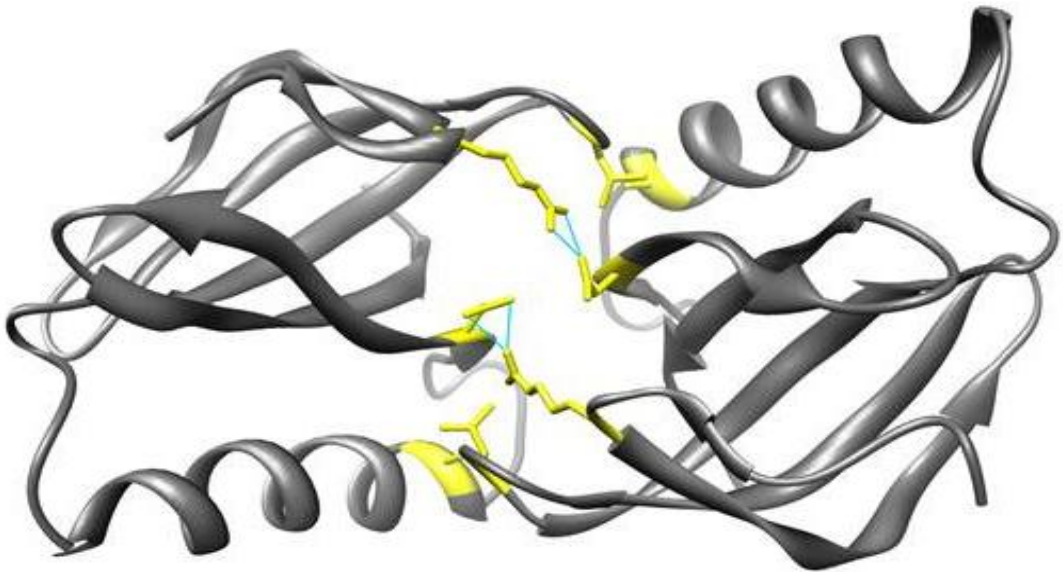

Figure 4.6 In this top-down view of the back-to-back PknB kinase domain dimer, critical residues are highlighted in yellow and H-bonds are depicted in aqua.

The comparison of active and inactive structures would elucidate the auto-inhibitory mechanism utilized by these Ser/Thr kinases.

By purifying the kinase domains of the 11 *Mtb* STPKs, I took a systematic approach to define the structural changes that activate a bacterial receptor STPK. PknH, a master regulator kinase in the DEH evolutionary clade, proved to be a tractable target for crystallography. In addition to phosphorylating PknE, PknF, PknG and PknJ, PknH phosphorylates EmbR, a DNA-binding transcription factor involved in regulating the synthesis of the cell-wall component arabinogalactan (Molle, Kremer et al. 2003). EmbR contains a phospho-peptide binding FHA domain that is hypothesized to recognize the active kinase. PknH is not essential in *Mtb*, but the knockout strain exhibits a hypervirulent phenotype *in vivo* (Papavinasasundaram, Chan et al. 2005). *PknH* is induced during macrophage infection, heat shock and low pH, and expression of this gene alters resistance to the anti-mycobacterial agent ethambutol (Sharma, Gupta et al. 2006). Phosphorylation of EmbR increases transcription of the *embA* and *embB* genes, resulting in the resistance phenotype. PknH contains a folded extracellular domain of unknown function, and is hypothesized to mediate cellular responses to environmental stress (Sharma, Gupta et al. 2006)

The majority of kinases are maintained in the inactive state. These proteins are activated by interaction with a signaling molecule that releases autoinhibition and triggers phosphorylation that stabilizes the active conformation. The structures of the PknH kinase domain in the active and inactive forms will provide insights into mechanisms of kinase activation and may reveal the *Mtb* STPK autoinhibition mechanism.

Results

Initial crystallization trials were conducted with the wild-type PknH kinase domain encompassing residues 1-280. Notably, this protein construct requires a minimum of 10% glycerol in the buffer at all times to prevent precipitation. Crystallization trials using the non-

hydrolyzable ATP analog ATPγS and $MnCl_2$ yielded hits in several conditions. The crystals proved difficult to reproduce, but data sets were collected from crystals harvested from the screening trays. The final crystallization condition was 0.1 M cacodylate pH 6.5, 0.2M LiSO4, and 20% PEG400, with 300 μM protein, 3 mM ATPγS and 1.5 mM $MnCl_2$. The crystals were frozen in well solution.

The structure was solved with molecular replacement using a PknB (1MRU) monomer poly-alanine model with two molecules in the asymmetric unit (Adams, Afonine et al. 2010). Refinement using PHENIX at 3.5-Å resolution yielded R/Rfree values of 0.257/0.28 (Table 4.1).

To trap the inactive form of the kinase domain, I introduced the Asp138Asn mutation, which alters the Asp in the RD motif. Mass spectrometry confirmed the absence of autophosphorylation on this PknH mutant. Crystals were obtained in >15 conditions including 0.2 M Potassium Acetate, 20% PEG 3350, 300 μM protein, 3 mM ATPγS and 1.5 mM $MnCl_2$. X-ray data was collected to 2.09-Å resolution. A poly-alanine model from the initial PknH molecular replacement solution was utilized as the MR search model. The structure was refined using PHENIX to R/R free values of 0.188/0.232 (Table 4.1).

To probe the impact of ligand binding on the PknH structural conformation, the inactive kinase was crystallized with an alternate nucleotide, AMP-PNP, and without nucleotide. A mixture of inactive PknH with 3 mM AMP-PNP and 1.5 mM $MnCl_2$ crystallized readily in 0.1M Bis-Tris pH 6.5, 45% Polypropylene glycol P400. These crystals were frozen in the well solution. The ligand-free and metal-free inactive PknH crystals grew in 30% Tacsimate pH 7.0 and were frozen in this solution with the addition of 30% glycerol. The crystal structures were determined at 2.08-Å and 2.07-Å resolution, respectively (Table 4.1).

Unexpectedly, the crystal structures of both the active and inactive PknH kinase domain constructs in the presence and absence of ligand formed the characteristic back-to-back dimer formed by the active forms of PknB and PknE (Figure 4.7). This structure was paradoxical for the unphosphorylated kinase domain, because dimerization actives the unphosphorylated PknB and PknD monomers (Greenstein, Echols et al. 2007; Lombana, Echols et al. 2010).

Based on the dimer interface in the crystal structure, I designed a series of dimer interface mutants. Previous crystal structures of the PknB Leu33Asp interface mutant revealed a variety of inactive conformations with large active site-distortions (Lombana, Echols et al. 2010). N-lobe dimer interface mutants of PknB and PknD block dimerization and phosphorylation of the kinase domain *in vitro* and block activation of full-length PknB in Msmeg. For these kinases, N-lobe dimerization appears necessary for activity (Greenstein, Echols et al. 2007).

To disrupt the PknH kinase domain dimer, Lys38, Glu39, Trp40, His80, and Tyr82 were individually replaced with Ala. Tyr82 was also changed to Val. The PknH dimer interface mutants purified readily using the standard purification protocol. Size-exclusion chromatography, native polyacrylamide gel electrophoresis (native PAGE) and western blotting with anti-phospho-Thr antibody were used to determine the oligomerization of each protein (Figure 4.8). Unlike the kinase domains of PknB and PknE, which form weak dimers, the active and inactive forms of PknH run as a dimer on a sizing column and native gel. Western blots of the dimer interface mutants revealed that all constructs are phosphorylated (Figure 4.8). Native PAGE and size exclusion chromatography analysis suggest that the dimer interface is weakened in these mutants with an increased population of monomers in solution (Figure 4.8). The PknH Tyr82Val and Glu39Ala mutants crystallized readily. The structure of the Tyr82Val construct bound to AMP-PNP and $MnCl_2$ was determined at 2.7-Å resolution (Table 4.1).

Table 4.1	PknH - ATPγS	PknH D139N - ATPγS	PknH D138N - AMP-PNP	PknH D138N	PknH D138N Y82V - AMP-PNP
Data Collection					
Space group	$P6_1$	$P6_1$	$P6_1$	$P6_1$	$P6_1$
Unit cell dimensions					
a,b,c (Å)	79.74, 79.74, 181.5	79.22, 79.22, 181.03	79.79, 79.79, 180.74	80.1, 80.1, 181.26	81.42, 81.42, 178.9
Resolution (Å)	69-3.53	68.1-2.09	90.3-2.08	69-2.07	89.46-2.71
R_{merge}	0.358	0.078	0.037	0.075	0.122
mean (I/σI)	8.1	22.9	25.8	20	17.9
Completeness (%)	99.6	99.9	97.5	99.8	99.9
Redundancy	7.7	8.2	5.5	6.1	8.1
Refinement					
Resolution (Å)	69-3.53	68.1-2.09	36.4-2.08	69-2.07	70.5-2.71
Unique Reflections		37760	35796	39636	18157
R_{work}/R_{free}	25.7/28.0	18.8/23.2	21.0/25.9	19.4/22.6	23/29.23
Atoms	3960	4482	4425	4348	3961
Protein	3926	4190	4073	4073	3789
Ligand/ion	34	77	87	0	79
Water	0	213	265	275	93
B-factors (overall)	32.7	33.35	48.436	34.022	43.147
r.m.s.d.					
Bond lengths (Å)	0.009	0.009	0.011	0.013	0.027
Bond angles (deg)	1.59	1.23	1.3	1.72	2.27

Figure 4.7 The unphosphorylated PknH D139N structure is depicted in purple and the wild-type PknH structure is pictured in turquoise. Both structures contain ATPγS and $MnCl_2$.

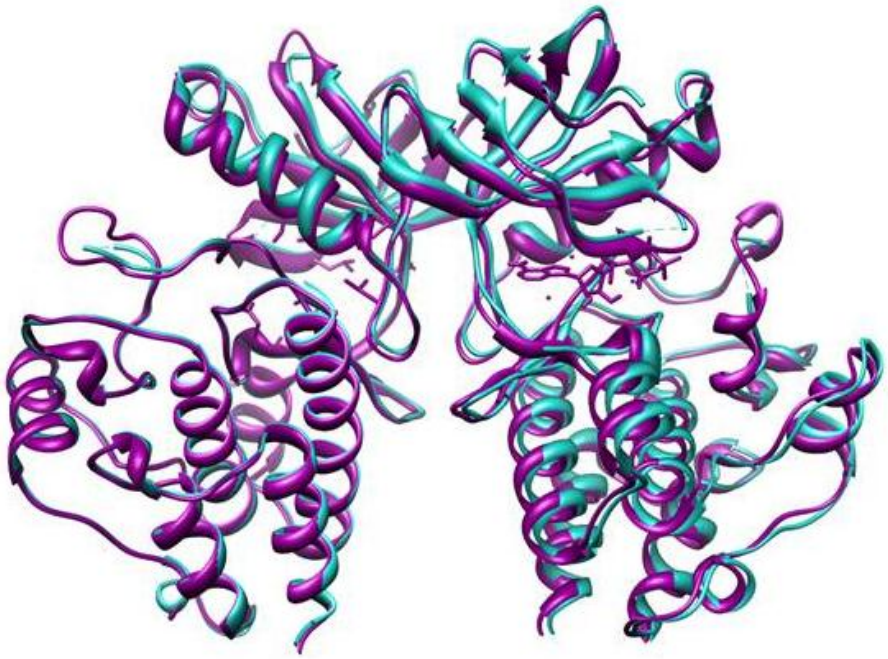

Despite the presence of the substitution in the dimer interface, the PknH Tyr82Val variant forms the classic back-to-back dimer in the crystals (Figure 4.13). The substitution introduces a cavity at the replacement site and the C-terminus of the Cα-helix unwinds (Figure 4.13). Although other shits in the dimer are small, these results emphasize how the dimer interface communicates with the active site >30 Å across the protein by controlling the position of the Cα-helix.

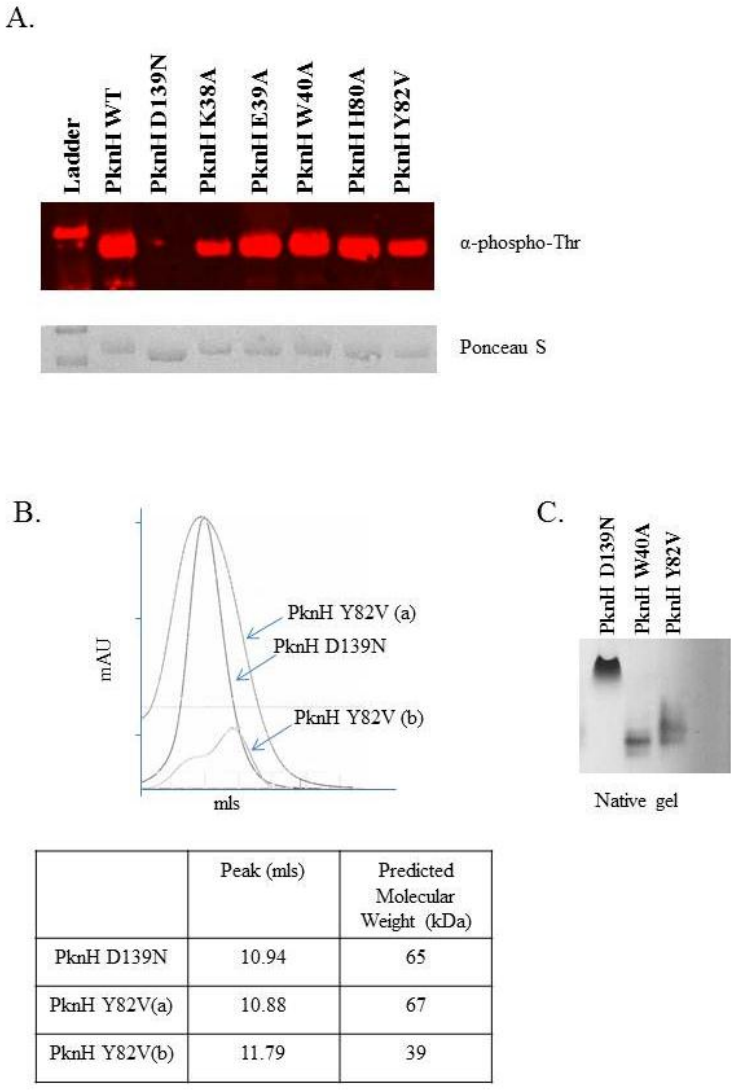

	Peak (mls)	Predicted Molecular Weight (kDa)
PknH D139N	10.94	65
PknH Y82V(a)	10.88	67
PknH Y82V(b)	11.79	39

Figure 4.8 A) An anti-phospho-Thr western blot of the dimer interface mutants reveals that these proteins are still phosphorylated and therefore still capable of forming dimers. PknH Asp138Asn acts as the unphosphorylated negative control. **B)** Chromatograms of analytical size exclusion chromatography show the differences in oligomeric state for the PknH Asp139Asn mutant and the PknH Tyr82Val dimer interface mutant. At low concentrations, PknH Tyr82Val contains more monomer than dimer. The predicted molecular weights for each peak are listed in the table. **C)** A native gel of the PknH mutants demonstrates that the PknH Asp139Asn mutant is a dimer while the PknH Trp40Ala and Tyr82Val mutants are significantly smaller, indicative of a monomer.

Discussion

Multiple crystal structures of active *Mtb* kinases have been determined, but the inactive conformations of these proteins remain unknown. PknH structures in phosphorylated and unphosphorylated forms were solved to enable the exploration of intramolecular remodeling that may occur as the kinase switches from the off-state to the on-state. Structural analysis of many eukaryotic kinases provides multiple metrics for determining the activation state of a STPK. In general, active kinases contain intact R- and C-spines, a DFG-in conformation coordinating the ligand and Mg^{2+} ions in the proper positions for catalysis, a Cα-helix engaged by a conserved salt bridge, and an ordered activation loop. Examination of the PknH structures in light of these characteristic features enables the classification of each conformation as 'active' or 'inactive'.

An overlay of the wild type and Asp139Asn PknH kinase domain structures reveals an unexpected degree of similarity (Figure 4.7). The crystals had the symmetry of space group $P6_1$ with nearly identical unit-cell dimensions despite widely differing crystallization conditions. The structures invariably had two kinase molecules in the asymmetric unit forming a characteristic back-to-back dimer very similar to active, phosphorylated PknE and PknB.

The regulatory and catalytic spines are intact in the PknH structures (Figure 4.9). Superposition of the kinase spines from the PknB with the wild-type PknH kinase domain PknH wild-type structures demonstrates that these residues are in nearly identical positions in the two kinases.

The Cα-helix of PknH is tilted toward the active site, assuming the active conformation and enabling proper formation of the C-spine. Intriguingly, the R-spine is fully assembled in the inactive PknH structure with and without nucleotide. This result is unexpected as the adenine ring of ATP is considered essential for proper assembly of this structural feature. Unassigned density is visible in the apo-PknH structure (Figure 4.10). This density may indicate partial occupancy of the ATP binding cleft, despite purification of the protein without adding nucleotide prior to crystallization. A partially occupied active site may be responsible for the unphosphorylated PknH Asp139Asn mutant assuming a conformation nearly identical to the active kinase.

In the phosphorylated and unphosphorylated PknH kinase domains, the ATP-binding cleft adopts a conformation characteristic of in an active kinase. The magnesium binding loop DFG motif is flipped 'in' to engage the metal ions. The unphosphorylated Asp139Asn PknH mutant adopts the active conformation even though the activation loop is not phosphorylated. Unlike the activation loop of the wild-type PknH kinase domain, this segment is ordered in the structure of the unphosphorylated Asp139Asn variant (Figure 4.11)

These results, particularly the unexpected similarity of the phosphorylated and unphosphorylated PknH kinase domain structures, are subject to different interpretations. While activation loop phosphorylation leading to conformational remodeling and ligand binding is the accepted activation pathway for multiple eukaryotic kinases (Nolen, Taylor et al. 2004), these structures suggest that movement from the off-state to the on-state may occur through a different series of steps for the *Mtb* STPKs.

Phosphorylation may activate PknH by controlling the recognition specificity of the activation loop. This model almost certainly applies to substrates like GarA and EmbR, in which RHA domains recognize phospho-Thr sites on the kinase. The unphosphorylated PknH activation loop extends outward from the ATP binding cleft. This conformation may permit substrate binding or alternatively sequester the activation loop in a conformation that does not

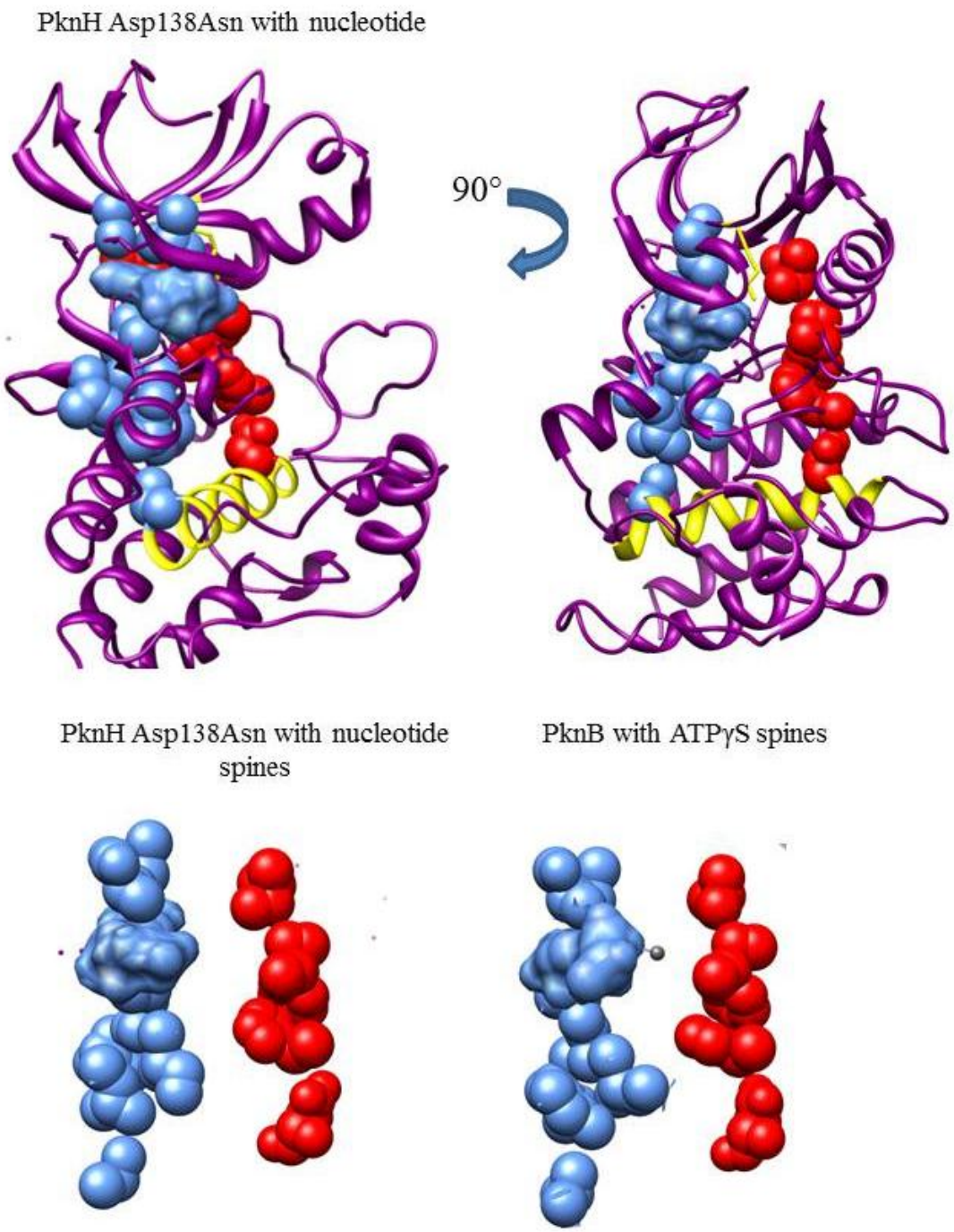

Figure 4.9 Intact C- (blue) and R-spines (red) are present in the Asp138Asn PknH:ATPγS complex. The PknH D139N with ligand structure is shown in purple. The C-spine is highlighted in blue, the R-spine is in red and the F helix is in yellow. For comparison, the PknH and PknB spines are shown below the ribbon diagram. These two proteins display fully intact kinase spines

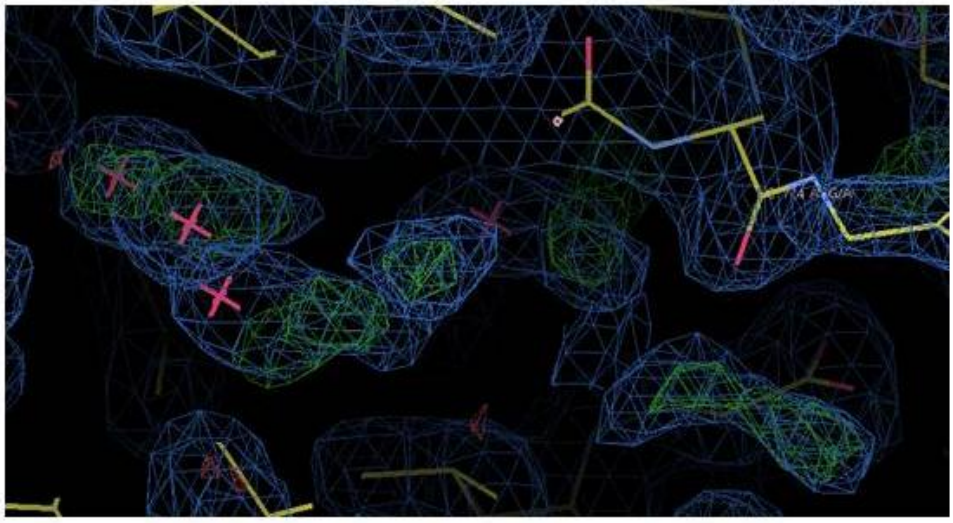

Figure 4.10 Unassigned active site density in the apo-PknH D138N structure may be representative of partial occupancy. As a place holder, waters (red asterisks) have been added to some of this density (depicted in blue and in green).

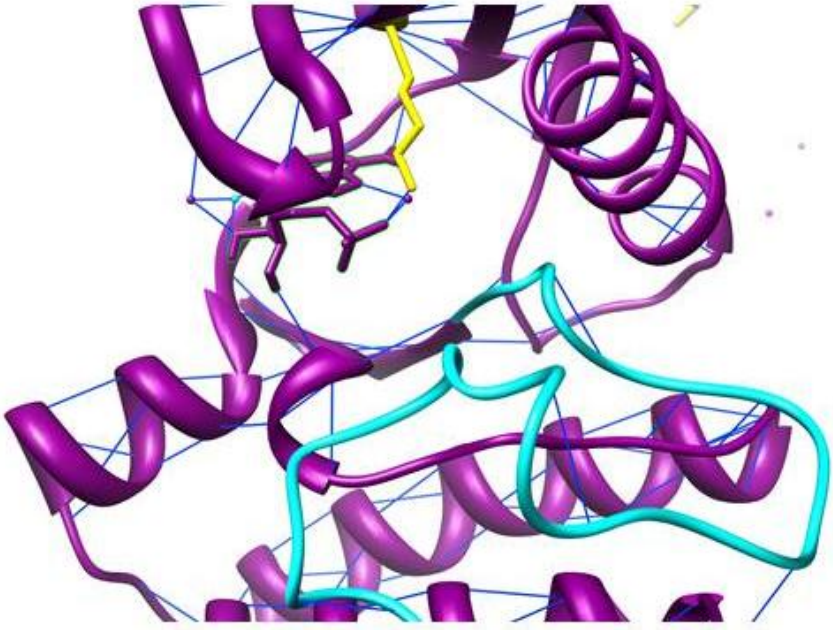

Figure 4.11 The activation loop (turquoise) is visible in the PknH Asp139Asn structure. H-bonds (dark blue) help stabilize the activation loop in an open conformation.

recognize substrates.

In contrast, the phosphorylated activation loop is disordered in the wild-type PknH kinase domain. The structure of the activation loop has not been observed for an *Mtb* STPK in the 'activated' back-to-back dimer form. The clear identification of this peptide in the unphosphorylated structure lends credence to the idea that the phosphorylated activation loop is disordered in the wild-type kinase structures due to hyper- or heterogeneous phosphorylation. The N-terminal anchor of the unphosphorylated PknH activation segment is stabilized by the hydrogen bonds between this peptide and the catalytic loop. The extended conformation of this loop is further stabilized by back-bone-mediated hydrogen bonds between the activation loop and the peptide N-terminal to the F-helix. Backbone interactions serve to stabilize the half-turn located in the middle of the activation loop. One of the two Thr phosphorylation sites, Thr170, is located in the middle of this turn. Phosphorylation of this amino acid will alter the local electrostatic charge, perhaps promoting activation loop flexibility. The second phosphorylation site, Thr 174, is located at the C-terminal end of the activation loop. Like Thr170, this residue resides in an area of neutral charge in the unphosphorylated PknH structure. Phosphorylation of Thr174 likely contributes to activation loop disorder.

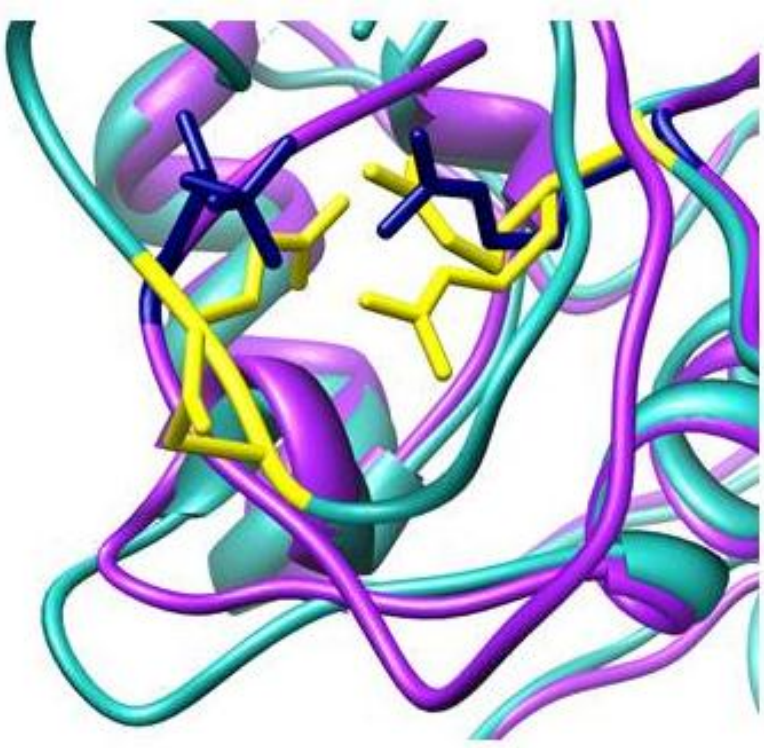

Figure 4.12 An overlay of the PknH Asp139Asn activation loop (turquoise) with the PKA activation loop (purple) highlights the similarity between these two structures. The phosphorylated residue, Thr197, and the interacting Arg are depicted in navy blue for PKA. Glu167, Asp166, and Arg138 from PknH are highlighted in yellow.

Ser/Thr protein kinases commonly exhibit a binding pocket, known as the RD pocket, which locks the phosphorylated activation loop in place. In PKA, the phosphorylated Thr197 in the activation loop forms an ion pair with a conserved Arg in the catalytic loop to help rotate the DFG into position (Huse and Kuriyan 2002). This binding surface is conserved in PknB, but the activation loop disorder makes any conclusion about side chain interactions in this region impossible (Ortiz-Lombardia, Pompeo et al. 2003). Three of the RD-pocket residues are conserved in PknH: Arg60 and Arg63 in the Cα-helix and Arg138 in the catalytic loop. In PknH, Glu167 is located in the Thr197 position (Figure 4.12). The Arg138 side chain is positioned to interact with the Glu167 side chain. Asp166 is located immediately N-terminal to this residue and may also interact with the Arg138 side chain. This Arg exhibits multiple side-chain conformations in the crystal structure. The occurrence of a negatively charged residue in place of the Thr may enable activation loop binding in this area of the protein and possibly eliminates the requirement for phosphorylation on this portion of the activation segment.

The unphosphorylated PknH Asp139Asn mutant crystallized with ATPγS and $MnCl_2$ is the only *Mtb* STPK kinase domain structure to exhibit full activation loop density. The other PknH structures exhibit disorder in this region to varying extents. Despite variation in the phosphorylation state of the crystallized protein, little Cα-helix movement is observed. In the MAP kinase, ERK2, phosphorylation of the activation loop residues leads to closing of the N- and C-lobes (Huse and Kuriyan 2002). Movement of this sort is not observed in the PknH kinase domain structures.

A third model holds that PknH, in particular, is regulated by a different mechanism than the other *Mtb* receptor kinases. PknH includes a folded, extracellular sensory domain, but, unlike PknB, PknD, and PknE, this domain does not appear to the essential for kinase-domain dimerization. Mutations in the N-lobe dimer interface of PknB and PknD disrupt the dimer interface, resulting in inactive, unphosphorylated monomeric kinases (Greenstein, Echols et al. 2007; Lombana, Echols et al. 2010). In contrast, the wild-type PknH kinase domain forms a stable, preformed dimer in solution and the PknH dimer interface mutants are phosphorylated (Figure 4.8). This PknH dimer may be constitutively active and capable of autophosphorylation. The stability of the isolated PknH dimer may indicate that, rather than stabilizing the association of the kinase domains, ligand binding to the extracellular domain may separate the monomers to inactivate the kinase.

The PknH Tyr82Val mutant in complex with AMP-PNP and $MnCl_2$ crystallizes as a back-to-back dimer. Disorder is observed in the N-lobe. The mutation in the dimer interface disrupts the C-terminus of the Cα-helix (Figure 4.13). This result indicates that the PknH dimer interface is essential for maintaining the active conformation of the kinase. The PknB monomeric variant structures exhibit altered N-lobe conformations with unraveling of the Cα-helix relative to the active back-to-back dimer. These similar structural effects suggest that the dimer interface may be a conserved feature for kinase activation.

Analysis of the unphosphorylated PknH kinase-domain structure in light of the features considered essential for kinase activity suggests that this structure captures an activated, but unphosphorylated conformation. Phosphorylation of Thr170 and Thr174 are essential for autophosphorylation and trans-phosphorylation of GarA (Chapter 3), suggesting that the unphosphorylated kinase is inactive in solution. This apparent paradox could be resolved by a fourth model in which the unphosphorylated PknH dimer represents not the inactive form, which may be monomeric, but rather provides a view of an activated conformation poised to catalyze autophosphorylation. Thus, although the kinase domain is unphosphorylated, the high kinase

domain concentration used for crystallization may trap the N-lobe dimer in the crystals, mimicking the ligand-activated dimer.

The structures of the phosphorylated and unphosphorylated PknH kinase do not reveal the structure of an unphosphorylated, inactive *Mtb* STPK monomer or resolve the mechanism of bacterial STPK activation. Nonetheless, the crystal structures of the PknH kinase domain reveal important structural motifs that may be characteristic of the *Mtb* Ser/Thr kinome. Importantly, the back-to-back N-lobe dimer formation is stabilized in PknH, strengthening the idea that this interaction is a conserved allosteric activating feature of bacterial STPKs. The unphosphorylated PknH kinase domain structure also provides the first view of the conformation of the activation loop. The conformation of the unphosphorylated activation loop is incompatible with phosphorylation of Thr170 and Thr174, revealing why the loop conformation is sensitive to phosphorylations. The disorder of the phosphorylated activation loop also appears to be a general feature of the *Mtb* receptor STPKs that may be preserved to allow this segment to adapt to a diverse set of substrates.

Figure 4.13 Superposition of the N-lobes of PknH Asp138Asn (purple) and PknH Asp138Asn Tyr82Val (turquoise) reveals unraveling of the Cα-helix (circled) due to the dimer interface mutation.

Methods

Protein expression and purification

PknH constructs were expressed using the auto-induction protocol described previously. The cells were lysed and the initial Ni-IMAC column was run as detailed above. The PknH 6XHis-MBP construct was purified with Ni-IMAC from *E.coli* lysate, and the 6X-His-MBP tag was cleaved with TEV protease. TEV cleavage was performed during dialysis into 30 mM NaCl, 25 mM HEPES pH 8.0, 0.5 mM TCEP, 25 mM Imidazole and 20% glycerol. A paired ion-exchange-Ni-IMAC purification scheme was utilized to remove the tag. The protein was loaded onto an anion-exchange HQ column directly attached to a Ni-IMAC column. The columns were washed with 10 column volumes of low salt, low imidazole buffer. Protein was eluted off the HQ column with a gradual gradient of 1 M NaCl, 25 mM HEPES pH 8.0, 0.5 mM TCEP, 25 mM imidazole, and 20% glycerol. The untagged protein flowed through the columns during elution, while the tag and His-tagged TEV protease were retained on the Ni-IMAC column. Many protocols were tested for this purification protocol because the kinase and cleaved His-MBP tag tend to co-purify. The tandem column method at pH 8.0 yields the largest amount of pure protein. Following the second IMAC run, the protein was concentrated and aggregate was removed with size-exclusion chromatography. The protein was desalted into 75 mM NaCl, 12.5 mM HEPES pH 8.0, 10% glyercol, and 0.25 mM TCEP for crystallization trials.

Western Blot

Proteins were quantified with A280 readings to ensure equal loading and run on a 4-20% TGX MiniPROTEAN gel (BioRad). Transfer to nitrocellulose membrane was performed in a XCell II™ Blot chamber (Invitrogen) at a constant voltage of 25 V for 1 hr. Following transfer, the membrane was incubated with Ponceau S stain for 5 minutes, washed with H_2O to remove excess stain and imaged. The Ponceau S stain was removed with Tris-Buffered-Saline with Tween (TBST). The membrane was blocked overnight at room temperature with shaking using LI-COR Odessey® Blocking Buffer (LI-COR). Washes were performed with a 1:1 dilution of blocking buffer and TBST. Anti-phospho-Thr primary antibody (20 ul; Invitrogen) was diluted in 10 ml of blocking buffer. The membrane was incubated with antibody for 4 hours at room temperature with shaking. Following incubation with a secondary antibody (IRDye 800CW Goat anti-Rabbit IgG, LI-COR), the blot was imaged on an Odessey® imaging system (LI-COR).

Native Gel

Sample concentration was normalized after quantification by Bradford assay to 0.5 mg/ml. Non-denaturing PAGE loading dye and Native PAGE running buffer were used. Samples were run on a 4-20% TGX MiniPROTEAN gel at 60 mV for ~4 hours at room temperature.

Analytical Size Exclusion Chromatography

Samples were run on a Superdex HR 10/300 analytical sizing column using an ÄTKA FPLC (GE Life Sciences) in 150 mM NaCl, 25 mM HEPES pH 8.0, 0.5 mM TCEP, 25 mM imidazole, and 20% glycerol. A molecular weight standards run was preformed immediately prior to the sample run.

Crystallization and structure determination

PknH wild-type with ATPγS – Purified protein with the addition of 3 mM ATPγS and 1.5 mM $MnCl_2$ crystallized when mixed with an equal volume of 0.1 M sodium cacodylate pH 6.5, 0.2 M $LiSO_4$, and 20% PEG400 and equilibrated against precipitant at 18 °C. Crystals that formed in 2-4 weeks were harvested by transferring to mother liquor and flash frozen in liquid N_2.

PknH Asp139Asn with ATPγS – Initial crystallization trials with 3 mM ATPγS and 1.5 mM $MnCl_2$ yielded multiple hits. The best diffraction was obtained from crystals that grew when the protein/ligand solution was mixed with an equal volume of 0.2 M potassium acetate and 20% PEG3350 and equilibrated against precipitant at 18 °C. Crystals formed in ~1 week and were flash frozen in mother liquor with the addition of 25% glycerol.

PknH Asp139Asn with AMP-PNP – A mixture of purified protein with 3 mM AMP-PNP, 1.5 mM $MnCl_2$, 0.1 M Bis-Tris pH 6.5 and 45% Polypropylene glycol P 400 crystallized readily in ~1 week at 18 °C when equilibrated against precipitant. The crystals were harvested and flash frozen in mother liquor.

PknH Asp139Asn – Ligand- and metal-free inactive PknH crystals grew when purified protein was mixed with 30% Tacsimate solution at pH 7.0. Crystals that formed in ~2 weeks were harvested by transferring to the mother liquor supplemented with 30% glycerol and flash frozen in liquid N_2.

PknH Asp139Asn Tyr82Val with AMP-PNP– Purified protein with the addition of 3 mM ATPγS and 1.5 mM $MnCl_2$ crystallized when mixed with an equal volume of 0.08 M sodium cacodylate pH 7.5, 0.16 M calcium acetate, 20% glycerol and 10% PEG8000 and equilibrated against precipitant at 18 °C. Crystals that formed in 2 weeks were harvested by transferring to mother liquor and flash frozen in liquid N_2.

X-ray data were collected at the Lawrence Berkeley National Laboratory Advanced Light Source Beamline 8.3.1 at 100 K and 11111 eV. The data was indexed and data collection strategies were determined using ELVES (Holton and Alber 2004). Data were processed and scaled using XDS and HKL2000 (Otwinowski 1997; Kabsch 2010). Molecular replacement was carried out using Phenix with a poly-alanine model of the PknB wild-type protein bound to ATPγS as the search model (Adams, Afonine et al. 2010). Two molecules were located in the asymmetric unit. Models were modified using Coot and refined with Phenix (Emsley, Lohkamp et al. 2010). Structures were superimposed using Chimera (Pettersen, Goddard et al. 2004). The quality of the models was evaluated using MolProbity (Chen, Arendall et al. 2010).

Chapter 5

X-ray crystal structures of the *Mtb* solution kinase PknK in various phosphorylation states

Introduction

The phosphorylated and unphosphorylated structures of the master regulatory kinase PknH raise many questions concerning the impact of activation loop phosphorylation on STPK conformation. As the unphosphorylated structure has not been solved for any of the remaining STPKs, it is difficult to judge whether the lack of major structural remodeling between these crystal structures and the stability of the unphosphorylated activation loop are general features of unphosphorylated prokaryotic STPKs that hold for the rest of the *Mtb* kinome. The pattern of cross-phosphorylation revealed by the kinase-kinase interaction map presented in Chapter 2 supports a three tiered classification of the *Mtb* STPKs into master regulatory kinases, signal propagation kinases that both receive and transmit the phospho-signal, and substrate kinases. The currently available *Mtb* crystal structures in the PDB include multiple structures of the master regulator kinase PknB and the apo-structure of the signal propagation kinase PknE. However, the structure of a substrate kinase is unknown. The substrate kinases offer the unique opportunity of utilizing the kinase-kinase interactions to trans-phosphorylate the protein on specific sites prior to crystallization. By taking advantage of the ability of various kinases to place differing numbers of phosphates on the substrate kinase, it is possible to visualize the three dimensional structure of this protein in various stages of activation.

PknK, one of the two soluble kinases in *Mtb*, is an appealing target for crystallography as this protein is cross-phosphorylated by multiple kinases. Mass spectrometry revealed that the PknK-PknK interaction resulted in two to three phosphates on the inactive substrate protein, while the interaction with PknB and PknJ leads to the addition of just one phosphate. Crystallizing the protein in the unphosphorylated form, with a single phosphate, with two to three phosphates and in the wild-type, hyperphosphorylated form will enable analysis of the structural changes that may occur as a result of activation loop phosphorylation.

The structure of the other soluble kinase, PknG, in complex with the inhibitor AX20017 allows a comparison of the differences between soluble kinases and membrane-bound enzymes (Scherr, Honnappa et al. 2007). However, PknG differs substantially from other members of the *Mtb* kinome as this protein lacks the Arg preceding the Asp in the catalytic group, making it the only non-RD kinase in *Mtb*. PknG, like other non-RD kinases, is the only *Mtb* STPK that is not activated by phosphorylation on the activation segment (Nolen, Taylor et al. 2004). In the PknG structure, the activation loop is fully ordered and extended in an open conformation. The lack of activation loop phosphorylation may explain the folded nature of the PknG activation loop, in contrast to the other structures of active *Mtb* kinases. Unlike PknG, PknK is an RD kinase that appears to be activated by auto- and trans-phosphorylation in the activation loop region (Chapters 2 and 3).

PknK contains a putative PDZ domain and large C-terminal domain in addition to the N-terminal STPK fold. PDZ domains, common in eukaryotes, consist of 80-90 amino acids and act

as scaffolds for the assembly of signaling complexes (Ranganathan and Ross 1997). The PknK C-terminal domain is homologous to the MalT ATPase domain found in *E. coli*. Phosphorylation sites have been identified on this region, but the functional purpose of these residues is unknown (Kumar, Kumar et al. 2009). MalT is part of the signal transduction ATPase with numerous domains (or STAND) family of large signaling hubs. STAND proteins have a conserved 40 kDa core domain that has ATP activity and is known as the nucleotide-binding oligomerization domain (Danot, Marquenet et al. 2009). These proteins appear to have two states: a monomeric, resting, ADP-bound off-form and an ATP-bound, oligomeric on-state competent for downstream signaling. Curiously, homologs have been purified with bound ADP and AMP, contradicting the model of a static off-state only transiently activated by ATP binding. The effect of MalT domain activation on the associated STPK region in PknK is unknown. The MalT protein in *E.coli* does not have an associated kinase domain, but STPKs are found linked to STAND domains in other organisms, an indication that there is a canonical functional relationship between these two motifs.

PknK phosphorylates multiple substrate proteins in the monooxygenase operon, mymA; however, the role of this phosphorylation is not yet understood (Kumar, Kumar et al. 2009). Transcription of this operon appears to be induced when VirS, as PknK substrate, and PknK are co-expressed. This enhance transcription appears to be dependent on PknK activity, but these results remain speculative as a direct link between phosphorylation and transcriptional control has yet to be demonstrated. Phosphorylation by multiple membrane-bound kinases that are implicated in a wide variety of cellular processes suggests a complex role for PknK in intracellular signaling.

Crystallization of a single protein in multiple phosphorylation states to examine the structural changes at each stage in the activation pathway is an approach previously applied to the eukaryotic tyrosine kinase, Insulin Receptor Kinase (IRK) (Pautsch, Zoephel et al. 2001). Structures of the unphosphorylated (inactive) IRK and fully phosphorylated (active) forms of IRK reveal the significant conformational rearrangement that occurs as a result of activation loop phosphorylation. The unphosphorylated activation segment folds into the ATP binding cleft, sterically blocking ligand binding. In the active form, the activation loop is fully extended for substrate binding, stabilized in this conformation by the interaction of a phosphoryl group and the RD-pocket cluster of basic residues.

The structure of the IRK homolog, the insulin-like growth-factor receptor, IFG-1R, in the bi-phosphorylated form provides a snapshot of the kinase as it moves from the off-state to the on-state (Pautsch, Zoephel et al. 2001). Analysis of the distances in the ATP binding cleft reveals that the doubly phosphorylated-form of IFG-1R is in a half-closed state. The activation segment folded into the ATP binding cleft of the autoinhibited form prevents the N- and C-lobes from closing into the active conformation. This steric block remains present in the bi-phosphorylated structure. The addition of the third phosphate enables final activation loop remodeling into the active conformation. To achieve the active form, the N-lobe undergoes two perpendicular rotations with the result being closure of the active site. These crystal structures represent snapshots of low-energy conformations of intermediates in kinase activation. The comparison of these three structures helps to elucidate the role played by each phosphorylation site. Phosphates are added sequentially to the three IRK Tyr residues with a clear, stepwise impact on protein conformation.

IRK activation is hypothesized to occur through the following steps: autophosphorylation of the first and second Tyr residues introduces negative charges, and the activation loop

compensates by moving to the bi-phosphorylated position. This shift readies the active site for ATP binding, but not for phosphoryl transfer. The addition of the third phosphate gives rise to an ordered activation loop (Pautsch, Zoephel et al. 2001). This step finalizes activation by enabling the lobe closure that moves the ATP toward the substrate, enabling catalysis. This sequential addition of phosphoryl-groups has also been reported for PknA and PknB (Mieczkowski, Iavarone et al. 2008; Thakur, Chaba et al. 2008), leading to speculation that the *Mtb* STPKs undergo a similar step-by-step activation process. Crystallographic studies of the *Mtb* solution kinase PknK in various phosphorylation states of will uncover the steps in kinase activation.

Results

The catalytic domain of PknK is an active enzyme. The kinase domain construct consisting of residues 1-290 proved amenable to crystallographic studies. A cloning artifact leaves an additional 8-residue extension on the C-terminus, but this linker did not appear to impact kinase activity and is not visible in the crystal structures. Based on a multiple sequence alignment to identify the catalytic sequence motifs, the Asn149Asp mutant was constructed to inactivate the kinase domain. Both the mutant and the active protein consistently behave as monomers in solution. Wild-type PknK and unphosphorylated PknK crystallized readily and the structures of complexes with ATPγS were deteremined at 2.3-Å and 2.1-Å respectively (Table 5.1). To define the effects of nucleotide binding, the structure of apo-Asp149Asn PknK kinase domain was determined at 2.2-Å resolution.

The initial inactive, PknK kinase-domain structure proved challenging to solve using molecular replacement. Various search models utilizing poly-alanine monomeric kinase models generated from the PknB, PknG and PknE structures failed to produce a molecular replacement solution. Because kinase C-lobes are relatively rigid, I searched with poly-alanine models encompassing the C-lobes of the *Mtb* kinase structures. While these models provided the first potential solutions, the electron density for the N-lobe remained un-interpretable. The structure was solved by holding the C-lobe solution constant and using poly-alanine models of the N-lobe β-sheets from the PknB structure with all connecting loops deleted. This combination of search models proved feasible only when using the Rotate Around function in Phaser to limit the N-lobe rotational axis to 30 degrees (McCoy, Grosse-Kunstleve et al. 2007). Refinement of this structure revealed significant changes in the orientation of the N-lobe relative to the C-lobe, the root cause of the difficulty with molecular replacement.

To define the effects of phosphorylation on the PknK conformation, I crystallized the hyperphosphorylated wild-type and singly phosphorylated PknK kinase domains. PknB catalyzes the addition of a single phosphate on PknK. This interaction was utilized to generate mono-phosphorylated Asp149Asn PknK kinase domain for crystallization. Following the tag cleavage and Ni-IMAC purification steps, the unphosphorylated Asp149Asn PknK kinase domain was incubated with 6xHis-MBP tagged PknB, ATP and $MnCl_2$overnight at 4 degrees. The PknB was removed with Ni-IMAC followed by size exclusion chromatography. After this purification step, the single phosphorylated PknK was further purified by anion exchange. Given the substantial difference in molecular weight, 75 kDa for tagged PknB *versus* 30 kDa for PknK, and differing isoelectric points, this combination of purification steps effectively removed the PknB from the reaction. The structure of the mono-phosphorylated PknK:ATPγS:$MnCl_2$ complex was determined at 1.7-Å resolution (Table 5.1). The nucleotide complex of the inactive

PknK kinase domain proved to be a suitable search model for the molecular replacement solution of the wild-type PknK kinase domain and the mono-phosphorylated PknK:ATPγS:$MnCl_2$ complex .

Table 5.1	PknK D149N - ATPγS	PknK D149N	PknK D149N - ATPγS +1 PO_4	PknK - ATPγS
Data Collection				
Space group	P3221	P3221	P3221	P3221
Unit cell dimensions				
a,b,c (Å)	62.93, 62.93, 119.86	63.2, 63.2, 120.36	63.61, 63.61, 120.28	63.55, 63.55, 120.0
Resolution (Å)	59.86-2.27	120.23-2.17	60.14-1.7	119.99-2.06
R_{merge}	0.089	0.105	0.059	0.079
mean (I/σI)	16.6	17.9	18	17.1
Completeness (%)	99.6	99.67	99.8	99.9
Redundancy	7.5	7.7	7.8	5.9
Refinement				
Resolution (Å)	49.6-2.37	40.5-2.17	40-1.7	40.57-2.06
Unique Reflections	11696	15206	31458	17893
R_{work}/R_{free}	25/28.3	21.5/28.0	23.45/28.26	21.8/27.9
Atoms	2100	2018	2165	2228
Protein	2016	1895	1953	1993
Ligand/ion	40	0	18	49
Water	44	123	194	186
B-factors (overall)	51.96	37.013	33.078	33.265
r.m.s.d				
Bond lengths (Å)	0.009	0.007	0.007	0.008
Bond angles (deg)	1.27	1.047	1.11	1.13

Discussion

PknK, the sole soluble RD STPK in *Mtb,* is phosphorylated to different extents by other *Mtb* kinases. Like nine of the other *Mtb* STPKs, phosphorylation of the PknK activation loop activates the PknK kinase domain. I determined the crystal structures of the PknK kinase domain in three phosphorylation states. These structures provide valuable images of the kinase at intermediate points during activation.

The PknK kinase domain crystallized as a monomer in all three phosphorylation states. The back-to-back, N-lobe dimer typically observed for the transmembrane (TM) STPKs was not observed with this soluble kinase domain. The back-to-back dimer stabilizes the TM STPKs in the active conformation (Chapter 4). The lack of this interaction interface may enable greater conformational flexibility and allow visualization of the monomeric, unphosphorylated off-state of an *Mtb* kinase for the first time.

The PknK kinase domain exhibits the classical kinase fold with a mainly α-helical C-lobe and an N-lobe containing the Cα-helix and β-sheets. The PknK fully phosphorylated (wild-type) and mono-phosphorylated Asn149Asp mutant structures are nearly identical to the unphosphorylated structures (Figure 5.1). Residues near the active site display multiple side chain conformations when the structures are compared. Notably, His106 appears to flip in and out of the ATP binding cleft (Figure 5.1). The position of this side chain may contribute to the preservation of the C-spine in the nucleotide-free, unphosphorylated, kinase-domain structure.

Clear electron density for the nucleotide in the ATP-binding cleft demonstrates that unphosphorylated, mono-phosphorylated and wild-type PknK can bind ATP analogs. These results show that activation loop phosphorylation is not required for nucleotide recognition and binding. In contrast to the PknH wild-type structure, there is no unassigned density in the active site of the apo-PknK structure, an indication that the conformation is maintained regardless of nucleotide binding (Figure 5.2).

The lack of clear electron density hinders the analysis of the activation loop anchor region. Very little activation loop electron density is visible in the unphosphorylated PknK kinase-domain structures, in contrast to the unphosphorylated PknH kinase-domain structure in which the full activation loop is well ordered (Chapter 4). Multiple conformations of this peptide may account for the lack of electron density for this area of the protein. This result indicates that heterogeneous phosphorylation of the activation loop is not the sole reason for the conformational disorder of the activation loop.

The comparison between the nucleotide-bound and apo-unphosphorylated PknK structures reveals that Mn:ATPγS binding results in improved activation loop density. The increased electron density may indicate improved stability of the activation loop resulting from nucleotide binding. Nonetheless, the majority of this loop remains unstructured. The presence of nucleotide in the ATP-binding cleft likely serves as part of the protein activation mechanism, resulting in conformation changes that support the formation of a stable-substrate binding region proximal to the activation loop. Intriguingly, the lack of ATP does not result in global conformational changes.

The structures of the PknK kinase domain, with and without phosphates, exhibit significant conformational differences in comparison to phosphorylated PknB. Initial difficulties generating a molecular replacement solution hinted at the conformational differences between

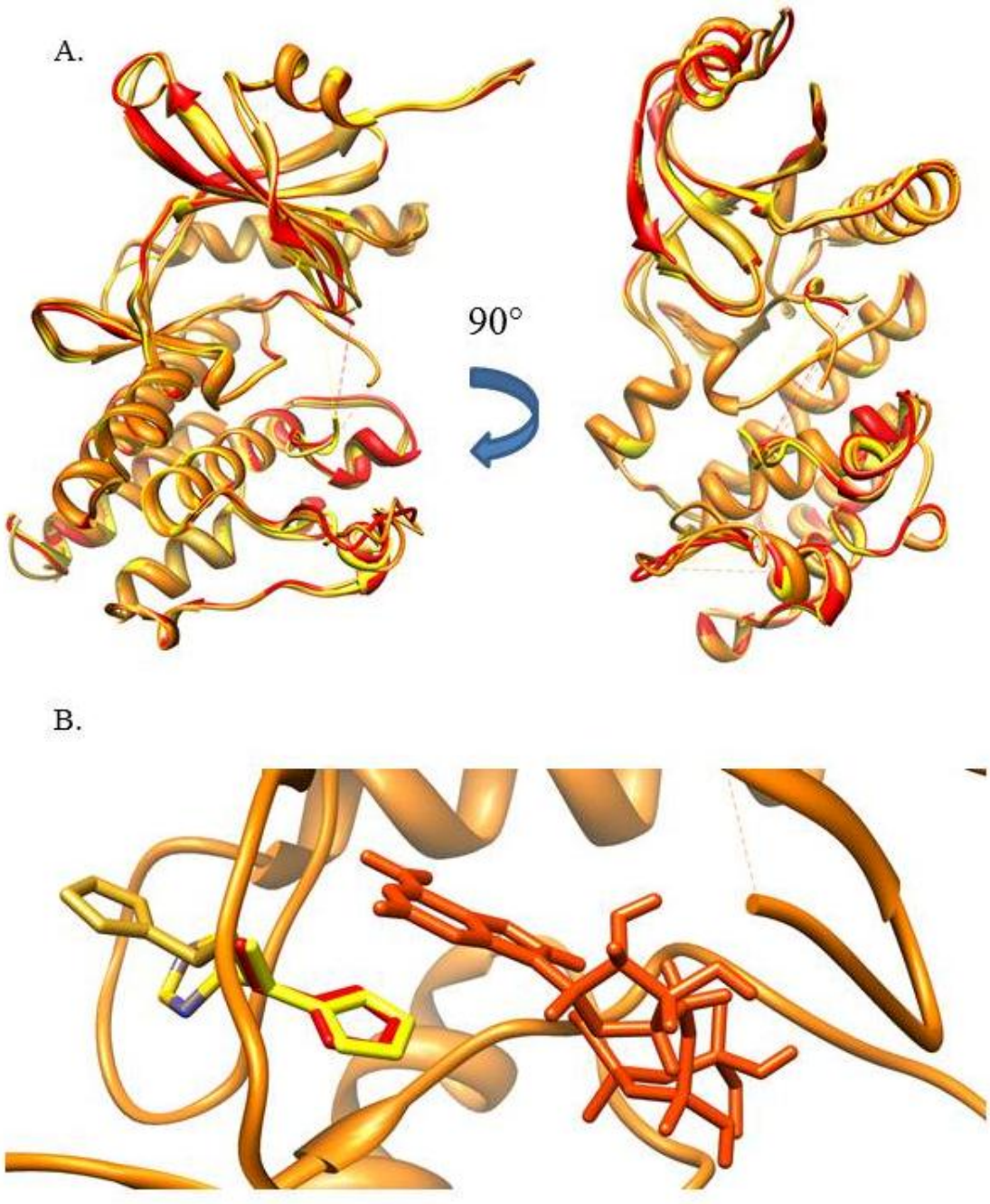

Figure 5.1 A) The superposition of the unphosphorylated apo (mustard yellow), unphosphorylated:ATPγS (orange), monophosphorylate: ATPγS (yellow), and wild-type (red) PknK kinase domain structures reveals that activation loop phosphorylation induces little conformational change. **B)** His106 displays multiple side chain conformations in the PknK kinase domain structures.

A.

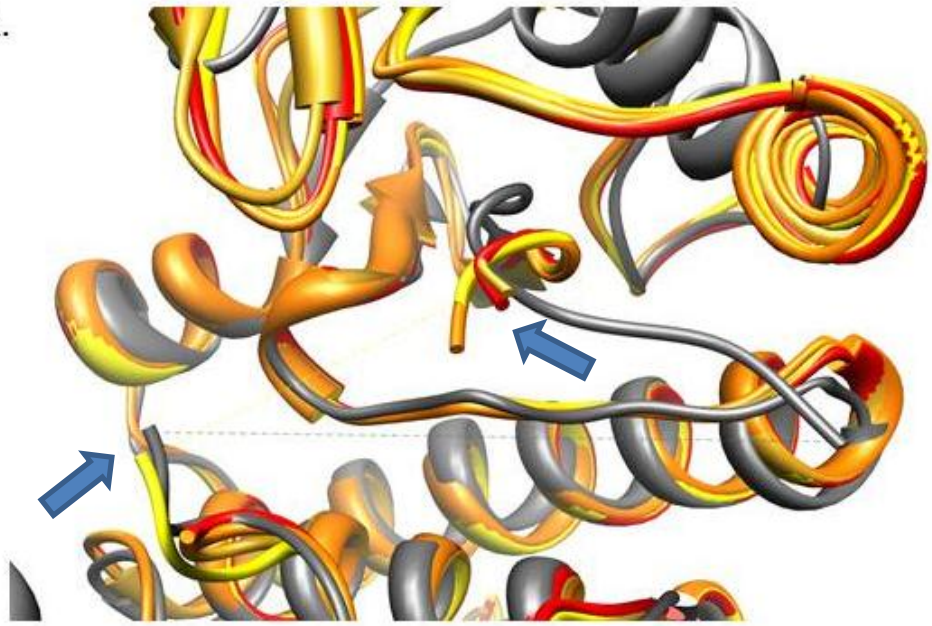

B.

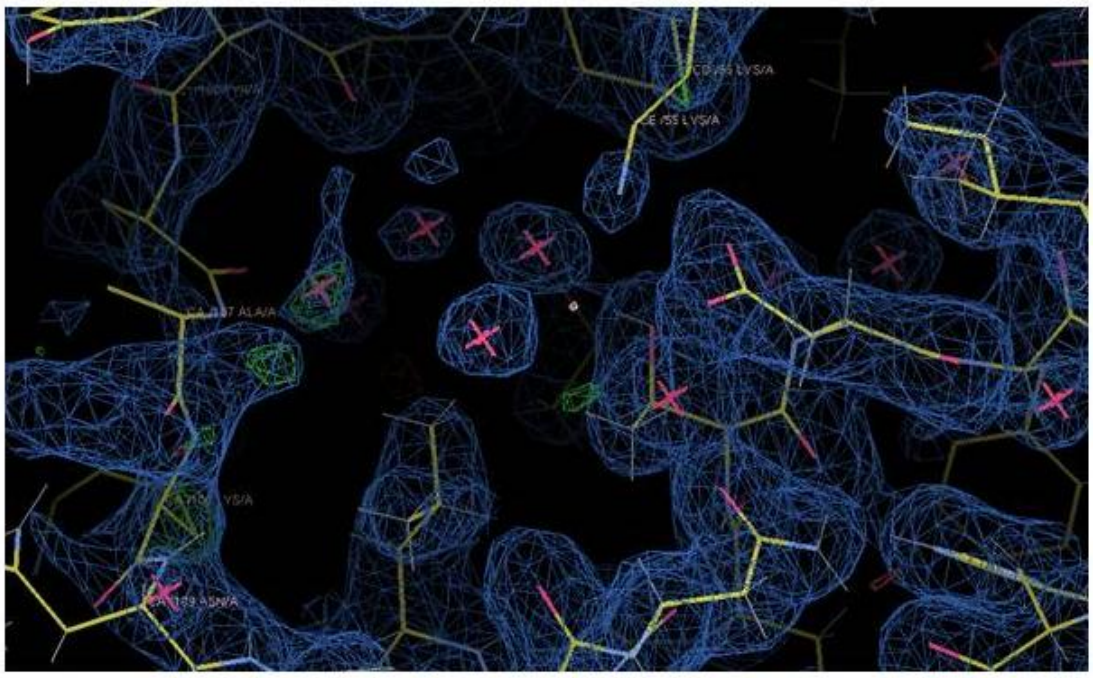

Figure 5.2 A) Ribbon diagram of the superposition of the four PknK structures (shades of orange and yellow) with PknB (dark gray) reveal the positioning of the activation-loop termini (blue arrows). **B)** The active site of the apo-PknK kinase domain structure contains no additional electron density aside from waters (red asterisks).

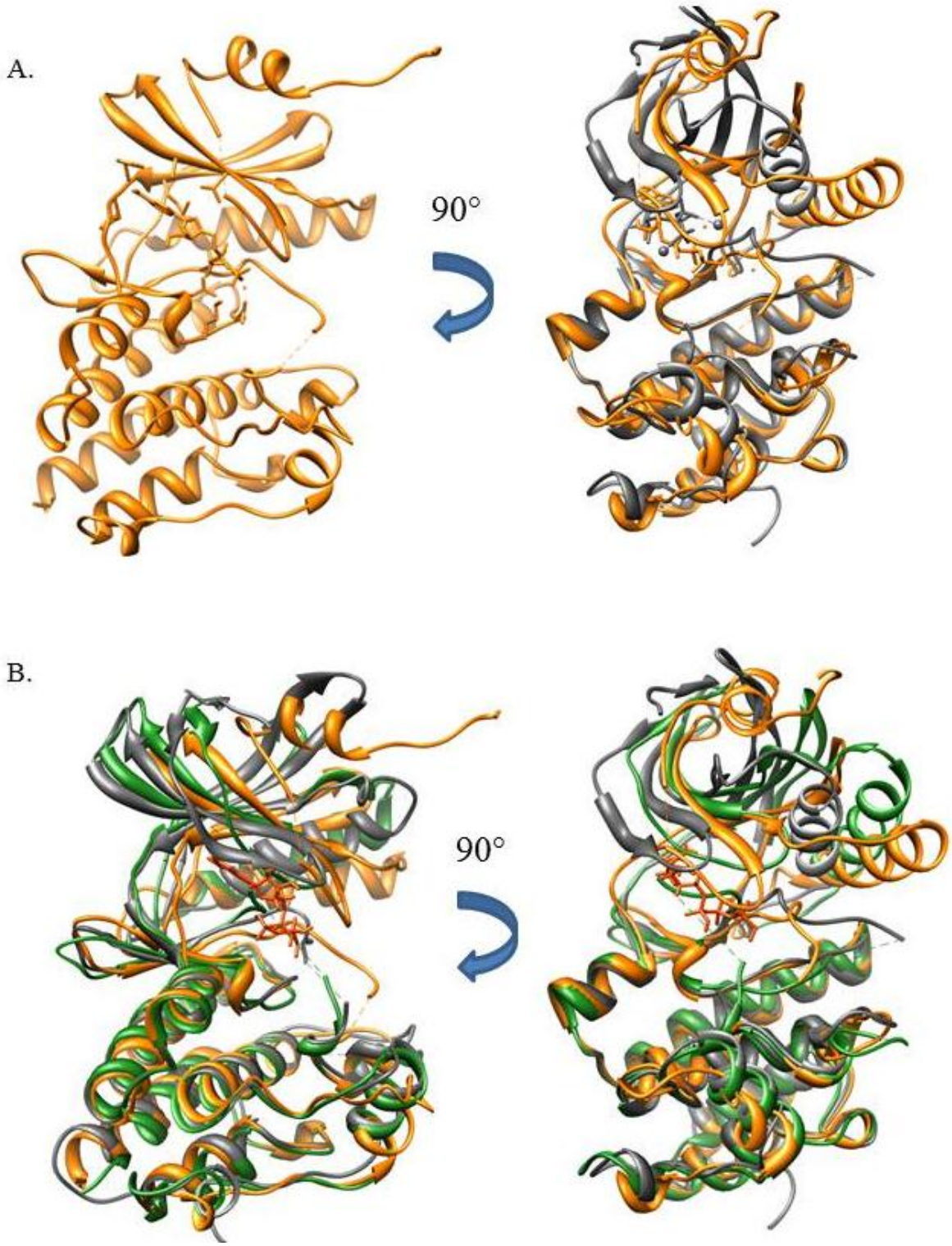

Figure 5.3
A) Superpositions of the Asp149Asn PknK structure (orange) with PknB (dark gray) highlight the difference in N-lobe orientation between the two kinases.
B) The superposition of PknE (green) with the Asp149Asn PknK structure (orange) and PknB (dark gray) reveals differences in N-lobe conformation.

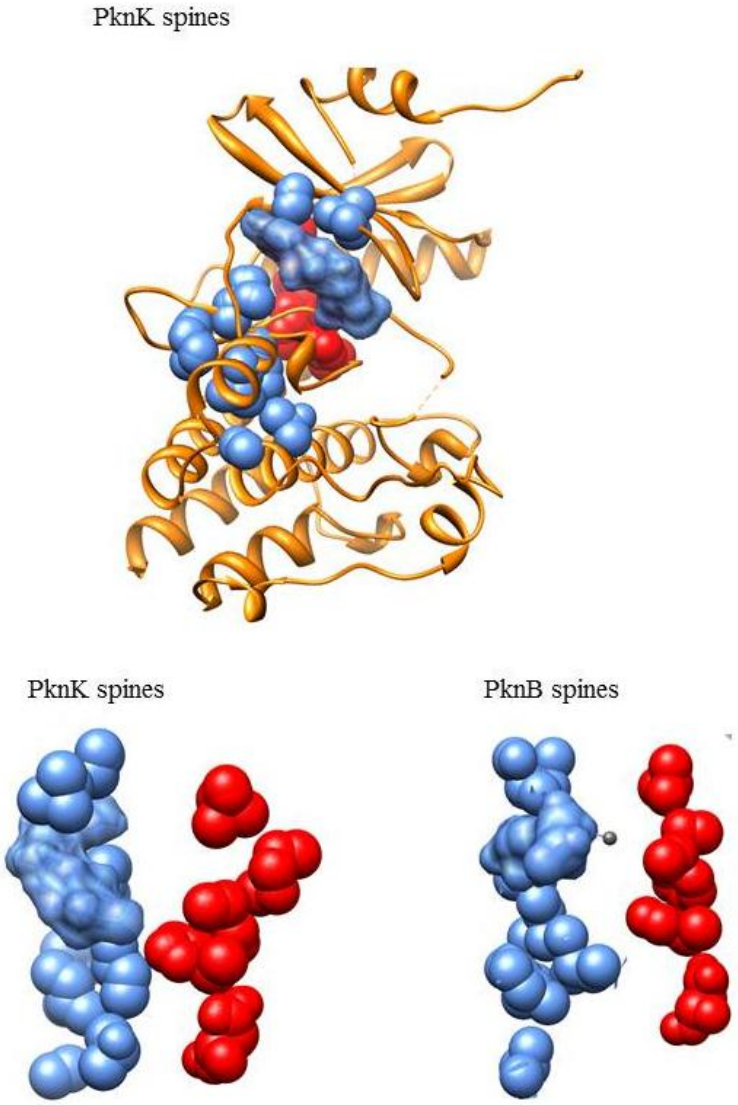

Figure 5.4 The PknK kinase spines are highlighted in blue (C-spine) and in red (R-spine). While the C-spine remains intact, the R-spine is disordered. A comparison between the PknK spines and the PknB spines demonstrates the conformational differences between the two structures.

this PknK structure and the extant STPK crystal structures (Figure 5.3). Superposition of these PknK and PknB kinase domains highlights the altered N-lobe and Cα-helix orientations relative to the C-lobe. In particular, the PknK Cα-helix wings outward, away from the ATP-binding cleft. The N-lobe β-strands rotate slightly and slip down toward the activation segment, covering the active site.

This positioning of the N- and C-lobes also differs significantly from the apo-PknE kinase domain structure (Figure 5.3). While the Cα-helix in the PknE structure rotates away from the active site, the equivalent helix in the PknK structures is shifted even farther along the same path. The relative opening and closing of the ATP-binding cleft due to movement of the

N- and C-lobes is a dynamic feature of the kinase fold (Nolen, Taylor et al. 2004). Analysis of a number of kinase crystal structures revealed extensive conformational diversity in the β-sheets of the N-lobe (Sowadski, Epstein et al. 1999). Altered positioning of these lobes can be a basis for inactivity, but, many active kinases display rotation of the N-lobe relative to the canonical STPK fold.

While the C-spine is intact in the PknK structures, the R-spine is disassembled. The C-spine depends on the presence of ATP, because the adenine ring forms the connection between the N- and C-lobes (Kornev, Taylor et al. 2008). The R-spine depends on the activation loop conformation and Cα-helix position for proper formation. The PknK R-spine appears misaligned (Figure 5.4). However, analysis of the hydrogen bonds in this region reveals that the misaligned residue H-bonds with the Mg-binding loop, stabilizing the conformation. The comparison of the PknK Asp149Asn structure with the wild-type PknK structure reveals that this altered N-lobe conformation is maintained in the active form of the kinase (Figure 5.1).

A structured activation loop is considered a hall mark of an active eukaryotic STPK. The phosphorylated residues in the activation loop interact with one or more basic pockets in the C-lobe to enable assembly of the substrate binding platform near the active site of the protein. Activation loop electron density is not observed in any active *Mtb* STPK structure, indicating that an altered mechanism for assembly of the protein-substrate platform may be utilized by these proteins. Csk and PDK1 also have disordered activation loop residues in the active site (Biondi, Komander et al. 2002; Ogawa, Takayama et al. 2002). In each of these structures, only 3 to 6 residues are disordered, contrasting with the completely disordered activation segment observed in the structures of PknB, PknE, PknH and PknK. The lack of an anchored activation loop, prepared for substrate binding, indicates that novel recognition mechanisms may be utilized by the *Mtb* STPKs. Substrate-kinase co-crystal structures would greatly add to the understanding of the *Mtb* kinase substrate recognition and phospho-transfer processes.

In summary, for the first time I determined the structures of a bacterial STPK kinase domain in the unphosphorylated, singly phosphorylated and multiply phosphorylated forms. All three forms bound the ATP analog, ATPγS, at concentrations typical of ATP in cells. Phosphorylation did not result in large changes in the conformation of the PknK kinase domain. The activation loop was disordered in all three phosphorylation states, in contrast to large changes in this segment that accompany phosphorylation-dependent activation of eukaryotic kinases. Nucleotide binding to the unphosphorylated PknK kinase domain caused little conformational change, suggesting that this form is pre-organized to bind nucleotides. The PknK kinase-domain structures suggest paradoxically that this *Mtb* STPK does not undergo a series of global conformational changes as the protein transitions from the on-state to the off-state. The lack of structural plasticity between all four structures suggests that biochemical processes rather than conformational transitions mediate PknK activation. Potential changes that may be regulated by PknK phosphorylation include differences in the localization of the kinase, assembly of kinase complexes with partner proteins, or the relative affinity of ATP and the nonproductive nucleotides ADP and AMP.

Methods

Protein expression and purification

PknK constructs were expressed as described in Chapter 2. Proteins were purified as described in Chapter 2 through the second Ni-IMAC column. To remove the 6XHis-MBP affinity tag, both the mutant and the active protein required some adaptation of the purification techniques utilized earlier. Briefly, the proteins were expressed with autoinduction and initially separated from the lysate with Ni-IMAC. TEV protease was used to cleave the 6xHis-MBP tag, and the tag and protease were removed with a second round of Ni-IMAC. Following desalting into 30 mM NaCl, 25 mM Tris-HCl pH 8.0, 0.5 mM TCEP, and 20% glycerol buffer, the protein was chromatographed on a MonoQ anion-exchange column to further remove contaminating His-MBP tag. The resulting protein was concentrated and subjected to size exclusion chromatography (SEC) in 150 mM NaCl, 25 mM Tris-Hcl pH 8.0, 0.5 mM TCEP and 20% glycerol. As an alternative to ion exchange and SEC, contaminating tag was removed with a third round of Ni-IMAC, if necessary. The protein was buffer exchanged in 75 mM NaCl, 12.5 mM Tris-HCl pH 8.0, 0.25 mM TCEP, and 10% glycerol for crystallography.

PknK modified with a single phosphate group was generated through a series of additional purification steps. Following the second Ni-IMAC purification step, PknK Asp149Asn was incubated with active 6XHis-MBP tagged PknB, 1 mM ATP and 1 mM $MnCl_2$ overnight at 4 °C. The active kinase was removed with an additional Ni-IMAC purification step and with SEC. Full kinase removal was confirmed by SDS-PAGE. The purified protein was then desalted into 75 mM NaCl, 12.5 mM Tris-HCl pH 8.0, 0.25 mM TCEP, and 10% glycerol for crystallography.

Crystallization and structure determination

PknK Asp149Asn with ATPγS – Purified protein with the addition of 2 mM ATPγS and 2 mM $MnCl_2$ crystallized when mixed with an equal volume of 0.2 M ammonium acetate, 0.1 M sodium acetate trihydrate pH 5.2, and 15% PEG 4000 and equilibrated against precipitant at 18 °C. Crystals that formed in 48 hours were frozen in mother liquor with the addition of 15% glycerol.

PknK Asp149Asn – Apo-PknK Asp149Asn with 2mM $MnCl_2$ crystallized when combined with 0.1 M sodium citrate tribasic pH 5.0 and 30% PEG 550. Crystals were harvested and frozen in mother liquor.

PknK Asp149Asn with ATPγS, + 1 phosphate group – A mixture of purified protein with 2 mM ATPγS, 2 mM $MnCl_2$, 0.04 M potassium phosphate monobasic, 20% glyercol and 8% PEG 8K crystallized readily in 24 week at 18 °C when equilibrated against precipitant. The crystals were harvested and flash frozen in mother liquor.

PknK with ATPγS – Purified protein with the addition of 2 mM ATPγS and 2 mM $MnCl_2$ crystallized when combined with 0.2 M potassium phosphate monobasic pH 4.8 and 20% PEG3350 in 1 week at 18 °C when equilibrated against precipitant. Crystals were frozen in mother liquor with the addition of 20% glycerol.

X-ray data were collected at the Lawrence Berkeley National Laboratory Advanced Light Source Beamline 8.3.1 at 100 K and 11111 eV. The data was indexed and data collection strategies were determined using ELVES (Holton and Alber 2004). Data were processed and scaled using XDS and HKL2000 (Otwinowski 1997; Kabsch 2010). Molecular replacement was carried out using Phaser with a poly-alanine version of the PknB wild-type kinase domain

monomer. After initially placing a search model of the C-lobe alone, the N-lobe was located using a search model comprising the PknB N-lobe with all loops connecting secondary structural elements manually deleted. The molecular replacement solution was obtained using these two search models and the Rotate Around function limited to 30 degrees (McCoy, Grosse-Kunstleve et al. 2007). Models were modified using Coot and refined with Phenix (Emsley, Lohkamp et al. 2010). Structures were superimposed using Chimera (Pettersen, Goddard et al. 2004). The quality of the models was evaluated using MolProbity (Chen, Arendall et al. 2010).

Bibliography

(2003). Finnigan LTQ Getting Started, revision B San Jose Thermo Electron Corporation

(2009). Global Tuberculosis Control: A short update to the 2009 report W. H. Organization.

Adams, P. D., P. V. Afonine, et al. (2010). "PHENIX: a comprehensive Python-based system for macromolecular structure solution." Acta Crystallogr D Biol Crystallogr **66**(Pt 2): 213-221.

Alber, T. (2009). "Signaling mechanisms of the Mycobacterium tuberculosis receptor Ser/Thr protein kinases." Curr Opin Struct Biol **19**(6): 650-657.

Anderson, E. and J. L. Cole (2008). "Domain stabilities in protein kinase R (PKR): evidence for weak interdomain interactions." Biochemistry **47**(17): 4887-4897.

Arora, G., A. Sajid, et al. (2010). "Understanding the role of PknJ in Mycobacterium tuberculosis: biochemical characterization and identification of novel substrate pyruvate kinase A." PLoS One **5**(5): e10772.

Av-Gay, Y., S. Jamil, et al. (1999). "Expression and characterization of the Mycobacterium tuberculosis serine/threonine protein kinase PknB." Infect Immun **67**(11): 5676-5682.

Barthe, P., G. V. Mukamolova, et al. (2010). "The structure of PknB extracellular PASTA domain from mycobacterium tuberculosis suggests a ligand-dependent kinase activation." Structure **18**(5): 606-615.

Biondi, R. M., D. Komander, et al. (2002). "High resolution crystal structure of the human PDK1 catalytic domain defines the regulatory phosphopeptide docking site." EMBO J **21**(16): 4219-4228.

Biondi, R. M. and A. R. Nebreda (2003). "Signalling specificity of Ser/Thr protein kinases through docking-site-mediated interactions." Biochem J **372**(Pt 1): 1-13.

Boitel, B., M. Ortiz-Lombardia, et al. (2003). "PknB kinase activity is regulated by phosphorylation in two Thr residues and dephosphorylation by PstP, the cognate phospho-Ser/Thr phosphatase, in Mycobacterium tuberculosis." Mol Microbiol **49**(6): 1493-1508.

Buckstein, M. H., J. He, et al. (2008). "Characterization of nucleotide pools as a function of physiological state in Escherichia coli." J Bacteriol **190**(2): 718-726.

Busso, D., B. Delagoutte-Busso, et al. (2005). "Construction of a set Gateway-based destination vectors for high-throughput cloning and expression screening in Escherichia coli." Anal Biochem **343**(2): 313-321.

Canman, C. E., D. S. Lim, et al. (1998). "Activation of the ATM kinase by ionizing radiation and phosphorylation of p53." Science **281**(5383): 1677-1679.

Chao, J., D. Wong, et al. (2010). "Protein kinase and phosphatase signaling in Mycobacterium tuberculosis physiology and pathogenesis." Biochim Biophys Acta **1804**(3): 620-627.

Chao, J. D., K. G. Papavinasasundaram, et al. (2010). "Convergence of Ser/Thr and two-component signaling to coordinate expression of the dormancy regulon in Mycobacterium tuberculosis." J Biol Chem **285**(38): 29239-29246.

Chaurasiya, S. K. and K. K. Srivastava (2009). "Downregulation of protein kinase C-alpha enhances intracellular survival of Mycobacteria: role of PknG." BMC Microbiol **9**: 271.

Chen, V. B., W. B. Arendall, 3rd, et al. (2010). "MolProbity: all-atom structure validation for macromolecular crystallography." Acta Crystallogr D Biol Crystallogr **66**(Pt 1): 12-21.

Chenna, R., H. Sugawara, et al. (2003). "Multiple sequence alignment with the Clustal series of programs." Nucleic Acids Res **31**(13): 3497-3500.
Chopra, P., B. Singh, et al. (2003). "Phosphoprotein phosphatase of Mycobacterium tuberculosis dephosphorylates serine-threonine kinases PknA and PknB." Biochem Biophys Res Commun **311**(1): 112-120.
Cohen-Gonsaud, M., P. Barthe, et al. (2009). "The Mycobacterium tuberculosis Ser/Thr kinase substrate Rv2175c is a DNA-binding protein regulated by phosphorylation." J Biol Chem **284**(29): 19290-19300.
Cowley, S., M. Ko, et al. (2004). "The Mycobacterium tuberculosis protein serine/threonine kinase PknG is linked to cellular glutamate/glutamine levels and is important for growth in vivo." Mol Microbiol **52**(6): 1691-1702.
Danot, O., E. Marquenet, et al. (2009). "Wheel of Life, Wheel of Death: A Mechanistic Insight into Signaling by STAND Proteins." Structure **17**(2): 172-182.
Dasgupta, A., P. Datta, et al. (2006). "The serine/threonine kinase PknB of Mycobacterium tuberculosis phosphorylates PBPA, a penicillin-binding protein required for cell division." Microbiology **152**(Pt 2): 493-504.
Deol, P., R. Vohra, et al. (2005). "Role of Mycobacterium tuberculosis Ser/Thr kinase PknF: implications in glucose transport and cell division." J Bacteriol **187**(10): 3415-3420.
Duran, R., A. Villarino, et al. (2005). "Conserved autophosphorylation pattern in activation loops and juxtamembrane regions of Mycobacterium tuberculosis Ser/Thr protein kinases." Biochem Biophys Res Commun **333**(3): 858-867.
Durocher, D. and S. P. Jackson (2002). "The FHA domain." FEBS Lett **513**(1): 58-66.
Emsley, P., B. Lohkamp, et al. (2010). "Features and development of Coot." Acta Crystallographica Section D **66**(4): 486-501.
England, P., A. Wehenkel, et al. (2009). "The FHA-containing protein GarA acts as a phosphorylation-dependent molecular switch in mycobacterial signaling." FEBS Lett **583**(2): 301-307.
Fernandez, P., B. Saint-Joanis, et al. (2006). "The Ser/Thr protein kinase PknB is essential for sustaining mycobacterial growth." J Bacteriol **188**(22): 7778-7784.
Fiuza, M., M. J. Canova, et al. (2008). "From the characterization of the four serine/threonine protein kinases (PknA/B/G/L) of Corynebacterium glutamicum toward the role of PknA and PknB in cell division." J Biol Chem **283**(26): 18099-18112.
Gao, T., A. Toker, et al. (2001). "The carboxyl terminus of protein kinase c provides a switch to regulate its interaction with the phosphoinositide-dependent kinase, PDK-1." J Biol Chem **276**(22): 19588-19596.
Gay, L. M., H. L. Ng, et al. (2006). "A conserved dimer and global conformational changes in the structure of apo-PknE Ser/Thr protein kinase from Mycobacterium tuberculosis." J Mol Biol **360**(2): 409-420.
Gee, C. L., K. G. Papavinasasundaram, et al. (2010). "A Ser/Thr phosphosignaling system controls cell-wall synthesis in mycobacteria " In preparation. .
Good, M. C., A. E. Greenstein, et al. (2004). "Sensor domain of the Mycobacterium tuberculosis receptor Ser/Thr protein kinase, PknD, forms a highly symmetric beta propeller." J Mol Biol **339**(2): 459-469.
Gopalaswamy, R., P. R. Narayanan, et al. (2004). "Cloning, overexpression, and characterization of a serine/threonine protein kinase pknI from Mycobacterium tuberculosis H37Rv." Protein Expr Purif **36**(1): 82-89.

Gopalaswamy, R., S. Narayanan, et al. (2009). "The serine/threonine protein kinase PknI controls the growth of Mycobacterium tuberculosis upon infection." FEMS Microbiol Lett **295**(1): 23-29.
Gopalaswamy, R., S. Narayanan, et al. (2008). "Mycobacterium smegmatis biofilm formation and sliding motility are affected by the serine/threonine protein kinase PknF." FEMS Microbiol Lett **278**(1): 121-127.
Greenstein, A. E., N. Echols, et al. (2007). "Allosteric activation by dimerization of the PknD receptor Ser/Thr protein kinase from Mycobacterium tuberculosis." J Biol Chem **282**(15): 11427-11435.
Greenstein, A. E., C. Grundner, et al. (2005). "Structure/function studies of Ser/Thr and Tyr protein phosphorylation in Mycobacterium tuberculosis." J Mol Microbiol Biotechnol **9**(3-4): 167-181.
Greenstein, A. E., J. A. MacGurn, et al. (2007). "M. tuberculosis Ser/Thr protein kinase D phosphorylates an anti-anti-sigma factor homolog." PLoS Pathog **3**(4): e49.
Grundner, C., L. M. Gay, et al. (2005). "Mycobacterium tuberculosis serine/threonine kinases PknB, PknD, PknE, and PknF phosphorylate multiple FHA domains." Protein Sci **14**(7): 1918-1921.
Hanks, S. K. and T. Hunter (1995). "Protein kinases 6. The eukaryotic protein kinase superfamily: kinase (catalytic) domain structure and classification." FASEB J **9**(8): 576-596.
Holton, J. and T. Alber (2004). "Automated protein crystal structure determination using ELVES." Proc Natl Acad Sci U S A **101**(6): 1537-1542.
Huse, M. and J. Kuriyan (2002). "The conformational plasticity of protein kinases." Cell **109**(3): 275-282.
Jang, J., A. Stella, et al. (2010). "Functional characterization of the Mycobacterium tuberculosis serine/threonine kinase PknJ." Microbiology **156**(Pt 6): 1619-1631.
Jayakumar, D., W. R. Jacobs, Jr., et al. (2008). "Protein kinase E of Mycobacterium tuberculosis has a role in the nitric oxide stress response and apoptosis in a human macrophage model of infection." Cell Microbiol **10**(2): 365-374.
Kabsch, W. (2010). "Xds." Acta Crystallogr D Biol Crystallogr **66**(Pt 2): 125-132.
Kang, C. M., D. W. Abbott, et al. (2005). "The Mycobacterium tuberculosis serine/threonine kinases PknA and PknB: substrate identification and regulation of cell shape." Genes Dev **19**(14): 1692-1704.
Kang, C. M., S. Nyayapathy, et al. (2008). "Wag31, a homologue of the cell division protein DivIVA, regulates growth, morphology and polar cell wall synthesis in mycobacteria." Microbiology **154**(Pt 3): 725-735.
Kannan, N., S. S. Taylor, et al. (2007). "Structural and functional diversity of the microbial kinome." PLoS Biol **5**(3): e17.
Kelley, L. a. S., MJE (2009). "Protein structure prediction on the web: a case study using the Phyre server." Nature Protocols **4**: 363-371
Knight, Z. A., B. Schilling, et al. (2003). "Phosphospecific proteolysis for mapping sites of protein phosphorylation." Nat Biotechnol **21**(9): 1047-1054.
Kornev, A. P. and S. S. Taylor (2010). "Defining the conserved internal architecture of a protein kinase." Biochim Biophys Acta **1804**(3): 440-444.
Kornev, A. P., S. S. Taylor, et al. (2008). "A helix scaffold for the assembly of active protein kinases." Proc Natl Acad Sci U S A **105**(38): 14377-14382.

Koul, A., A. Choidas, et al. (2001). "Serine/threonine protein kinases PknF and PknG of Mycobacterium tuberculosis: characterization and localization." Microbiology **147**(Pt 8): 2307-2314.

Kumar, P., D. Kumar, et al. (2009). "The Mycobacterium tuberculosis protein kinase K modulates activation of transcription from the promoter of mycobacterial monooxygenase operon through phosphorylation of the transcriptional regulator VirS." J Biol Chem **284**(17): 11090-11099.

Lakshminarayan, H., S. Narayanan, et al. (2008). "Molecular cloning and biochemical characterization of a serine threonine protein kinase, PknL, from Mycobacterium tuberculosis." Protein Expr Purif **58**(2): 309-317.

Leonard, C. J., L. Aravind, et al. (1998). "Novel families of putative protein kinases in bacteria and archaea: evolution of the "eukaryotic" protein kinase superfamily." Genome Res **8**(10): 1038-1047.

Lombana, T. N., N. Echols, et al. (2010). "Allosteric activation mechanism of the Mycobacterium tuberculosis receptor Ser/Thr protein kinase, PknB." Structure (in press).

Madhusudan, P. Akamine, et al. (2002). "Crystal structure of a transition state mimic of the catalytic subunit of cAMP-dependent protein kinase." Nat Struct Biol **9**(4): 273-277.

Manning, G., D. B. Whyte, et al. (2002). "The protein kinase complement of the human genome." Science **298**(5600): 1912-1934.

Marshall, A. G. and C. L. Hendrickson (2008). "High-resolution mass spectrometers." Annu Rev Anal Chem (Palo Alto Calif) **1**: 579-599.

McCoy, A. J., R. W. Grosse-Kunstleve, et al. (2007). "Phaser crystallographic software." J Appl Crystallogr **40**(Pt 4): 658-674.

Mieczkowski, C., A. T. Iavarone, et al. (2008). "Auto-activation mechanism of the Mycobacterium tuberculosis PknB receptor Ser/Thr kinase." EMBO J **27**(23): 3186-3197.

Molle, V., C. Girard-Blanc, et al. (2003). "Protein PknE, a novel transmembrane eukaryotic-like serine/threonine kinase from Mycobacterium tuberculosis." Biochem Biophys Res Commun **308**(4): 820-825.

Molle, V., L. Kremer, et al. (2003). "An FHA phosphoprotein recognition domain mediates protein EmbR phosphorylation by PknH, a Ser/Thr protein kinase from Mycobacterium tuberculosis." Biochemistry **42**(51): 15300-15309.

Molle, V., R. C. Reynolds, et al. (2008). "EmbR2, a structural homologue of EmbR, inhibits the Mycobacterium tuberculosis kinase/substrate pair PknH/EmbR." Biochem J **410**(2): 309-317.

Molle, V., I. Zanella-Cleon, et al. (2006). "Characterization of the phosphorylation sites of Mycobacterium tuberculosis serine/threonine protein kinases, PknA, PknD, PknE, and PknH by mass spectrometry." Proteomics **6**(13): 3754-3766.

Narayan, A., P. Sachdeva, et al. (2007). "Serine threonine protein kinases of mycobacterial genus: phylogeny to function." Physiol Genomics **29**(1): 66-75.

Nariya, H. and S. Inouye (2005). "Identification of a protein Ser/Thr kinase cascade that regulates essential transcriptional activators in Myxococcus xanthus development." Mol Microbiol **58**(2): 367-379.

Nolen, B., S. Taylor, et al. (2004). "Regulation of protein kinases; controlling activity through activation segment conformation." Mol Cell **15**(5): 661-675.

Nott, T. J., G. Kelly, et al. (2009). "An intramolecular switch regulates phosphoindependent FHA domain interactions in Mycobacterium tuberculosis." Sci Signal **2**(63): ra12.

O'Hare, H. M., R. Duran, et al. (2008). "Regulation of glutamate metabolism by protein kinases in mycobacteria." Mol Microbiol **70**(6): 1408-1423.
Ogawa, A., Y. Takayama, et al. (2002). "Structure of the carboxyl-terminal Src kinase, Csk." J Biol Chem **277**(17): 14351-14354.
Ortiz-Lombardia, M., F. Pompeo, et al. (2003). "Crystal structure of the catalytic domain of the PknB serine/threonine kinase from Mycobacterium tuberculosis." J Biol Chem **278**(15): 13094-13100.
Otwinowski, Z. a. W. M. (1997). "Processing of X-ray Diffraction Data Collected in Oxcillation Mode." Methods Enzymol **276**(Macromoleulcar Crystallography, part A): 307-326.
Pallen, M., R. Chaudhuri, et al. (2002). "Bacterial FHA domains: neglected players in the phospho-threonine signalling game?" Trends Microbiol **10**(12): 556-563.
Papavinasasundaram, K. G., B. Chan, et al. (2005). "Deletion of the Mycobacterium tuberculosis pknH gene confers a higher bacillary load during the chronic phase of infection in BALB/c mice." J Bacteriol **187**(16): 5751-5760.
Parish, T., D. A. Smith, et al. (2003). "Deletion of two-component regulatory systems increases the virulence of Mycobacterium tuberculosis." Infect Immun **71**(3): 1134-1140.
Pautsch, A., A. Zoephel, et al. (2001). "Crystal structure of bisphosphorylated IGF-1 receptor kinase: insight into domain movements upon kinase activation." Structure **9**(10): 955-965.
Pettersen, E. F., T. D. Goddard, et al. (2004). "UCSF Chimera--a visualization system for exploratory research and analysis." J Comput Chem **25**(13): 1605-1612.
Prisic, S., S. Dankwa, et al. (2010). "Extensive phosphorylation with overlapping specificity by Mycobacterium tuberculosis serine/threonine protein kinases." Proc Natl Acad Sci U S A **107**(16): 7521-7526.
Ranganathan, R. and E. M. Ross (1997). "PDZ domain proteins: scaffolds for signaling complexes." Curr Biol **7**(12): R770-773.
Roepstorff, P. and J. Fohlman (1984). "Proposal for a common nomenclature for sequence ions in mass spectra of peptides." Biomed Mass Spectrom **11**(11): 601.
Rost, B. G. Y. a. J. L. (2004). "The PredictProtein Server." Nucleic Acids Research 32(Web Server Issue): W321-W326.
Savitzky, A. and M. J. E. Golay (1964). "Smoothing and Differentiation of Data by Simplified Least Squares Procedures." Analytical Chemistry **36**(8): 1627-1639.
Scherr, N., S. Honnappa, et al. (2007). "Structural basis for the specific inhibition of protein kinase G, a virulence factor of Mycobacterium tuberculosis." Proc Natl Acad Sci U S A **104**(29): 12151-12156.
Schultz, C., A. Niebisch, et al. (2009). "Genetic and biochemical analysis of the serine/threonine protein kinases PknA, PknB, PknG and PknL of Corynebacterium glutamicum: evidence for non-essentiality and for phosphorylation of OdhI and FtsZ by multiple kinases." Mol Microbiol **74**(3): 724-741.
Sharma, K., M. Gupta, et al. (2006). "Transcriptional control of the mycobacterial embCAB operon by PknH through a regulatory protein, EmbR, in vivo." J Bacteriol **188**(8): 2936-2944.
Simard, J. R., M. Getlik, et al. (2010). "Fluorophore labeling of the glycine-rich loop as a method of identifying inhibitors that bind to active and inactive kinase conformations." J Am Chem Soc **132**(12): 4152-4160.

Simard, J. R., C. Grutter, et al. (2009). "High-throughput screening to identify inhibitors which stabilize inactive kinase conformations in p38alpha." J Am Chem Soc **131**(51): 18478-18488.

Singh, A., Y. Singh, et al. (2006). "Protein kinase I of Mycobacterium tuberculosis: cellular localization and expression during infection of macrophage-like cells." Tuberculosis (Edinb) **86**(1): 28-33.

Skerker, J. M., M. S. Prasol, et al. (2005). "Two-component signal transduction pathways regulating growth and cell cycle progression in a bacterium: a system-level analysis." PLoS Biol **3**(10): e334.

Sowadski, J. M., L. F. Epstein, et al. (1999). "Conformational diversity of catalytic cores of protein kinases." Pharmacol Ther **82**(2-3): 157-164.

Studier, F. W. (2005). "Protein production by auto-induction in high density shaking cultures." Protein Expr Purif **41**(1): 207-234.

Sureka, K., T. Hossain, et al. (2010). "Novel role of phosphorylation-dependent interaction between FtsZ and FipA in mycobacterial cell division." PLoS One **5**(1): e8590.

Thakur, M., R. Chaba, et al. (2008). "Interdomain interaction reconstitutes the functionality of PknA, a eukaryotic type Ser/Thr kinase from Mycobacterium tuberculosis." J Biol Chem **283**(12): 8023-8033.

Wehenkel, A., M. Bellinzoni, et al. (2008). "Mycobacterial Ser/Thr protein kinases and phosphatases: physiological roles and therapeutic potential." Biochim Biophys Acta **1784**(1): 193-202.

Wehenkel, A., P. Fernandez, et al. (2006). "The structure of PknB in complex with mitoxantrone, an ATP-competitive inhibitor, suggests a mode of protein kinase regulation in mycobacteria." FEBS Lett **580**(13): 3018-3022.

Xu, W., A. Doshi, et al. (1999). "Crystal structures of c-Src reveal features of its autoinhibitory mechanism." Mol Cell **3**(5): 629-638.

Young, M. A., S. Gonfloni, et al. (2001). "Dynamic coupling between the SH2 and SH3 domains of c-Src and Hck underlies their inactivation by C-terminal tyrosine phosphorylation." Cell **105**(1): 115-126.

Young, T. A., B. Delagoutte, et al. (2003). "Structure of Mycobacterium tuberculosis PknB supports a universal activation mechanism for Ser/Thr protein kinases." Nat Struct Biol **10**(3): 168-174.